NASA TECHNICAL MEMORANDUM

NASA TM X-62,083

NASA TM X-62,083

A FLIGHT EVALUATION OF A VTOL JET TRANSPORT UNDER VISUAL AND SIMULATED INSTRUMENT CONDITIONS

Curt A. Holzhauser, Samuel A. Morello, Robert C. Innis, and James M. Patton

Ames Reseach Center
Moffett Field, Calif. 94035
and
Langley Research Center
Hampton, Va. 23365

August 1971

A FLIGHT EVALUATION OF A VTOL JET TRANSPORT UNDER VISUAL AND SIMULATED INSTRUMENT CONDITIONS

By

Curt A. Holzhauser*, Samuel A. Morello**,
Robert C. Innis *, and James M. Patton**

*Ames Research Center
**Langley Research Center

TABLE OF CONTENTS

SUMMARY

A flight investigation was performed with the Dornier DO 31 VTOL transport to evaluate the performance, handling, and operating characteristics that are considered to be important when operating a commercial VTOL transport in the terminal area. The DO 31, a 20,000-kilogram transport, has a mixed jet-propulsion system; i.e., there are main engines with nozzles that deflect from a cruise to a hover position, and vertical lift engines that operate below 170 knots. In this VTOL mode, pitch and roll attitude and yaw rate stabilization are incorporated. The main and lift engines are used to control the VTOL forces and moments.

The tests concentrated on the transition, approach, and vertical landing. The mixed jet-propulsion system provided a large usable performance envelope that enabled simulated IFR approaches to be made on 7° and 12° glideslopes. In these approaches management of thrust magnitude and direction was a primary problem, and some form of integrating the controls will be necessary. The handling qualities evaluation pointed out the need for additional research to define flight-path criteria.

The aircraft had satisfactory control and stability in hover out of ground effect. The recirculation effects in a vertical landing were large below 15 meters.

INTRODUCTION

Commercial V/STOL aircraft offer the possibility of overcoming many of the shortcomings of present short-haul air travel. The low-speed characteristics make it possible to operate from small airfields which can be conveniently located near the centers of population. Additionally, these characteristics should red air and ground maneuver time, and improve reliability under adverse weather conditions (refs. 1 to 5). Although considerable research and development have been done over the past decade in the United States and abroad in studying the performance, handling qualities, and operating characteristics of different types of V/STOL aircraft (refs. 6 to 14), it has been difficult to realistically assess the potential of commercial V/STOL transport aircraft and to define the desired characteristics, particularly for IFR conditions. Each aircraft tested had limitations either due to size, stability and control, inherent characteristics, or inability to represent IFR flight; consequently, there is a continuing need to update available information by terminal-area tests with V/STOL aircraft that permit a better simulation of terminal-area operation.

A flight evaluation was made with the Dornier DO 31 jet VTOL transport because this aircraft has several features that offered a better assessment of the terminal-area operation than other research aircraft tested. First, it is sufficiently large (20,000 kg) to

represent a first generation transport. Second, it has a mixed propulsion system (main fan-jets with vectoring nozzles plus lift-jet engines) that provides a very broad performance envelope. Third, it has an advanced control and stabilization system that can reduce pilot workload. Fourth, the controls and displays are duplicated so that IFR operation can be simulated. The NASA flight tests were primarily concentrated on the transition, approach, and vertical landing phases of operation since these are generally considered to be the most demanding phases in terms of aircraft performance and handling qualities. The tests were conducted on 7° and 12° glideslopes with some simulated IFR operation.

The tests were conducted by NASA personnel from Ames and Langley Research Centers in cooperation with the Dornier Company, Bundesministerium für Wissenshaft und Forschung (BWF), Bundesministerium für Verteidigung (BMVg), and the Deutsche Forschungs und Versuchsanstalt für Luft und Raumfahrt (DFVLR).

NOTATION

A_X	Longitudinal acceleration of center of gravity as measured by an accelerometer, $\sin \Theta + \frac{1}{g} \frac{dv_x}{dt}$, g
a_X	Longitudinal acceleration of aircraft, $\frac{dv_x}{dt}$, m/s^2
A_Y	Lateral acceleration of center of gravity as measured by an accelerometer, $\sin \phi + \frac{1}{g} \frac{dv_y}{dt}$, g
a_Y	Lateral acceleration of aircraft, $\frac{dv_y}{dt}$, m/s^2
A_Z	Normal acceleration of center of gravity as measured by an accelerometer, $\cos \Theta + \frac{1}{g} \frac{dv_z}{dt}$, g
a_Z	Normal acceleration of aircraft, $\frac{dv_z}{dt}$, m/s^2
C_D	Drag coefficient, including propulsive thrust
$C_{L_{1g}}$	Lift coefficient in steady-state flight, including propulsive thrust
C_{L_α}	Power-off lift curve slope, per deg
FCU_L	Position of fuel control unit for left lift engines, deg
FCU_R	Position of fuel control unit for right lift engines, deg
g	Acceleration of gravity, 9.81 m/s^2
h	Height above the runway, m

I_{xx}, I_{yy}, I_{zz}	Moments of inertia, Kg-m^2
L	Rolling moment, newton - m
m	mass, kg
N_1	Speed of lift engine furthest forward in left pod, rpm
N_5	Speed of lift engine furthest forward in right pod, rpm
N_F	Main engine fan speed, measured for left engine in percent of maximum speed, percent
q_∞	Free stream dynamic pressure, Kg/m^2
R/C	Rate of climb, m/s
R/S	Rate of sink, m/s
s	Horizontal distance, m or km
S	Wing area, m^2
t	Time, s
T	Thrust, newtons
T_A	Ambient air temperature, °C
T_1	Average temperature at main engine inlet, °C
V	True airspeed, knots or m/s
V_C	Calibrated airspeed, $V\sqrt{\sigma}$, knots
v_x, v_y, v_z	Velocities in body axes, m/s

W	Weight, newtons
X	Longitudinal displacement, m
Y	Lateral displacement, m
α	Uncorrected angle of attack measured at nose boom, deg
β	Uncorrected angle of sideslip measured at nose boom, deg
γ	Flight path angle (climb, positive), deg
γ_G	Glideslope angle at centerline of ILS (descent, negative), deg
δ_A	Left aileron deflection (trailing-edge down, positive), deg
δ_E	Elevator deflection (trailing-edge down, positive), deg
δ_F	Flap deflection (trailing-edge down, positive), deg
δ_{LP}	Lateral stick deflection (right, positive), deg
δ_{MP}	Longitudinal stick deflection (aft, positive), deg
δ_{NP}	Rudder pedal deflection (right pedal forward, positive), mm
δ_{PN}	Pitch nozzle deflection (nose-up pitching moment, positive), deg
δ_R	Rudder deflection (trailing-edge left, positive), deg
ϵ_G	Glideslope error (above, positive), dots or deg
ϵ_L	Localizer error (to right, positive), dots or deg
ξ_M	Pitch stabilization actuator position (nose-up pitching moment, positive), deg
ξ_L	Roll stabilization actuator position (right rolling moment, positive), deg

ξ_N	Yaw stabilization actuator position (right yawing moment, positive), deg
ξ_{VTOL}	VTOL roll rate damper actuator position (right roll rate, positive), deg
θ	Pitch attitude (nose up, positive), deg
θ_{TRIM}	Pitch trim position (nose up, positive), deg
$\dot{\theta}$	Pitch rate (nose up, positive), deg/s
σ	Density ratio
σ_{FCU}	Lift engine thrust lever position, deg
σ_M	Main engine nozzle lever position, deg
σ_{NL}	Nozzle deflection for left lift engines (aft, positive), deg
σ_{NR}	Nozzle deflection for right lift engines (forward positive), deg
σ_T	Main engine thrust lever, measured for left engine, deg
ϕ	Bank angle (right wing down, positive), deg
$\dot{\phi}$	Roll rate (right wing down, positive), deg/s
$\ddot{\phi}$	Angular acceleration in roll (right wing down, positive), rad/s^2
ψ	Heading angle, from measured clockwise, true north, deg
$\dot{\psi}$	Yaw rate (nose right, positive), deg/s

DESCRIPTION OF AIRPLANE AND EQUIPMENT

The DO 31-E3 is a high-wing, mixed-propulsion, jet V/STOL transport with two main engines (vectored lift-cruise) and eight lift engines. The aircraft was designed and constructed by the Dornier Company for a V/STOL research program which was initiated in 1962 and sponsored by the German Federal Ministry of Defense. Figure 1(a) is a photograph of the airplane in the VTOL mode. A three-view drawing is given in Figure 1(b) with additional details in Table 1. The first flight of the aircraft was in 1967, and it was followed by 24 hours of flight tests primarily to define the operational envelope and document the performance. The subsequent NASA program for 11 flight hours primarily evaluated and documented handling qualities in the V/STOL mode and simulated IFR operation. The normal operating mass of the aircraft was about 19,500 kilograms (43,000 pounds).

Propulsion

The E-3 aircraft is equipped with two Rolls Royce (Bristol Division) Pegasus 5-2 turbofan engines and eight Rolls Royce RB-162-4D lift-jet engines. The two Pegasus 5-2 engines are mounted under the wing and have nozzles to vector the thrust. Each engine has four nozzles that vector the total thrust force from a 10° thrusting to a 120° braking position. This engine and nozzle arrangement is essentially the same as used on the Hawker-Siddeley P.1127 aircraft. Each Pegasus 5-2 engine is rated at 69,000 newtons (15,500 pounds force)

of uninstalled sea-level static thrust. At each wing tip are four RB-162-4D lift engines housed in pods. Each RB-162-4D engine is rated at 19,600 newtons (4,400 pounds force) of uninstalled thrust at sea level.

Flight Controls

Figure 2 is a schematic of the separate control functions, and figure 3 is a photograph showing the cockpit layout. The flight attitude controls are a stick and rudder pedals. In cruise the controls are linked to conventional ailerons, elevator, and rudder.

In hover, rolling moments are produced by differential thrust between left and right sets of lift engines. The thrust is commanded by the fuel control units (FCU) which are linked in each pod to the stabilization system and the stick. The pitching moments are produced by reaction controls located at the aft end of the fuselage; high pressure air is supplied from each main engine through separate ducts and nozzles. Yawing moments are created from fore and aft movements of nozzles on the tail pipes of the lift engines. As with roll control, the pitching and yawing motions can be controlled by either the pilot or stabilization system. In the transition the moments are produced by a combination of the hover and conventional controls because the latter move at all speeds. In addition to the stick and rudder pedals, one set of main engine throttles, two main engine nozzle control levers (one for each pilot), and one lift engine thrust lever are used for flight control and are located in the center console.

The DO 31 flight control system is powered by dual hydraulic actuators with control rods, summing bars, etc. The relation between the control forces and deflections are given in figure 4. The stick deflection in millimeters is given on the secondary scale of the deflection in degrees. It is of interest to note that this transport has a stick rather than a wheel, and also that the lateral control motion is obtained by movement about a pivot near the center of the stick (figure 3(a)). The pilots found the use of a stick acceptable, and in fact was preferable to a wheel for a transport VTOL because there was less obstruction to the view, and it was more natural with the one-hand method of control required during transition and hover. The forces and deflections were quite satisfactory.

Figures 5(a) and (b) relate the throttle and engine characteristics. The lift engines are started together with the lever at 17° FCU; after about 10 seconds a stable subidle is achieved and the individual warning lights go out. Then the lever is advanced to 30°, and 10 seconds later a stable flight idle is attained as indicated by another set of lights going off. The forces and deflections of the engine levers were satisfactory except for the fact that it was unsatisfactory to have the height control in the VTOL mode split between the main and lift engines; one control combining the two functions would be desirable. The main engine nozzle control was also satisfactory, but the deflection indicator on the panel had to be monitored and a better display was warranted.

Stabilization System

The aircraft is equipped with a full authority single channel attitude command control system for the pitch and roll axes and rate command for the yaw axis. Figure 6 presents the block diagrams of the stabilization and control system of each axis in the VTOL mode. Figure 7 is a schematic of the stabilization system for each axis. The pitch and roll attitude stabilization system compares the commanded attitude from the control stick signal to the actual aircraft attitude derived from the attitude gyro signal. In the yaw axis, rate is compared rather than attitude. These error signals are then used through the servo-motors to drive the aircraft to the commanded steady-state conditions shown in figure 8. The control signals are introduced additively through a mechanical linkage; thus, in the event of a stabilization system failure, the control reverts to a direct mechanical control immediately. If the control is deflected beyond the position of the limit switch (figure 8), the stabilization system is disengaged to provide safety in the event of a "hard over" failure. The pilots noted a reluctance to use large control deflections because of fear of disengaging the stabilization system. They considered this method of disengaging the system unsatisfactory. A roll damper is incorporated to improve the lateral controllability throughout all flight modes. In the VTOL mode, trim is provided in pitch only. The pilot can control the pitch trim in two manners; one, by a trim switch on his stick, and two, by a preselect switch

located on the instrument panel (figure 3(a)). For the latter case, he can dial in the desired pitch attitude at any time, and by pressing a button on the stick the attitude will change to the preselected value at the rate of 3° per second. The preselect trim system was a desirable feature, but the panel mounted switch was somewhat awkward to use. In the conventional mode, trim is provided for each control.

Cockpit Instrumentation and Displays

Figure 3(b) illustrates the arrangement of the cockpit instruments and displays for the evaluation pilot. Glideslope and localizer error information was displayed on the attitude director indicator (ADI); no steering information was used. True airspeed was obtained from the "Fluglog" (a free-turning, self-alining propeller utilizing the anemometer principle with optical pickups to sense rpm) developed by Dornier and mounted on the end of the nose boom. The face of the standard production airspeed indicator was changed to display 5-knot increments of true airspeed. Angle of attack and sideslip were taken from the deflection of the fluglog and displayed to the pilot.

Data Acquisition

The airborne equipment was capable of registering 208 different data channels simultaneously. One portion of the data was stored in analog form on magnetic tape onboard the aircraft, and at the same time transmitted to a ground station onto magnetic tape. The remaining data were sampled and then stored in digital form on a tape recorder in

the aircraft. Safety of flight information was telemetered to a ground station to be recorded and monitored during the flights. Computers were used to reduce the data to engineering units on plots and tabulated printouts for data analysis.

A ground-based radar operated by DFVLR was used to obtain the position of the aircraft during the approach and landing phase of the flights. The measurements were printed out at 1-second intervals and were time correlated with airborne data.

Guidance

Guidance for the instrument approaches was provided by ILS equipment based at the airfield and operated by DFVLR. This system provided a wide range of glidepath angles and sensitivities. Figure 9 illustrates the profiles and sensitivities used during this investigation. The semi-beam width provided a full-scale deflection of three dots on the ADI. No other approach or navigational aids were available. The glideslope transmitter was located adjacent to the VTOL landing area, see figure 9.

TEST PROCEDURES AND CONDITIONS

Test Location

All of the tests were made at the Dornier Flugplatz in the outskirts of Munich, Germany. The field elevation was 600 meters and the temperature ranged between 0° and 12° C. The flights were made under visual flight rules (VFR) over a range of wind conditions. The wind speeds, measured near the ground with an anemometer, ranged from 0 to 10 meters per second and included headwind, crosswind, and tailwind. For all flights, the Dornier pilot was in command in the left seat.

Hover-Rig Tests

A hover rig simulating the VTOL mode of the DO 31 was used for pilot checkout and training. This rig, shown on the pedestal in figure 10, was also flown in free flight over a range of speeds up to 40 knots (forward and sidewards) and a range of altitudes up to 100 meters above the runway. The tests were limited to a 5-minute duration by the fuel available and the continuous lift engine running time. The rig was similar to the DO 31 in terms of the VTOL propulsion, control, and stabilization systems, and it had similar response. It had three lift engines in each pod rather than four, and the mass and inertia were lower. When mounted on the pedastal in its raised, operating position, the hover rig had restricted angular movement and no vertical movement. It was very useful because the pilots could evaluate the angular response in hover

with and without stabilization and also the response due to shutting down a lift engine or main engine. After a few pedestal runs, each pilot made several free-flight tests. These free-flight tests included tests with the stabilization system turned off, but did not include engine failures.

DO 31-E3 Tests

All flight tests were within the operational envelope established by the manufacturer. Engine failures were not simulated or performed. All tests were made with the stabilization system engaged, except for limited tests with the yaw rate stabilization disengaged during the approach.

Most of the tests were started with a conventional takeoff at a mass of about 21,500 kg (47,000 pounds), and consisted of three to five approaches, terminating at 70 meters of altitude either in a waveoff at 50 knots or a hover and a vertical landing at a mass of about 18,500 kg (41,000 pounds). These procedures were used primarily to maximize research time with the limited lift engine time and fuel. The lift engine time was limited to 5 minutes per start by the simple oil system, and each flight was about 20 minutes total. Several vertical takeoffs were also made. One flight was devoted to a climb to 3,000 meters to document and evaluate the use of the main engine thrust deflection for rapid descent and deceleration from cruise altitude and speed. The total of 11 flight hours was equally divided between the Langley and Ames pilots. This flight time permitted 90 approaches to be made of which 40 simulated IFR operation.

The glideslope angles and sensitivities were varied during the program. Tests were made primarily with a -7° glideslope with a beam width of ±2°. Limited tests were made with -7° ±1° and with -12° ±2°. The variations in flight profile tested are tabulated below:

Glideslope, deg	Intercept Altitude, meters (feet)	Lift engine starting condition
-7	600 (2,000)	Level flight
-7	450 (1,500)	Level flight
-7	300 (1,000)	Level flight
-7	600 (2,000)	On glideslope
-7	450 (1,500)	On base leg in turning flight
-12	600 (2,000)	Level flight
-12	450 (1,500)	Level flight
-12	900 (3,000)	On glideslope

During the majority of these tests, the location of the aircraft was recorded and correlated with onboard measurements.

STOL tests were not performed in these NASA tests primarily because of the high risk due to the nature of the runway. The entire runway, except for the VTOL landing area (figure 9), was surfaced with high friction asphalt that eroded rapidly by hot gases emitted by the lift engines and also by the main engines when they were deflected downward. This erosion was of concern not only because it could damage the runway, but also because of potential damage to the DO 31 engines.

RESULTS AND DISCUSSION

To fully realize the commercial potential of VTOL transports, it will be required to operate routinely to low visibility minimums under Instrument Flight Rules (IFR) and to minimize ground and air maneuver time, fuel, airspace, and noise. These requirements clearly indicate the landing approach to be the most critical flight condition for these aircraft. Further, previous NASA research has shown the approach phase to be the most demanding in terms of pilot workload and has indicated that a number of unresolved questions exist. Therefore, the NASA flight tests of the DO 31 concentrated on evaluating the performance, handling and operating characteristics of this mixed jet-propulsion concept with an advanced stabilization system in simulated IFR approaches.

It must be recognized that the flight test time of the program was limited, and included the time required to familiarize the 2 NASA pilots. Consequently, the operating procedures and patterns used were primarily those developed by Dornier personnel, and the documentation and evaluation of handling qualities was limited. For these reasons the pilot comments are given in an adjective and commentary form rather than in a quantitative form.

The section entitled "Performance and Test Procedures" contains static climb and descent characteristics supplied by Dornier to describe the operating envelope, and also time histories that illustrate a typical vertical takeoff and transition to conventional flight and a transition to VTOL configuration, approach, and vertical landing. The "Handling Qualities" section contains the measured characteristics to support the NASA pilots' evaluation of workload in approach and landing. The last section "Terminal Area" presents primarily the results of complete approaches. There are also some results of translating near hover, and a simplified comparison of different approach and landing techniques in terms of airspace and time used.

Performance and Basic Operating Procedures

Low speed operational envelope: The operational envelope for the DO 31 is illustrated in figure 11 as climb and descent for unaccelerated flight versus airspeed. Included in these figures are lines of 10 and 20 degrees climbing and descending flight paths in unaccelerated flight. Since the majority of the tests were in accelerating or decelerating flight, it should be recognized that these lines also approximate 0.17 and 0.35 acceleration and deceleration in level flight; i.e. $\gamma_{rad} + \frac{1}{g}\left(\frac{dV}{dt}\right) = -\frac{C_D}{C_{L_{1_g}}}$. First, examining the conventional mode (lift engines inoperative), figure 11 (a), it can be seen that with the two main engines operating at high power setting, an extremely large range of flight paths can be obtained by deflecting the nozzles of the main engines from 10° (thrusting) to 120° (braking). Buffet occurs with nozzle deflections greater than 85° at the higher airspeed; however, more than sufficient descent performance is provided for a rapid let down. Although 20 to 30 knot reductions in stalling speeds were achieved over the power off value, the operational speed could not be reduced because of the minimum control speed requirement, V_{MC}. The V_{MC} was defined with the nozzles at 10°, and it was limited by the directional control of the conventional rudder. For this condition with an engine inoperative, a rate of climb of 5 meters per second (1000 feet per minute) was obtained.

In the VTOL mode (lift engines operating), a very large range of operation can be obtained (figure 11(b)). The curves shown are for all engines running and are illustrative of the configurations used during NASA tests. The range of lift engine throttle settings shown provide sufficient range for lateral control, for a margin above the flight idle setting, and to

compensate for engine failure. The curve with $\sigma_{FCU} = 40°$, $N_F = 80\%$, $\sigma_M = 120°$ is about the maximum descent capability of the DO 31. The main engine speed, N_F, was not reduced below 80 percent so that sufficient bleed air could be provided for pitch control. Steady descent rates below 50 knot airspeed were not defined, but it can be presumed that instantaneous values greater than 10 meters per second are attainable. In hover, the maximum descent rate is dictated by the landing gear touchdown design speed of 4 meters per second. The wave off case is with a typical approach power setting and the nozzle deflection reduced from 120° to 70°. The takeoff case is with reducing nozzle deflection as speed increases, (artificially presented at 0 acceleration for comparitive purposes). Obviously, different performance curves can be established for different power settings, nozzle deflection, and angle of attack, dependent on the desired feature to be optimized. The maximum airspeed at which the lift engines have been operated is 170 knots; normally, the maximum airspeed was 160 knots to have a margin and to avoid instability of the fixed-gain stabilization system. Although it is not shown in the figure, a positive climb can be achieved over the entire speed range with one lift engine inoperative; and over a large part of the range with a main engine inoperative.

The thrust-weight ratios available in hover, out of ground effect are given in figure 12 for an aircraft mass of 18,500 kilogram and a field elevation of 600 meters. Three curves are shown: the upper curve is with all lift engines operating at maximum continuous thrust and both main engines at 2-1/2 minute rating, the middle and lower curves show the effect of a lift engine failure and a main engine failure, respectively; both curves

are with lateral symmetry maintained. It should be noted that the vertical force can be further increased by utilizing a main engine emergency thrust which increases the thrust-weight ratio by as much as 0.05 (dependent on the bleed and control used). These curves illustrate the magnitude of thrust-weight ratio that is installed to compensate for an engine failure and that might be available to develop normal acceleration for maneuvering near hover out of ground effect. It is seen that the effect of a lift engine failure is small compared to a main engine failure; however, even in the latter case the aircraft can be ballanced and a thrust-weight ratio in excess of one can be developed.

The proximity of the ground ($h < 15$ meters) was estimated to reduce the vertical force by about 10 percent; this reduction was caused by recirculation and re-ingestion of gases into the main engines.

Vertical takeoff and transition: The takeoff performance and procedures are illustrated in figure 13. Once the lift engines have been started it is necessary to proceed rapidly with the takeoff for two reasons; 1) the idle thrust is so high that the aircraft is very light on the gear, and 2) it is desirable to move away from the large hot gas cloud developing. A nozzle deflection of 75° is used for takeoff to minimize the recirculation effects. Even though the main engine nozzles and the lift engines are now both deflected 15° aft of the vertical, there is practically no ground roll in the takeoff because of the large thrust-to-weight ratio applied to takeoff. The result is a steep, high acceleration takeoff and transition with an average acceleration of more than 0.2g's. In just over 20 seconds sufficient airspeed is attained to shut off the lift engines. A steep climbout

can be continued because of the high thrust-weight ratio of the main engines (T/W = 0.6).

Approach and vertical landing: The procedures and flight paths used for two different approaches to a vertical landing are illustrated in figure 14. The three primary phases of the approach for this VTOL are:

1) The conversion from conventional mode to the VTOL mode;
2) The initial transition where the aircraft is decelerated from about 150 knots to 50 knots during which time a precision approach is made;
3) The final transition from 50 knots to hover at 60 meters followed by a vertical landing.

In the following discussion of handling qualities the longitudinal aspects of these three phases will be discussed first; this will be followed by the lateral-directional characteristics.

In order to complete these three phases of the approach with repeatable precision and with a reasonably low pilot workload, it was desirable to fly the aircraft with prescribed discrete operations that the pilot could perform at selected locations on the path. In addition, the recommended procedure was to track the glide slope at a negative angle of attack (near zero aerodynamic lift); the engines were then near a hover setting so that a hover could be attained with no change in main engine throttle setting and only a small adjustment to the lift engine throttle setting. Approaches were made where the lift engines were started before the glide slope was acquired, and also where the lift engines were started after the glide slope was acquired.

The first phase of the approach, the conversion, starts with the pilot establishing the pre-conversion configuration; i.e., the gear and flaps are lowered, and the airspeed is reduced to about 140 knots; the lift engine pod doors are opened; the attitude stabilization system is engaged; and the desired pitch attitude is pre-selected by the pilot. The airspeed has to be lowered to 140 knots to avoid instability of the stabilization system caused by a fixed gain system which was designed for hover, and also to avoid high starting RPM's of the lift engines. Next, the lift engines are started and advanced from a sub-idle to an idle speed ($\sigma_{FCU} = 30°$); this cycle automatically starts all 8 engines, and requires about 20 seconds to obtain a stable idle. During this period, the pre-select trim button is depressed to change the pitch attitude so that the added vertical force of the idle lift engines ($T/W_{idle} = 0.35$) is compensated by reducing the wing lift to minimize "ballooning", and the nozzles are deflected to maintain constant airspeed.

During the second phase, the precision approach, corrections were primarily made by modulating the lift engines with the aircraft stabilized at the selected pitch attitude. The main engine nozzle deflection for this phase was generally at 120° (maximum braking) to provide the desired deceleration schedule; in some cases smaller values were selected to adjust for head winds. When an altitude of about 60 meters was reached, the third and final phase of the approach commenced by rotating the aircraft to +5° attitude (through the pitch attitude pre-select trim system), by changing the nozzle to 95°, and making small lift engine corrections to attain a stable hover. Then the lift engine throttles were adjusted to set up the desired sink rate for the vertical touchdown.

Handling Qualities

The NASA handling qualities tests concentrated on selected stability and control characteristics of the aircraft and stabilization system that would be of general interest for future commercial V/STOL transports. Figure 15 gives a detailed range and time history of one of the simulated IFR approaches where the lift engines are started in level flight, a 7^{o} glide slope was tracked to 75 meters of altitude, after which the aircraft was flared to commence the vertical landing under visual conditions. These data are presented as a basis for the following discussion of handling.

A major element in the success of the DO 31 to perform a precision approach and to make a safe vertical landing is the pitch and roll attitude stabilization system. This system has 100 percent authority and dominates the basic aerodynamic stability and control characteristics. This system is designed so that the pilot can command pitch and roll attitude and yaw rate in proportion to control deflection over the major range of pilot inputs (see figure 8) and over the speed range for the VTOL configuration (from about 160 knots to hover). In addition, an automatic trim feature is provided that permits the pilot to pre-select the desired pitch attitude which is then commanded with a button on the stick. The system has been optimized for the hover task, and it minimizes aircraft disturbance by atmospheric condition, configuration change, or asymmetry such as produced by engine failure.

Because of the limited test time, extensive documentation was not performed and the information should be considered as an overview rather than a detailed analysis. It should also be noted that prevailing atmospheric

conditions of winds and gusts were accepted and they may have affected some of the initial and transient conditions.

Conversion: The preconversion configuration is established prior to acquiring the localizer. It was noted that little time was needed to engage and verify that that stabilization system was in an operative mode. When the lift engines are started in level flight using the procedures described earlier, the conversion can be performed with little altitude change and only a small attitude change (figure 15(b)). In several cases the lift engines were started after the glide slope was acquired rather than in level flight. An example where this was performed on a 12° hooded approach is shown in figure 16. The conversion procedures were similar to those where the lift engines were started in level flight, and no major piloting problems occurred provided that the intercept altitude was raised to allow sufficient time for tracking.

No significant handling qualities problems existed in maneuvering the aircraft to intercept the localizer in the conventional flight regime. The aircraft handles as a large docile fighter with light control forces. The conventional surface deflection per unit control deflection is reduced with a gear changer as airspeed is increased to give good response, force and force per unit acceleration characteristics at higher speeds.

ILS acquisition and tracking, longitudinal flight path and control: At the higher speeds, say above 100 knots, changes in angle of attack produced by pitch attitude change were very effective in (1) maintaining flight path while the lift engines were advanced to the approach setting and (2) in changing the flight fath to acquire the ILS. For example, an acceleratior

of 0.1g normal to the flight path was obtained in response to a stick step that changed angle of attack only 1 or 2 degrees. When the pre-select feature of the stabilization system was used to change flight path angle, moderate pitch rates were produced (3 degrees per second). The longitudinal control (stick) was also very effective in producing a higher frequency input when the pilot desired to make additional corrections or to compensate for gusts, etc. When large attitude changes were used, such as to acquire the glide slope, a horizontal acceleration was produced at a time when the pilot desired either a constant airspeed or a reducing airspeed. The main engine nozzles were very effective and easy to use in controlling the airspeed at these times (see figures 15 (a), (b), and (c)).

As the airspeed was decreased below 100 knots the longitudinal control became less effective in producing flight path changes. For a decelerating approach not only does the angular response to control input change, but also the flight path response to angle of attack changes; consequently, the pilot must continually re-adjust his gains as the airspeed decreases. At the lower speeds large angle of attack changes must be made to develop the desired normal acceleration and these introduce undesirable airspeed changes because of the rotation of the engine thrust vector with respect to the flight path. Therefore, other methods of control were evaluated and documented. A comparison was made in the 60 to 90 knot speed range of using 1) lift engine thrust, 2) main engine thrust, 3) main engine nozzle deflection, and 4) pitch attitude to control flight path and airspeed while tracking the ILS and correcting for wind and shear conditions. At speeds

below 90 knots the pilots preferred to modulate lift engines for tracking, but noted that there was insufficient control for large upward corrections. The peak measured incremental normal and longitudinal accelerations produced by these controls are compared in fugure 17 with values calculated from the thrust components. Figure 18 presents time histories of the aircraft response to these controls; the incremental changes in velocity, altitude, and flight path were calculated from the accelerometer readings and represent the change due only to the control (see Appendix A).

Modulation of the lift engine produced a maximum of $\pm$ 0.1g normal acceleration (figure 17(a)). Only small acceleration parallel to the flight path was obtained because the lift engine axis is inclined 15° from the fuselage reference line (figure 2), and the aircraft was flown near zero degrees angle of attack. The peak acceleration was rapidly achieved because of the short engine time constant (about 1/4 second), and the measured accelerations agreed well with the values computed from the thrust components. It can be observed in figure 18(a) that the normal acceleration decreases rapidly after the throttle input. This decrease is caused by the damping in heave (change in lift with angle of attack) at constant pitch attitude. The result is a fairly constant increment in vertical velocity 3 seconds after the input to provide a flight path change. Referring to figure 18(a), it can be seen that the altitude change produced by a control input of about 60 percent of the maximum is small; after 10 seconds the altitude increased only 6 meters which is equivalent to only 1/10 of the glide-slope beam width at an altitude of 200 meters (assuming $\gamma_G = -7° \pm 1°$, figure 9).

For a main engine throttle step (figure 17(b)) the magnitude of normal acceleration was similar to that produced by the lift engine. However, a large longitudinal deceleration accompanied an increase in propulsive force because the nozzles were deflected 120°. In contrast to the reduction in the normal acceleration by heaving there is little reduction in the longitudinal acceleration; therefore, a large unwanted decrease in airspeed occurs. The magnitude of the speed change was sufficient that the pilot had to compensate with a change in nozzle deflection; therefore his workload increased. He considered the use of main engine thrust modulation with the nozzles at 120° to be an unsatisfactory flight path control. He felt that the time constant of either the main or lift engines (about 1/2 second and 1/4 second, respectively) did not detract from the tracking task during this portion of the approach.

Modulating only the nozzles of the main engines (figure 17(c) and 18(c)) was unsatisfactory for high frequency control of the flight path because little normal acceleration was developed compared to the longitudinal acceleration. Since a large longitudinal acceleration was rapidly produced, this nozzle control was useful in making airspeed corrections and in making long period adjustments for large flight path changes (such as required for intercepting the glide slope and adjusting for headwinds). The nozzle deflection could be rapidly changed, and 0.1g longitudinal acceleration was obtained with less than 15° nozzle movement.

Figure 18(d) shows the response of the aircraft to an attitude change. A normal acceleration of 0.15g was produced by pitching the aircraft 6°.

This change in attitude caused a deceleration of 0.1g along the flight path which resulted in an unwanted airspeed error of 8 knots after 6 seconds. The combination of normal acceleration and longitudinal deceleration was similar to that for a main-engine step, and when combined with the large attitude increment required to develop the desired normal acceleration produced an unsatisfactory flight path conrtol. Figure 17(d) shows that the normal acceleration and longitudinal deceleration changes can be approximated by the lift change with angle of attack and the rotation of the resultant force ($\Delta\theta/57.3$), respectively.

As illustrated in figures 15 and 16 good tracking of the glide slope could be achieved by using the lift engines provided the pilot was initially on the glide slope. In the process of evaluating flight path control, glide slope offsets were purposely introduced to simulate situations that might occur in normal operations such as caused by wind shears, turbulence, etc. With the glide slope set at $-7^{\circ} \pm 2°$, offsets below the glide slope of 1/2 dot (1/3°) or less and any offsets above the glide slope posed no major problems. Offsets below the glide slope of 1 dot (2/3°) or more brought about expected power management problems because of insufficient normal acceleration provided by the lift engines. This problem is illustrated in figure 19. At t = 14 seconds the pilot advanced lift engines to the maximum normal thrust level, but there was little change in glide slope error. At t = 30 seconds the nozzle deflection was reduced, but this also did not correct the glide slope error because the primary effect of reducing nozzle deflection was to increase airspeed. Finally at t = 39, the aircraft attitude was increased; then the glide slope error decreased, and the airspeed also decreased. If the aircraft had first been pitched, the glide

slope error could have been corrected earlier, but the airspeed would have dropped to a much lower value than desired. Figure 20 shows a tracking run done where main engine throttles were modulated rather than lift engines. Comparing the glide slope error with that of figure 15, it is seen that equally good tracking was obtained; however, the pilot workload was greater when tracking with the main engines because of the undesirable airspeed perturbations with the nozzles at 120° (120° used for the desired flight path and deceleration). This effect on the open loop deceleration is evident in figure 20 at t = 39 seconds where the main engine thrust was increased to avoid going lower on the flight path; shortly thereafter the airplane decelerated to below 60 knots which was below the desired speed scheduled. Then the pilot decreased the nozzle deflection to increase airspeed, but the increase to 80 knots was too large, and the nozzles were rotated back to the full braking position to arrest this overspeed. Thus, one large tracking error can possibly force the pilot to modulate two, three or four control levers at a time when he prefers to keep constant as many parameters as possible.

Reference 7 presented a criteria for satisfactory STOL flight path control during ILS tracking as $\pm$ 0.1g normal acceleration to be achieved in less than 1.5 seconds. This criteria was satisfied by the DO 31 operating in the 60-90 knot range with lift or main engine thrust modulation, but the pilots considered either control unsatisfactory for tracking an ILS. It is concluded that the criteria was inadequate because it only specified a maximum acceleration normal to the flight path to be achieved within a given time. It appears that the flight path control criteria

should include changes in altitude and/or flight path after several seconds, and should also limit airspeed and attitude changes. Such a criteria would be analogous to lateral control criteria where time to bank 30° is specified with the maximum permitted cross coupling. There are insufficient data at present to revise the criteria for tracking and ILS with V/STOL aircraft; however, the following recommendations are made:

(1) The control of acceleration normal to the flight path should be achieved with little acceleration along the flight path (i.e. "direct lift control" is desired). When normal acceleration is increased (upwards), an acceleration along the flight path is preferred over a deceleration; a deceleration along the flight path greater than 50 percent of the normal acceleration is unsatisfactory. The flight path should be changed at least 2 degrees within 2 seconds after the control and thereafter the flight path should not return towards the initial conditions.

(2) Independent control of the acceleration parallel to the flight path should have no appreciable downward acceleration, and a small upward acceleration is desired.

Additional simulation and flight tests are required to define the criteria and provide limits to cross coupling (such as unwanted airspeed changes).

Final transition and vertical landing, longitudinal and height control: The final transition to a vertical landing was shown in time history form in figure 15(d). To reduce the pilot workload the normal precision approach procedure was to fly the aircraft near zero lift so that the main and lift

engines settings were near hover values and to use a main nozzle deflection of about 120° to decelerate the aircraft to an airspeed of 50 to 60 knots by the time the altitude was down to 50 to 70 meters. At this point (t = 110 seconds in figure 15(d)) the aircraft is flared by pitching to +5° attitude with the pre-select trim system; then the lift engine thrust, main engine nozzle deflection, and aircraft heading is adjusted to maintain the aircraft over the touchdown area. The lift engine thrust is readjusted to produce a small sink rate (less than 2 meters per second). As the aircraft descends below 15 meters of altitude, the sink rate increases because of recirculation and reingestion. In the descent between 60 meters and 15 meters, the pilot can increase the lift engine thrust to reduce the sink rate; however, there was concern that the resulting increase in gas cloud could increase reingestion into the main engine and increase rather than decrease sink rate. Figure 21 illustrates the suckdown magnitude when making a vertical landing in the DO 31. This time history of altitude, sink rate, and vertical acceleration is typical for a low sink rate descent when there is no increase in lift engine thrust just prior to landing to compensate for (1) suckdown forces on the under surfaces of the airplane, and (2) main engine thrust loss due to exhaust gas reingestion. The result is a downward acceleration of approximately 0.10g one second before landing with a touchdown impact of about 2.5 meters per second induced by the combined suckdown and reingestion factors. For the example given in figure 15(e), the lift engines were increased to the maximum normal thrust setting just before touchdown, and yet the touchdown descent rate was more than 1 meter per second. Thus it can be seen that below 10 meters of altitude the

landing commitment is definite. Even though the main engine thrust could have been increased, the effect on the reingestion was of concern, and thus there was no "go around" capability in these tests. At any point down to 30 meters, waveoffs were easily accomplished by pitching the aircraft $\pm$ 5° and repositioning the nozzles to 65°.

The NASA pilots considered the available control from lift engine modulation insufficient for descent control in hover. Since the normal acceleration was less than 0.1g, the vertical velocity damping near zero, and the lift engine time constants small, these results are in agreement with those of references 12 and 14. When this limited control was coupled with the recirculation effects, the NASA pilots rated the vertical descent and landing unacceptable for a commercial VTOL transport.

ILS tracking, lateral-directional flight path control: At speeds above 50 knots large lateral corrections were difficult to make. The aircraft response to a lateral step with the stabilization engaged on all axes and with rudder pedals fixed is given in figure 22(a). For this test the stabilization system maintains zero yaw rate; there is no change in heading, and the sideslip is related to the bank angle. The pilots noted that large bank angles were needed to develop the desired lateral velocity, high sideslip angles developed, and it took longer to make the correction than was desired. It was concluded that large lateral corrections could not be made satisfactorily by only translating the aircraft. When the pilots used the directional control (which commanded yaw rate) to coordinate the maneuver, it was impossible to find the correct input to maintain small sideslip angles; the aircraft responded as if it had no directional stability.

Tests were also made with the yaw rate stabilization off. For this condition and no pedal input (figure 22(b)), the sideslip excursion was proprtional to the bank angle ($\Delta\beta/\Delta\phi = 1$), and the aircraft had a fairly long directional period (7-8 seconds) with low directional damping. It was concluded that additional augmentation for turn coordination was needed. Reference 7 pointed out that it was necessary that $\Delta\beta/\Delta\phi$ be less than 0.3 for satisfactory handling, and methods to achieve these levels were also discussed therein.

The requirement for large bank angles to develop suitable lateral velocities was not expected based on small-scale tests of the DO 31 (reference 8) nor on predictions made by Dornier personnel. The static lateral-directional characteristics measured in flight are given in figure 23. These data show that 10 degrees of bank angle are needed to achieve a lateral velocity of 10 knots at 60 knots forward speed. The bank angle per unit sideslip was 2 to 3 times that calculated from the tests of reference 8 where the lift engine flow was simulated but the main engine flow exhausted at zero degrees rather than 120 degees used in the flight tests.

For small corrections to be made while tracking the localizer beam, the easiest procedure was to use the directional control (with yaw stabilization engaged) and let the aircraft translate laterally with the wings held level by the attitude stabilization system. In this case the desired heading was maintained by the stabilization system and this avoided the wandering exhibited by other V/STOL aircraft at comparable approach speeds (reference 7).

The lateral control, sensitivity, and response were satisfactory at the transition speeds; however, the attitude command feature required a lateral force be maintained by the pilot in turning flight, and even though the force was low it was unnatural and uncomfortable to the pilot.

Final transition and vertical landing, lateral control: Considerable research has been performed by NASA and others on the maginitude of lateral control power needed for satisfactory performance of the hover task (references 9 and 10); however, there remains considerable postulation on the effects of aircraft size and degree of stabilization, (references 11 and 12). Since the DO 31 is the largest VTOL tested by NASA (45,000 lbs.) has an attitude command stabilization system, and has a relatively low lateral control power installed (0.8 rad/sec^2), it offered a unique opportunity to examine the lateral controllability in flight in a realistic environment and to compare the results with simulator prognostications. The following evaluation and discussion of the lateral control power characteristics of the DO 31 during very low speed flight (at or near hover) is in the form of reference 12 where the maneuver, trim (balance) and upset requirements were discussed. It is assumed that the aircraft is being operated as a commercial V/STOL transport; i.e., only modest VTOL maneuvering is required, an engine failure must be controlled, and the aircraft must be operated in adverse weather conditions.

First, the maneuvering characteristics will be examined. The effect of stick deflection on the static rolling moment available and on the angular acceleration is shown in figure 24. It is seen that the maximum

rolling moment is essentially independent of the lift engine throttle setting ($\mathcal{T}_{FCU}$). Figure 24(b) contains several measured peak roll acceleration values. These values are larger than the calculated values of $\frac{L}{I_x}$ because the rolling moment is based on a static value and the stabilization system initially commands higher acceleration to give more rapid angular response to a normal pilot input. The more rapid response is evident in the time histories of a stick step, figure 25. With stabilization (left hand figure) the lift engine fuel control units (FCU) are commanded to very large deflections shortly after a pilot's input of 1/4 stick deflection, and the initial response ($t < 2$ seconds) is greater than without stabilization (right hand figure). With stabilization, a 5^o bank angle was attained in 1 second for this input, and the bank angle reached 90 percent of the steady state commanded value, 10^o, in about 2-1/2 seconds. As the pilot input is increased in magnitude, the differences in aircraft response with and without stabilization will become less because there is less excess moment available to increase the acceleration. The pilot input for the bank step with stabilization is a stick step and is easy to perform; the pilots considered the response, damping, and sensitivity to be satisfactory. The lag of peak RPM behind the stick input reflects the lift engine time constant of 0.2 and 0.3 seconds. The aircraft response closely matched a calculated time history based on a natural frequency of 2.5 radians per second, a damping ratio of 1.1, and an initial lag of 0.2 seconds; these characteristics were within the optimum areas defined by the simulator study reported in reference 10. Since the pilots rated the lateral control

sensitivity and maximum control power (a value of 0.8 radians per second squared) as satisfactory, good agreement was obtained with the study of reference 10. The control inputs of figure 25 were taken to document the aircraft response, and do not provide a measure of the lateral control needed for maneuvering. To make this evaluation the pilot was given two tasks: one was to perform what he believed to be the most extensive lateral maneuvering around the hover area, and the other was to determine the maximum lateral velocities that he would expect to normally use with a commercial VTOL operation. Figure 26 illustrates the pilot input and control needed to extensively maneuver the aircraft near hover. Figure 27 shows the time history where the pilot slowly increased the bank angle in order to establish and measure lateral velocities. From these tests it was found that the maximum control power needed for control and stabilization during lateral maneuvering was ± 0.4 radians per second squared, and the maximum lateral velocity over the ground that would normally be expected in maneuvering V/STOL transports was 10 meters per second (20 kts). Higher lateral air speeds may be encountered when it is necessary to precisely position the aircraft in crosswinds.

Next, the trim, or balance aspects are examined. Some VTOL aircraft have required large amounts of lateral control to trim lateral moments developed in sideward flight. Referring to the lack of change in differential RPM as lateral velocity increased, figure 27, it is inferred that little or no control moment was required in sideward flight for the DO 31 configuration, at least for velocities of 10 meters per second. Another control requirement is to balance an engine failure. Figure 28 shows that

the static moment resulting from a lift engine failure can be easily balanced. Sufficient moment is also available to balance a main engine failure; however, little moment is available if the remaining main engine is advanced to a high setting to compensate for the lift loss. The dynamic response to a lift engine failure is shown in a time history of the shutdown of the #1 lift engine performed with the hover rig on the pedestal, figure 29. It is seen that with a fixed stick position the aircraft rolls only 2 degrees and within one second of engine shutdown ititiation, the bank angle starts to return to the wings level position. During this compensation the remaining lift engines are initially commanded to a near emergency FCU level in the left pod and a near idle in the right pod to limit the rolling; this represents about 80 percent of the available control moment. Shortly thereafter the difference in FCU levels is reduced to maintain static symmetry. A larger bank angle was produced by a main engine failure and it took longer to return to wings level. From a piloting viewpoint the response to an engine failure was satisfactory; however, since the asymmetric moment was automatically trimmed out without changing stick position or force, the pilot had no direct way of knowing that he was near a control limit except by reference to actuator positon gages on the instrument panel. From these data it can be ascertained that the greatest lateral trim requirement for the DO 31 is produced by an engine failure. No flight tests were performed with an engine failed, but since 3/4 of the lateral control was needed to statically balance the remaining main engine, it would be expected that marginal control remained for a vertical landing. For the case with the lift engine failed, less control moment

was needed; and the remaining lateral control power should be satisfactory for some maneuvering during the landing.

Finally, a few comments are given on the upset aspect. The control power needed to compensate for gusts could not be determined; however, it can be stated that the stabilization system was very effective in controlling upsets due to atmospheric conditions that were encountered. In fact, the pilots remarked that the aircraft was very stable in a large variety of conditions such as headwind, crosswind, and gusty air. This is further verified by the ability of the stabilization system to compensate for an engine failure (figure 29) which would be comparable to a gust producing an angular acceleration of about 0.4 radians per second squared.

It should also be noted that care was taken to keep the friction and force gradient of the control system low (figure 4(b)). The values correspond to those recommended in reference 12.

In conclusion, the lateral control power of the DO 31 (0.8 radians per second squared) was sufficient to provide a satisfactory hover control provided that attitude stabilization was utilized. It should be noted that engine failures were not adequately evaluated in these tests. Although the aircraft could be flown by a research pilot with the stabilization system off, the workload required to hover and land such a craft in commercial operation were considered unacceptable even for an emergency operation. Based on these tests significant reduction in control power cannot be recommended for this class and configuration of aircraft.

Trim considerations in transition and hover: Throughout the flight regime with lift engines operating, the attitude command stabilization system very effectively performed the trimming function so that the pilot was generally not aware of out-of-trim moments. Although this greatly simplified the pilot's task, some warning must be given to the pilot if control limits are approached. For example, the previous section pointed out that a large amount of control was needed to compensate for an engine failure, and yet the pilot is not aware of the remaining control because the stick remained centered. This situation also occurred during a vertical takeoff and transition, figure 13. Referring to the pitch nozzle position it is seen that at 40 knots 80 percent of the longitudinal control is required to compensate for the nose-up pitching moment due to the aerodynamics and propulsion system, and yet the stick is centered.

Another aspect that must receive additional attention when stabilization systems are incorporated is the complaint by the pilot that a force must be maintained in turning flight at transition speeds. In this respect a rate command with attitude hold may be preferable.

The ability to pre-select the desired pitch attitude and to actuate this with the button on the control stick, when desired, was a very desirable feature of the pitch attitude command system, because it reduced pilot workload during the approach when discrete pitch changes were required.

Terminal Area Operation

It was noted earlier that a wide range of ILS approaches could be made with this aircraft because of its large operational envelope and good control and stabilization system. This section will review the approach in terms of constraints that may be imposed on a commercial V/STOL transport operating in the terminal area.

Cruise letdown to pre-approach configuration: Figure 30 presents a time history of a letdown from cruise altitude where the deflection of the nozzles of the main engines is used for controlling descent rate. The descent started at an altitude of about 2500 meters and an airspeed of 260 knots and ended at an altitude of 450 meters and 140 knots with localizer capture; the engines were set at a moderate thrust level, N_F = 72%. The maximum nozzle deflection permitted from structural considerations was 90° between 250 - 200 knots, and 120° below 200 knots. A heavy buffet accompanied the 120° setting during the descent and would be unacceptable from an operational standpoint. It was determined that an 85° nozzle setting was about maximum to avoid buffet, and this setting resulted in descent rates in excess of 20 meters per second, a sufficiently high descent rate for rapid letdowns. The use of the nozzles is considered an excellent method of establishing a varying rate of descent during the letdown.

Conversion: Before converting to the VTOL configuration the pilot maneuvers to intercept the localizer; he then needed about 30 seconds of tracking time while the aircraft stabilizes from the pre-conversion changes of gear and flap deflection. Then he initiates the

start of lift engines. By properly combining pitch attitude, nozzle deflection, and main engine thrust, there was little altitude or airspeed change during this operation (figure 15(b)) even though the lift engine idle thrust-weight ratio was about 0.35. The time to attain a stable idle was about 20 seconds and the pilots considered that this was too long because it distracted them from other flying tasks. This distraction was minimized by assigning this monitoring task to the co-pilot. Since there was no ground based guidance information, such as distance measuring equipment or beacons, level flight conversions were difficult to initiate at the proper location except when landmarks were visually used for position.

The lift engines were also started on the glide slope (figure 16), and in this case a better reference for starting the lift engines was provided by reference to the altitude. Due to the length of time required to start the lift engines, the intercept altitude had to be raised when starting the lift engines on the glide slope.

ILS acquisition: Referring to figure 15, before the glide slope is intercepted, the desired pitch attitude for the approach is pre-selected (-10° for-7° glideslope). When the aircraft nears the glide-slope centerline, the acquisition is initiated by releasing the pre-selected trim, by advancing the lift engine throttle to a hover setting, by deflecting the nozzles from 65° to 120° (braking), and by increasing the main engine thrust. All of these changes are performed by the pilot in less than 4 seconds. It is seen that by following these procedures the flight path is changed with little overshoot, and about 15 seconds later the pilot is confident that the glide slope has been acquired.

At this point (t=70 seconds) the aircraft has decelerated to about 100 knots and is at an altitude of 250 meters; the pilot can then proceed to track the ILS. By properly combining main and lift engine throttles, main engine nozzle deflection and longitudinal pitch control, it was found possible to intercept 7 and 12 degree glide slopes and to track these slopes with acceptable accuracy while decelerating from 140 to 50 knots and descending to a breakout altitude of 70 meters. However, the NASA pilots considered the workload imposed by the numerous discrete control steps to be unacceptable for commercial VTOL transport operation.

In order to examine the feasibility of reducing the time in the V/STOL configuration glide slope intercept altitudes of 300, 450, and 600 meters were tested for the 7° glide slope approaches. The 450 meter intercept altitude was preferred when the lift engines were started in level flight since this permitted a reasonable glide slope acquisition and tracking time (approximately one minute). The 300 meter intercept did not allow enough tracking time with the given deceleration schedule. The 600 meter altitude was used when more time was needed; e.g. when the lift engines were started on the 7° glide slope. Because of the higher descent rates that occur during 12° approaches, the intercept was raised to 600 meters when the lift engines were started in level flight. To obtain adequate tracking time when the lift engines were started on the 12° glide slope instead of in level flight, the intercept altitude had to be raised to 900 meters.

Although these intercept altitudes may be peculiar to the DO 31 configuration and will vary for other concepts, this study and other similar studies (reference 15) show that with only simple, situation information displays the pilot needs 20 to 30 seconds for acquisition (time from intercepting the glideslope to confidently acquiring it) and 20 to 30 seconds for tracking to assess the approach so that he can confidently proceed to a landing.

ILS tracking: Once the glide slope was acquired, the ILS beam was tracked by modulating lift engine thrust. If the glide slope has been accurately acquired and no large errors have been introduced, the tracking performance is good (see figures 15 and 16), and the pilot noted that workload is relatively low. The simulated IFR portion of the approach is ended at a breakout altitude of 70 meters at which point the airspeed has stabilized at 50 - 60 knots. The use of attitude stabilization contributed significantly to making these approaches successful. The pilots commented on the usefulness of the main engine nozzles to match the approach schedule with the desired ground speed. By giving the copilot the task of controlling airspeed with the nozzle, the pilot workload was significantly reduced during the simulated IFR approaches. For some tests the glideslope beam width for the 7° approach was decreased from $\pm$ 2° to $\pm$ 1° with no apparent increase in pilot workload or degradation in tracking performance.

The reason that lift engines were used for glide slope tracking and their limitations were presented in the section "Handling Qualities." Even though there was insufficient flight path control available from any individual control during the approach and landing, it is believed

that the aircraft had sufficient normal acceleration capability by combining various controls; however, further research is required to properly integrate these controls in a more manageable form. It should be possible to integrate throttles and nozzle deflection, or it might be desired to add a servo-system to provide a speed or deceleration command system. Consideration should also be given to displays that give the pilot a better visualization of the thrust vector.

The majority of these ILS approaches were made at low lift to reduce the pilot workload. These approaches were made at an angle of attack of about -3°; the relationship, $\theta = \gamma + \alpha$ dictates a pitch attitude of -10° for a -7° approach and -15° for a -12° approach, respectively. Since these approaches were with a large nose down attitude and the aircraft decelerating, the resulting force on the pilot (and potential passengers) is impractical for commercial operation. Therefore, several approaches were attempted with the fuselage more nearly level. These were notably unsuccessful. Insufficient time was available to explore the problem; however, it can be partially attributed to the decelerating approach where the lift at a positive angle of attack significantly is reduced as the approach progresses. From static considerations, the lift deficit, at constant thrust, would be about 0.15 times the aircraft weight when decelerating from 100 knots to 60 knots; nearly the total range of lift engine thrust modulation. In addition, to properly increase the thrust to compensate for this lift deficit, the pilot must also modulate thrust to track the ILS. This problem requires further examination since future V/STOL concepts

envision the use of wing lift to reduce both nose-down approach attitudes for passenger acceptance and power requirements for noise acceptance.

Final transition and vertical landing: At an altitude of 70 meters and an airspeed of 50 knots, the IFR portion of the approach is terminated and a flare is initiated. The steps and procedures required to accomplish a safe vertical landing were discussed in the "Handling Qualities" section. It can be noted in figure 15(a) that shortly after breakout the pilot went below the flight path; this was done to assure himself that he would not overshoot the touchdown area. During the vertical descent it was difficult to see the touchdown area, and reliance had to be placed on the vertical descent rate obtained from the radar altimeter. Figure 21 showed the magnitude of the suckdown which precluded low altitude hovering. This condition is unacceptable for a commercial VTOL transport. For complete IFR hover and landing operation, displays must be developed that provide additional situation information.

Low speed translation: Forward translation in hover can be accomplished by either modulating main engines nozzle deflection (figure 31(a)) or by changing pitch attitude (figure 31(b)). Modulating nozzle deflection was attractive, because little lift engine thrust change was necessary to maintain altitude Stopping on a desired spot was difficult, however, because it was hard to predict the decel ration from a given nozzle setting. Accurately and quickly selecting a nozzle position during the demanding task of maintaining altitude while maneuvering was also difficult due to the small size of the nozzle

position instrument. When pitch attitude was used for translating, large attitude changes were required when stopping and visibility was impaired. Even though the lift engine thrust had to be coordinated with attitude change to maintain altitude, the use of pitch attitude change as the primary means of translating for short distances was preferred over the nozzle modulation, since it did not require looking in the cockpit to monitor nozzle deflection. The pilots felt that if (1) the nozzle position were more clearly displayed and (2) the stabilization system had a height control feature, nozzle deflection modulation may be the preferred control for translating, particularly for longer distances.

Lateral maneuvering in hover is accomplished by changing roll attitude and tilting the thrust vector. Figure 27 presented a time history of a lateral translation. The maximum speed obtained during this test was 10 meters per second, which the NASA pilot considered to be the maximum lateral velocity normally required for a commercial VTOL transport of this size. The stabilization system reduces aircraft disturbances from the unusual wind conditions near the ground and allows the translation to be executed with low pilot workload.

Environmental effects at transition speeds: In the course of the test program a large range of environmental conditions was encountered. The wind speed ranged from 12 meters per second (24 knots) to calm, and the direction ranged from head wind to crosswind to tailwind. Light to moderate turbulence was encountered on several flights. In the preconversion mode (airspeeds greater than 140 knots) the aircraft was quite disturbed in the lateral-directional mode; however,

when the stabilization system was engaged and lift engines started, the aircraft was no longer affected by the turbulence and "it felt steady as a rock." It was gratifying to note that the aircraft was relatively unaffected by gusts, adverse winds and crosswinds. This result was somewhat surprising in view of the large sideforce due to sideslip (figure 23). Tests could not be conducted to isolate the factor that produced the favorable response in gusty air; it can only be surmised that the ability to maintain constant attitude contributed to the favorable ride characteristic. This is borne out by recent tests with an attitude command stabilization system in a light plane, reference 16.

In the approach it was found that crosswinds could not comfortably be compensated by a sideslipping approach because large bank angles were required. At 60 knots a 10 knot crosswind necessitated a 10° bank which not only was uncomfortable in terms of a high sideforce, but also because a lateral force had to be held by the pilot; consequently, the preferred method of compensating for crosswinds was to crab the aircraft. In decelerating approaches the heading can be slowly changed to keep sideslip near zero as the aircraft slows to a hover. With proper displays, the workload should not be too high. Thus, the crosswind problem does not appear to be as serious as with some STOL aircraft where it is necessary to abruptly decrab the aircraft before touchdown (reference 7).

Environmental effects at very low speeds: Figure 32 illustrates the effect of wind and sink rate on the main engine intake temperature rise during vertical landing. The landings with increased head wind

and greater sink rate generally resulted in less hot-gas reingestion. For comparison purposes, one short landing data point has been added to the vertical landing data. Along with sink rate and wind, it appears the immediate shut down of lift engines and reduction of thrust on main engines after touchdown is very important. Greater peak temperatures occur when the power plants continue to exhaust their hot gases after the landing impact is made. This landing procedure is added to the pilot workload during the final phase of the landing.

The techniques and procedures minimizing recirculation effects have been discussed, and the effect of wind on vertical takeoff recirculation and hot gas ingestion is presented in figure 33. It can be seen in figures 33 (a) and (c), that a 60 - 90° crosswind at takeoff considerably increases the main engine inlet temperature on the upwind side (20 - 25°C). The crosswind might be pushing the gas cloud from the lift engines on that side into the inlet of the main engine. The same effect can be seen with a lesser crosswind in figure 33 (d), the difference being a somewhat smaller increase in main engine inlet temperature. The vertical takeoff with a 6 kt. headwind, figure 33 (b), yields the smallest rise in inlet temperature.

Each main engine inlet on the airplane had only four temperature probes; they were located at the 12, 3, 6, and 9 o'clock positions, and the plots show the average of these. The limited number of temperature probes did not show temperature distortion across the engine inlets that can cause compressor stalls. It should be pointed out that no compressor stalls were encountered during the NASA evaluation.

Comparison of approaches: Figure 34 compares two 12° approaches and two 7° approaches with different lift engine starting conditions. This figure illustrates the reduction in time and noise footprint that can be realized by starting the lift engines on the glide slope. Less time is spent on the approach since the airspeed is kept at a high level during the first part of the approach, and the lift engines are started after glide slope acquisition. This figure also indicates a reduction of the noise footprint because the lift engines were started while tracking the glide slope. By starting the lift engines on the glide slope, the high noise level due to the lift engines is 2000 to 3000 meters closer to the landing site with an additional 150 meters of altitude during the starting cycle. Reference 17 gives some measured noise values for the DO 31. The approaches and landings took 2 - 3 minutes; these times are shorter than predicted in reference 16; however, they are longer than theoretically achievable based on the aircraft's performance.

Previous studies (reference 7 and 9) have reported that the descent rates in an ILS approach should be less than 5 meters per second (1000 feet per minutes) at altitudes below 100 meters (300 feet). The descent rates used during these tests were greater. Figure 35 is a graphical representation of the relationship between glide slope angle, airspeed, and rate of descent. Considering the DO 31 approach airspeed range from 120 kts at glide slope intercept, to 50 kts at flare on a 7° approach, the rate of descent varies from approximately 7 meters per second at the start of the approach to 3 meters per second at breakout. For the 12° approach, the rate of descent varies from

13 to 5 meters per second. The pilots considered the high rate of descent at the beginning of the approach to be no problem because (1) the rate of descent was decreasing as the aircraft was decelerating on schedule, (2) the attitude command control system allowed more attention to be devoted to approach performance parameters, and (3) there was a high confidence level that the aircraft could be flared to arrest the sink rate because sufficient altitude was allotted (70 meters).

The NASA pilots felt that approaches steeper than 12° were not practical with the DO 31 primarily because of the nose-down attitude. Referring to figure 15 (a) it can be seen that the time to flare the aircraft and to land took as long as the time to acquire and track the glide slope. It would be expected that attempts to reduce the landing time, e.g. by not flaring to zero vertical velocity at 70 meters, would make the rate of descent in the approach more critical and these high values might not be tolerated.

The close-in pattern presented in figure 36 represents the type of approach that may be required in a restricted area. The lift engines are started during the turn made to acquire the localizer. The altitude during the turn is held at the intercept altitude (450 meters), and the distance of the turn from the landing point was dictated by length of time required to bracket the localizer prior to glide slope intercept. After the localizer was captured, the rest of the approach is the same as those approaches where the lift engines are started in level flight on the localizer. The pilots considered this pattern to be feasible if the appropriate terminal-area navigation aids were available.

CONCLUDING REMARKS

A flight investigation was performed with the Dornier DO 31 VTOL transport to evaluate the performance, handling, and operating characteristics that are considered to be important when operating a commercial VTOL transport in the terminal area. The DO 31, a 20,000 kilogram transport, has a mixed jet propulsion system; i.e. there are main engines with nozzles that deflect from a cruise to a hover position, and vertical lift engines that operate below 170 knots. In this VTOL mode pitch and roll attitude and yaw rate stabilization are incorporated, and the main and lift engines are used to augment the forces and moments. The tests concentrated on the transition, approach and vertical landing.

The flight tests showed that this mixed jet-propulsion system provided a large useable performance envelope which enabled a broad range of simulated IFR approaches to be made. Glide slopes of 7° and 12° were intercepted at 140 knots and tracked while decelerating to 50 knots and a breakout altitude of 70 meters; the transition to hover and a vertical landing had to be made visually because displays were lacking. The aircraft could be easily converted to the VTOL mode either before or after the glide slope was intercepted. Once the glide slope was acquired, it was easy to track because corrections could be made normal and parallel to the flight path (via lift engine thrust and main engine nozzle deflection, respectively), during which time the stabilization system maintained attitude. The pilots reported that the normal acceleration available from the lift engines ($\pm$0.1g) was insufficient for flight path control. Controlling the flight path by

pitching the aircraft was unsatisfactory because of the changing control power and lift in the decelerating approach, and also because of the large unwanted airspeed changes at the lower airspeeds.

During the transition and approach, the pilot's prime job was power management (control of thrust magnitude and direction); there were too many discrete changes in attitude, lift and main engine throttle, and main engine nozzle deflections. Most of the approaches were made with the fuselage attitude nearly parallel to the flight path. This simplified the pilot's power management problem. When the ILS was tracked with a more level fuselage attitude, the workload increased and the performance deteriorated. It was found that the current criteria for flight path control are inadequate because they do not consider the aircraft response after a period of time, and they do not define limitations to the crosscoupling. Further research is required to integrate the different longitudinal controls to simplify power management, and to define appropriate criteria.

Several other observations were made pertaining to the transition and approach mode. First, when maneuvering laterally at transition speeds, the roll attitude stabilization (combined with yaw rate command) created problems, and turn coordination should be provided. When not maneuvering, the heading hold feature of the yaw rate stabilization greatly assisted in maintaining the aircraft track. Second, with the stabilization system engaged and lift engines operating the aircraft was relatively unaffected by turbulence. Finally, crosswinds in the approach were easily compensated by the "crab" maneuver; a "sideslipped" approach was unsatisfactory.

In hover, the lateral control power (0.8 radians per second squared), sensitivity, attitude stability and damping were satisfactory. The results are in agreement with previously reported NASA simulation studies. The pilots felt that attitude stabilization is mandatory for satisfactory VTOL operation. A sudden failure to an acceleration system in the VTOL mode would be unacceptable. The vertical landing was unacceptable because of the recirculation effects below 15 meters and because of insufficient height control.

When the complete terminal area operation was considered, the time in the VTOL mode was shorter than observed in other IFR flight studies. An ILS approach, starting with intercepting the localizer beam at 140 knots and ending in a vertical landing, could be completed in less than 3 minutes. The pilot needed 20 to 30 seconds to track the localizer; 60 to 90 seconds to acquire the glide slope, start the lift engines, and track and decelerate to 50 knots at the breakout altitude (70 meters); and 45 to 60 seconds to hover and make the vertical landing. In a vertical takeoff the aircraft has a high acceleration and a steep climbout. In just over 20 seconds the aircraft attained 120 knots, a sufficient airspeed to shut off the lift engines.

APPENDIX A

COMPUTATION OF DATA PERTAINING TO FLIGHT-PATH DEVIATIONS

In order to relate the pilot comments on flight-path control with the aircraft characteristics and motion, it is necessary to realize the significant difference between the change in aircraft flight-path angle, $\Delta\gamma$, and the glideslope error displayed to the pilot, ε_G. This is schematically illustrated in figure A1 and additional comments follow to describe the computations that were made for the figures illustrating flight-path control in the body of the report. During ILS tracking, the pilot's reference is the ILS beam which is ground based, set at the desired flight path, γ_G, and his position information is in the form of deviation from the centerline of the ILS glideslope beam, ε_G, displayed on the ADI. When the pilot makes a correction with a control input, a normal acceleration is produced which integrates into a flight-path change, $\Delta\gamma$, which is <u>not</u> directly related to ε_G. The $\Delta\varepsilon_G$ is a function of the change in altitude which is an integration of $\Delta\gamma$ (hence a second integration of normal acceleration). The integration of the longitudinal acceleration produces a change in velocity that may or may not be desired by the pilot. In a constant speed approach, these perturbations can be observed by the pilot as a change in rate of climb and a change in airspeed. For the decelerating approaches of the

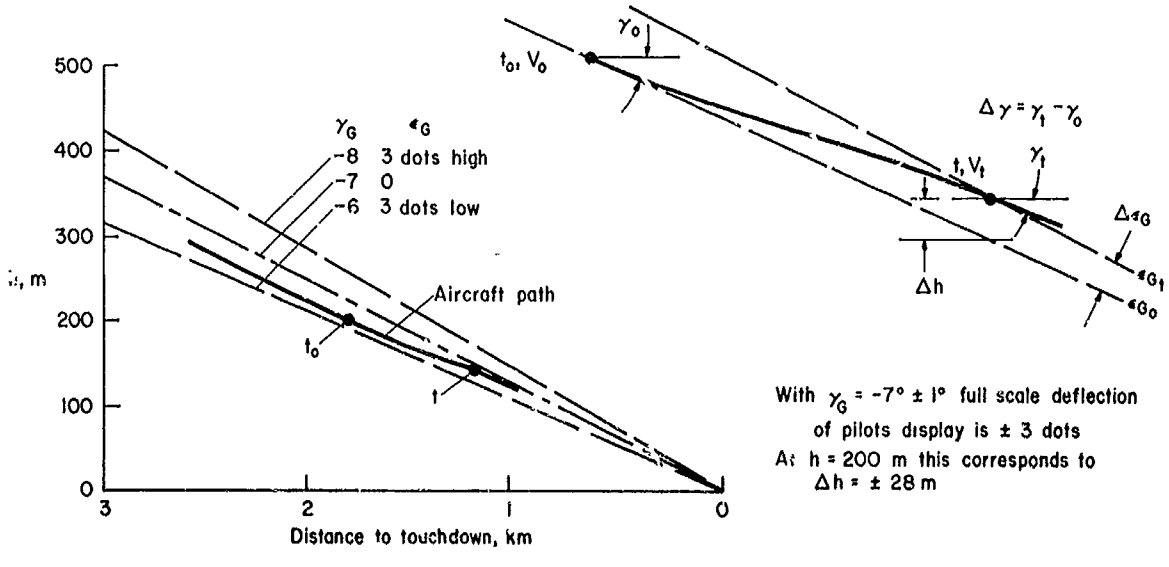

Figure A-1.- Flight path relations

present tests, the perturbations are obscured in the situation information (ADI) displayed to the pilot. In addition, these changes are also more difficult to measure by normal flight-test techniques. It was found that the radar data of the aircraft's position was not accurate enough to determine the changes in flight path produced by control inputs, and it was necessary to integrate the aircraft accelerometers.

First, an analysis will be made for the simple case where the aircraft is stabilized in pitch, the angle of attack is near zero, the initial flight path is -7°, and the aircraft is decelerating. For this case $\cos \theta = \cos \gamma \approx 1$.

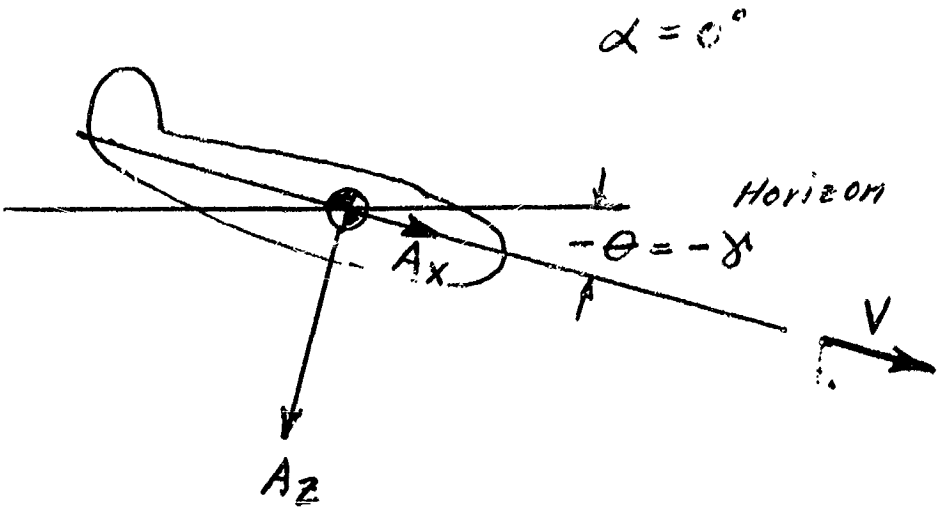

The perturbation of the aircraft to a control input is obtained by using the observed normal and longitudinal accelerometer readings (A_Z and A_X) minus the initial reference conditions to obtain the

incremental values, $\frac{\Delta a_z}{g}$ and $\frac{\Delta a_x}{g}$. For these decelerating approaches, it is assumed that the initial accelerations would have existed if no control input had been applied during the 10-second period of the integration. In figures 17 and 18, the ordinate of normal acceleration is inverted to have the direction of the curve in the sense of the aircraft motion. The change in vertical velocity is now obtained by $\Delta w = \int \Delta a_z dt$. Then $\Delta\alpha = -\frac{\Delta v_z}{V} \times 57.3$, and since the attitude is fixed, the change in flight path, $\Delta\gamma$, is equal to $\Delta\alpha$. This is also presented on the figures in comparison to the observed angle-of-attack changes; recognizing the poor quality of angle-of-attack information at the low speeds the agreement is reasonable. Conversely, it can be seen why it would be difficult to use the angle-of-attack information to compute flight-path changes. Next, the change in altitude is obtained by a second integration of normal acceleration; i.e., $\Delta h = \int\int -\Delta a_z dt^2$. For comparison, the change in altitude that corresponds to a 1-dot glideslope change (ε_G) at 200 meters altitude is shown for a glideslope of -7° with a beam width of ±1°. The change in velocity, Δv_x, is obtained as $\Delta v_x = \int \Delta a_x dt$; it should be noted that this does not correspond to the change in velocity that would be observed on the airspeed meter because the initial condition of the aircraft is decelerating flight, and Δv_x represents the perturbation due to control input only.

For the case where the flight-path change due to pitching the aircraft is evaluated, the computations are similar; however, the accelerations are transformed to earth-fixed axes before computations are performed. Since the cos $\theta \approx 1$, change in acceleration is retained in the form of $\frac{\Delta a_z}{g}$ to be more easily compared with the data at constant attitude. The change in longitudinal acceleration (along the flight path) is given as $\frac{\Delta\ dv/dt}{g}$. Because of the changing attitude and angle of attack, $\Delta\gamma$ is presented in lieu of Δv_z.

It should be noted that the previous derivations are only approximate, but are sufficiently accurate to assess the initial motions of the aircraft to relate aircraft characteristics and pilot comments.

APPENDIX B

MISCELLANEOUS ENGINE AND CONTROL RELATIONS

Thrust and fuel flow.- The thrust and fuel flow characteristics of one main and one lift engine are given in figure 37. The relations between throttle position and engine speed were presented in figure 5.

Control deflections.- The variation of the VTOL control deflection and of the conventional surface deflection with the pilot control are given in figures 38 to 40. Also included are the maximum hover control power about each axis for a nominal hover configuration. Since the conventional surfaces are simultaneously deflected with the VTOL control, the control power increases with forward speed. In the conventional flight regime above 155 knots, a gear changer reduces the surface deflection per unit of pilot control to maintain a better stick force per unit acceleration. The reduction in control surface deflection is illustrated in part (b) of these figures by the reduction in the maximum surface deflection with increased dynamic pressure. For each axis, the maximum deflection of the stabilization system actuator is 40°.

REFERENCES

1. Fry, Bernard L.; and Zabinsky, Joseph M.: Feasibility of V/STOL Concepts for Short-haul Transport Aircraft. NASA CR-743, 1967.

2. Marsh, K. R.: Study on the Feasibility of V/STOL Concepts for Short-Haul Transport Aircraft. NASA CR-670, 1967.

3. Anon.: Study on the Feasibility of V/STOL Concepts for Short-Haul Transport Aircraft. NASA CR-902, 1967.

4. Anon.: STOL-V/STOL City Center Transport Aircraft Study. McDonnell Aircraft Corporation, FAA-ADS-26, Oct. 1964.

5. Waldo, Richard K.; and Filton, Peter D.: An Economic Analysis of Commercial VTOL and STOL Transport Aircraft. Stanford Research Institute, FAA-ADS-25, Feb. 1965.

6. Kelley, Henry L. and Champine, Robert A.; Flight Investigation of a Tilt-Wing VTOL Aircraft in the Terminal Area Under Simulated Instrument Conditions. AIAA Paper No. 71-7, Jan. 1971.

7. Innis, Robert C.; Holzhauser, Curt A.; and Quigley, Hugh C.: Airworthiness Considerations for STOL Aircraft. NASA TN D-6094, 1970.

8. Smith, Charles C. Jr.; and Parlett, Lysle P.: Flight Tests of a 0.13-Scale Model of a Vectored - Thrust Jet VTOL Transport Airplane. NASA TN D-2285, 1964.

9. Garren, John F.; Kelly, James R.; and Reeder, John P.: A Visual Flight Investigation of Hovering and Low-Speed VTOL Control Requirements. NASA TN D-2788, 1965.

10. Greif, Richard K.; Fry, Emmett B.; Gossett, Terrence D.; and Gerdes, Ronald M.: Simulator Investigations of Various Control Systems for VTOL Aircraft. NASA SP-116, 1966.

11. Anderson, Seth B.: Considerations for Revision of V/STOL Handling Qualities Criteria. NASA SP-116, 1966.

12. Anon.: V/STOL Handling, I-Criteria and Discussion. AGARD Rep. 577, 1970.

13. Rolls, L. Stewart; and Gerdes, Ronald M.: Flight Evaluation of Tip Turbine-Driven Fans for Lateral Control and a Hovering VTOL Aircraft. NASA TN D-5491, 1969.

14. Kelly, James R.; Garren, John F.; and Deal, Perry L.: Flight Investigation of V/STOL Height-Control Requirements for Hovering and Low-Speed Flight under Visual Conditions. NASA TN D-3977, 1967.

15. Reeder, John P.: The Impact of V/STOL Aircraft on Instrument Weather Operations. NASA TN D-2702, 1965.

16. Loscke, Paul C.; Barber, Marvin G.; Jarvis, Calvin R.; and Enevoldsen, Einar E.: Handling Qualities of Lift Aircraft with Advanced Control Systems and Displays. NASA Aircraft Safety and Operating Problems NASA SP 270, May 4-6, 1971.

17. Flemming, M.; and Schotten, R. (Dornier GmbH): Noise Problems of VTOL with Particular Reference to t. Dornier DO-31. Royal Aeronautical Journal, August 1969.

TABLE I

AIRCRAFT DIMENSION AND DESIGN DATA

General:

Length, m, (ft.)	20.60 (67.6)
Height to top of vertical fin, m, (ft.)	8.53 (28.0)

Wing:

Area, m^2, ($ft.^2$)	57.0 (613)
Span, m, (ft.)	17.0 (55.8)
Mean aerodynamic chord, m, (ft.)	3.415 (11.2)
Aspect Ratio	5.05
Sweep, deg	8.5
Airfoil section, root	NACA 64(A412)-412.5
Airfoil section, tip	NACA 64(A412)-410
Incidence angle, deg	2
Dihedral angle, deg	1.5
Taper ratio, deg	0.615
Flap deflection (max), deg	45
Flap area, m^2, ($ft.^2$)	6.64 (71.4)
Flap chord, m, (ft.)	0.85 (2.8)
Aileron deflection, deg	$\pm$25

Horizontal Tail:

Area, m^2, ($ft.^2$)	16.4 (176)
Span, m, (ft.)	8.0 (26.2)
Mean aerodynamic chord, m, (ft.)	2.13 (7.0)
Airfoil section	NACA-63A-010
Aspect ratio	3.9
Elevator Deflection, deg	$\pm$25

TABLE I. - Continued

Vertical Tail:	
Total area, m^2, ($ft.^2$)	15.4 (166)
Span, m, (ft.)	4.4 (14.4)
Mean aerodynamic chord, m, (ft.)	3.61 (11.8)
Airfoil section	NACA-63A-010
Rudder area, m^2, ($ft.^2$)	5.59 (60)
Rudder deflection, deg	± 30
Mass:	
Maximum conventional takeoff, kg, (lb. mass)	24,500 (53,900)
Maximum vertical takeoff, kg, (lb. mass)	21,800 (48,000)
Standard empty, kg, (lb. mass)	16,594 (34,300)
Weight:	
Maximum vertical takeoff, newtons (lb. force)	213,000 (48,000)
Moment of Inertia for 20,500 kg mass (45,000 lb. mass) and gear down:	
I_{xx}, kgm^2, ($slug\text{-}ft.^2$)	385,000 (284,000)
I_{yy}, kgm^2, ($slug\text{-}ft.^2$)	277,000 (205,000)
I_{zz}, kgm^2, ($slug\text{-}ft.^2$)	606,000 (447,000)
Center of Gravity:	
Percent of mean aerodynamic chord	23.0

TABLE I. - Concluded

Propulsion System:

Main engine, 2 installed

Rolls Royce Pegasus 5-2 turbofan

Maximum thrust per engine at S. L. S. for 2 1/2 minutes

newton (lb. force) 67,200 (15,100)

Emergency thrust per engine at S. L. S.

newton (lb. force) 76,000 (17,200)

Weight, per engine, with nozzles

newton (lb. force) 16,000 (3,500)

Lift engine, 8 installed

Rolls Royce RB-162-4D lift jet

Maximum thrust per engine at S. L. S.

newton (lb. force) 18,700 (4,200)

Emergency thrust per engine at S. L. S.

newton (lb. force) 19,600 (4,400)

Weight, per engine, with yaw nozzle

newton (lb. force) 1,570 (350)

Total maximum thrust at S. L. S.

newton (lb. force) 285,000 (64,000)

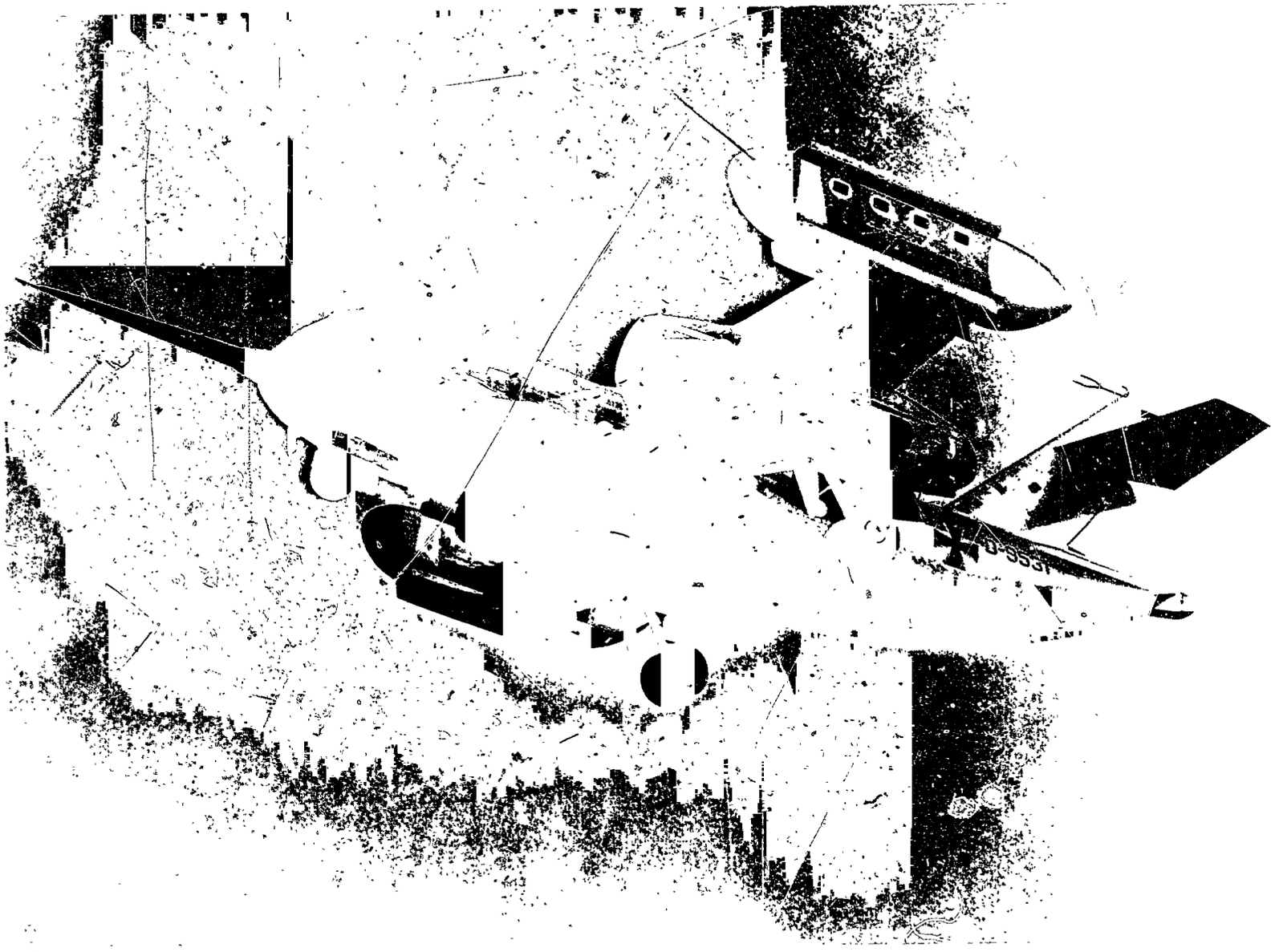

a) In VTOL mode.

Figure 1.- The test aircraft, Dornier DO 31 E-3.

NATIONAL AERONAUTICS AND SPACE ADMINISTRATION
AMES RESEARCH CENTER, MOFFETT FIELD, CALIFORNIA

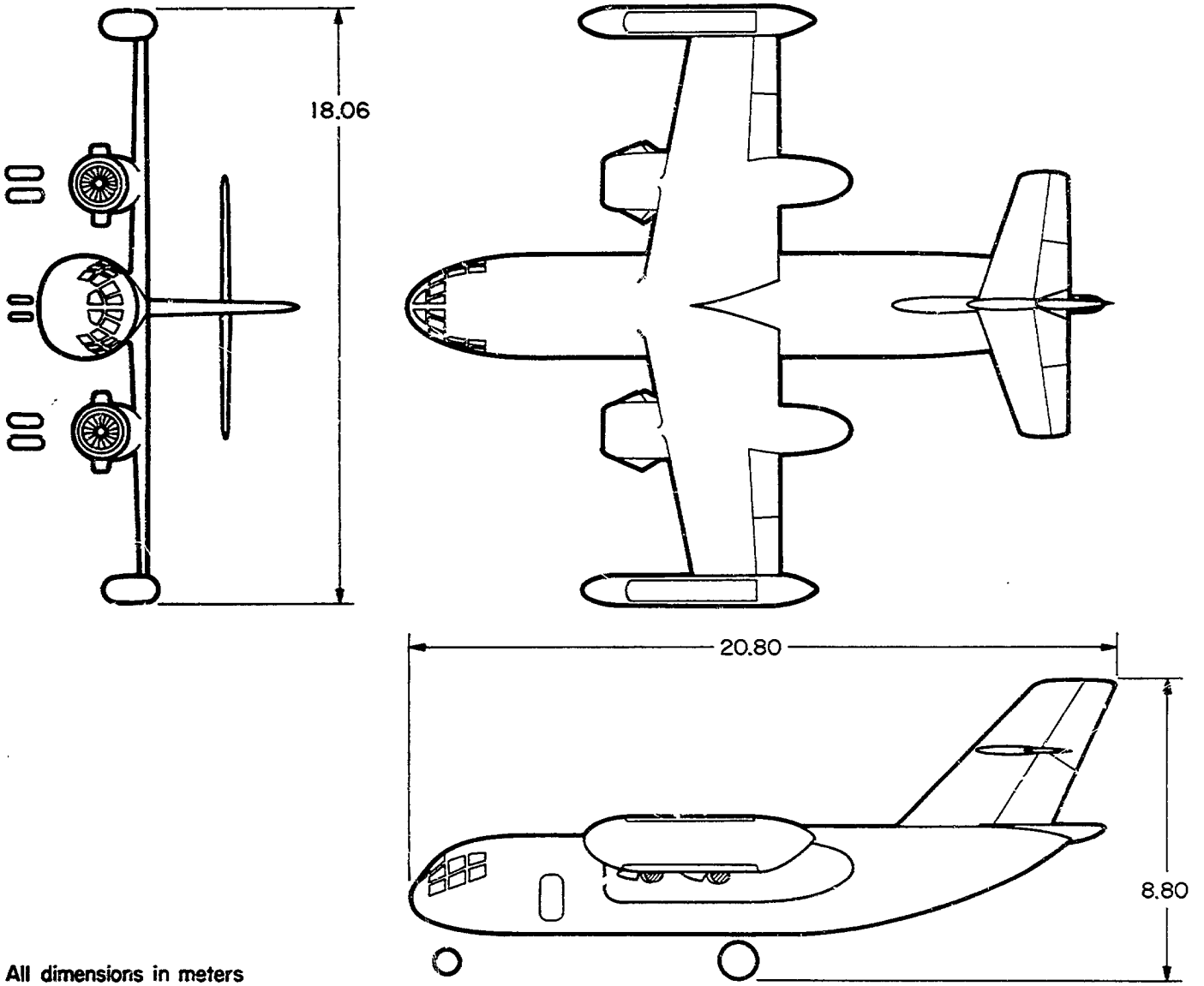

(b) Three-view sketch in conventional mode

Figure 1.- Concluded.

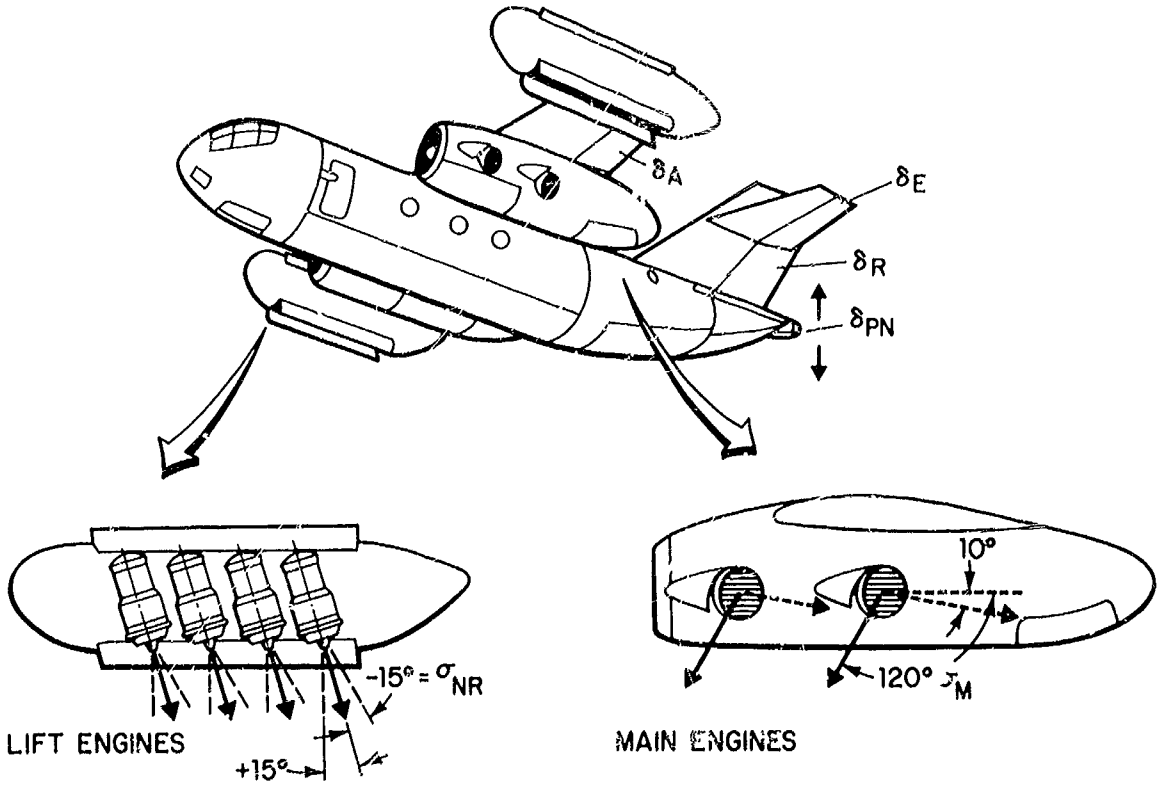

Rotation:

1. Longitudinal stick, δ_{MP}, controls elevator (δ_E) and pitch nozzle (δ_{PN})
2. Lateral stick, δ_{LP}, controls ailerons (δ_A) and differential thrust of lift engines ($FCU_L - FCU_R$)
3. Rudder pedal, δ_{NP}, controls rudder (δ_R) and differential lift engine nozzle deflection ($\sigma_{NL} + \sigma_{NR}$)

Translation:

1. One lift engine throttle, σ_{FCU}, controls thrust of lift engines collectively
2. Two main engine throttles, σ_{TL} and σ_{TR}, control thrust of each main engine
3. One main engine nozzle lever, σ_M, controls deflection of all main engine nozzles collectively

Figure 2.- Schematic of control functions.

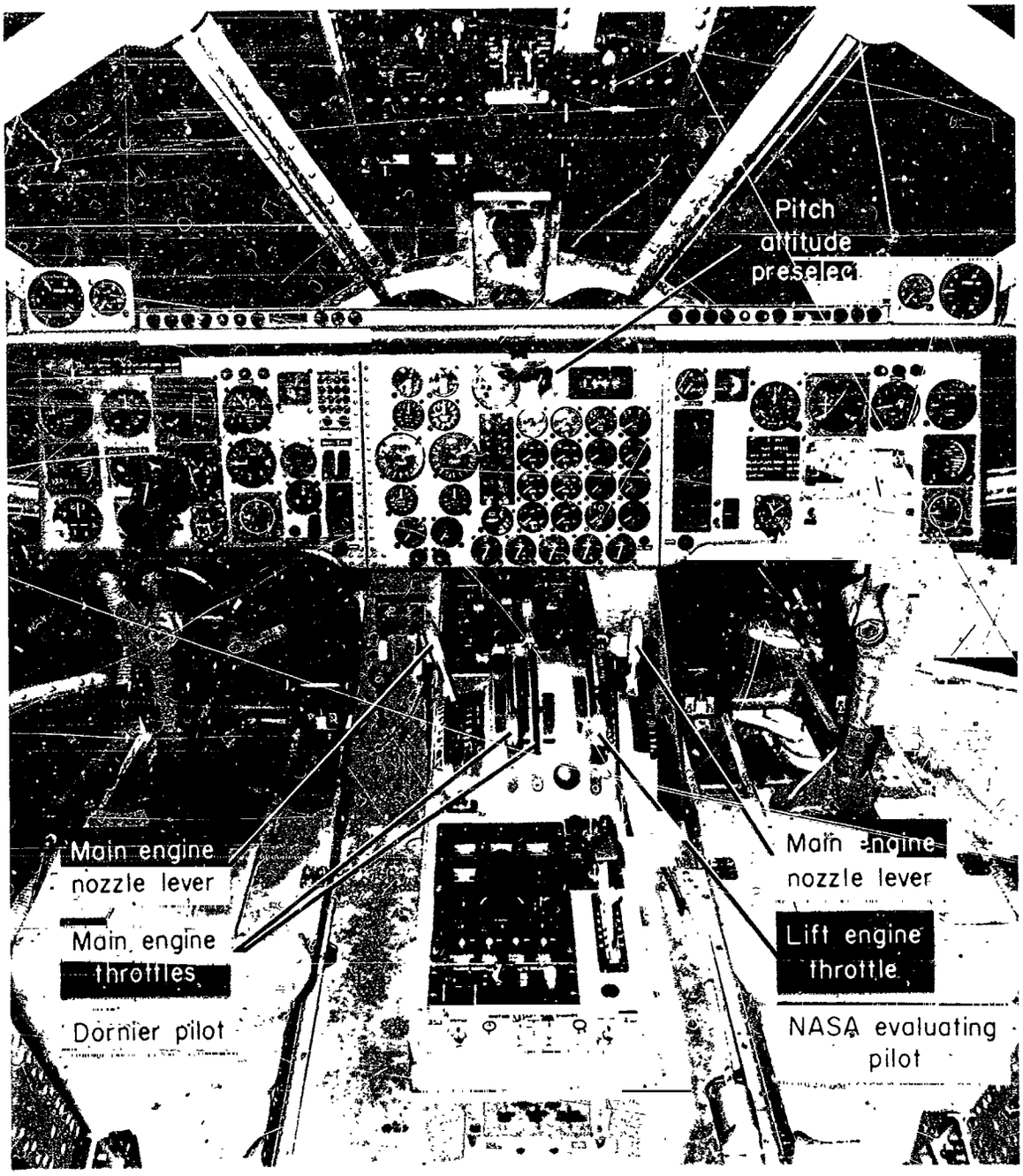

a) Control layout.

Figure 3.- Cockpit control and display layout.

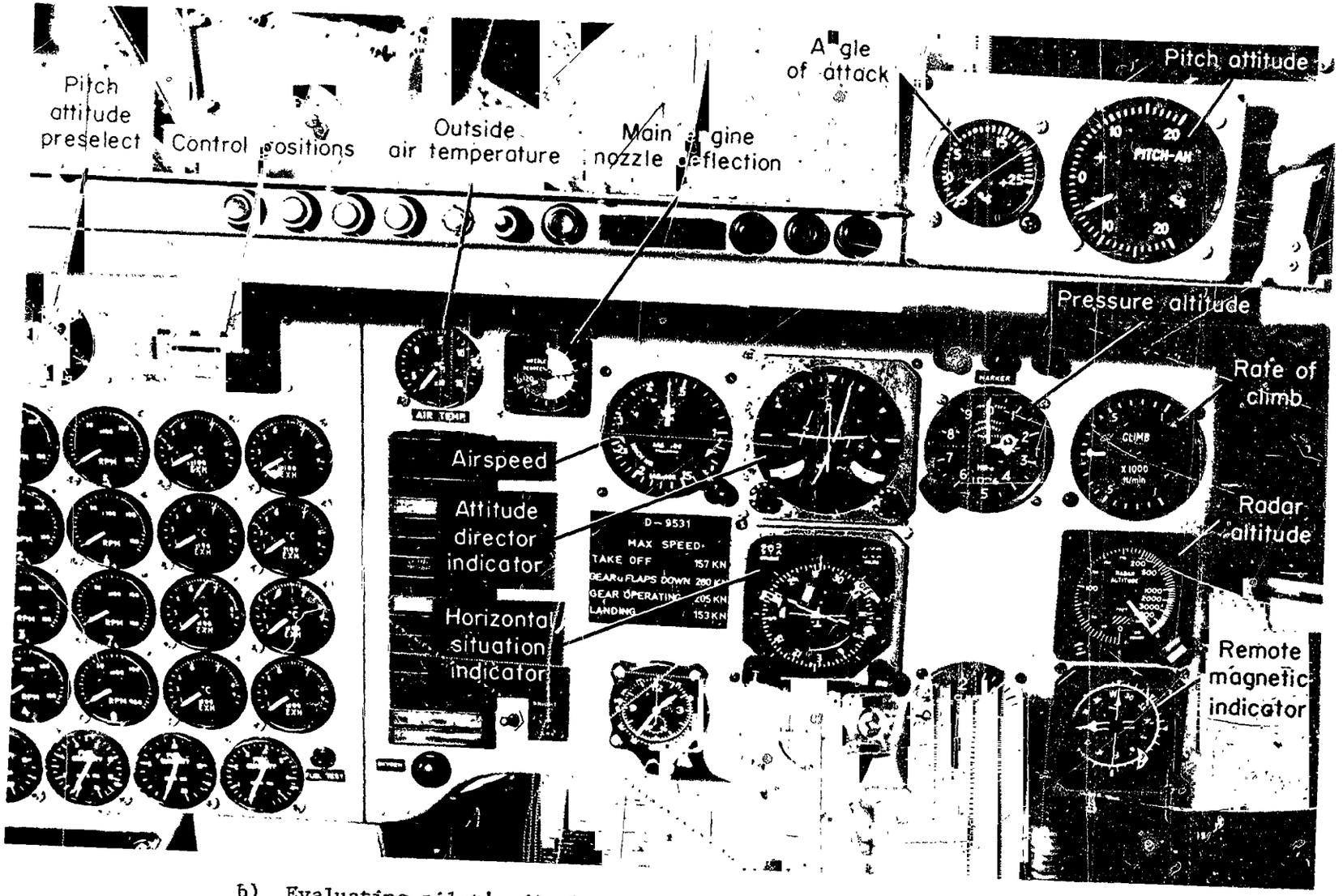

b) Evaluating pilot's display.

Figure 3.- Concluded.

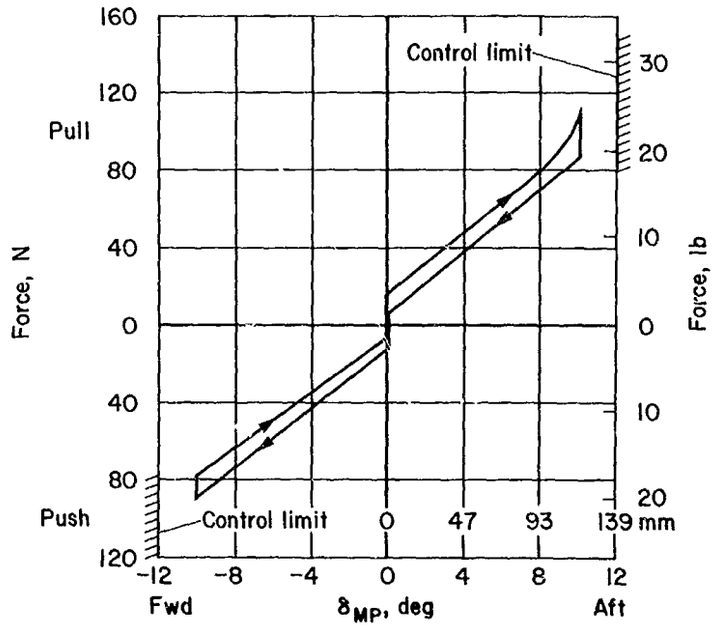

(a) Longitudinal control

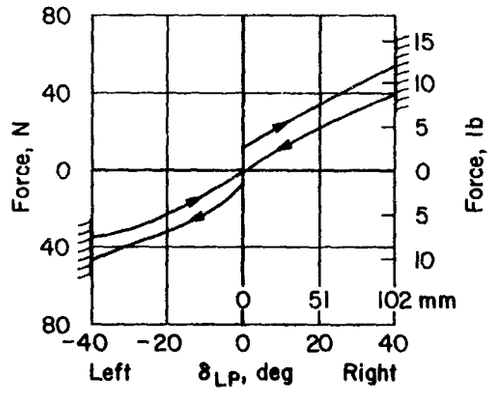

(b) Lateral control

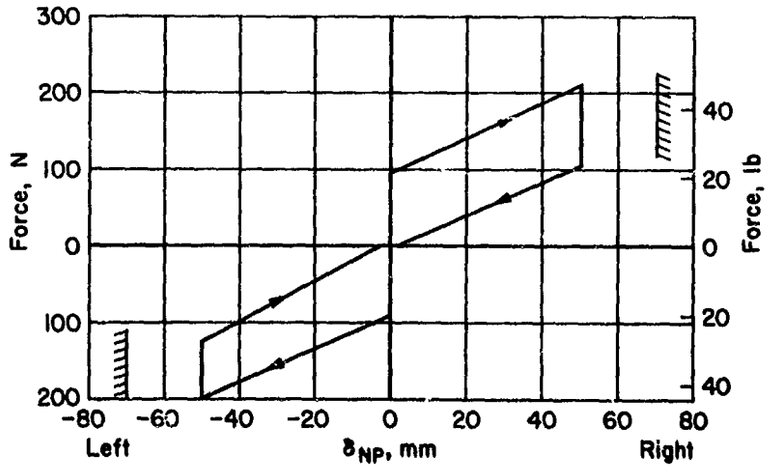

(c) Directional control

Figure 4.- Pilot control force-deflection relations.

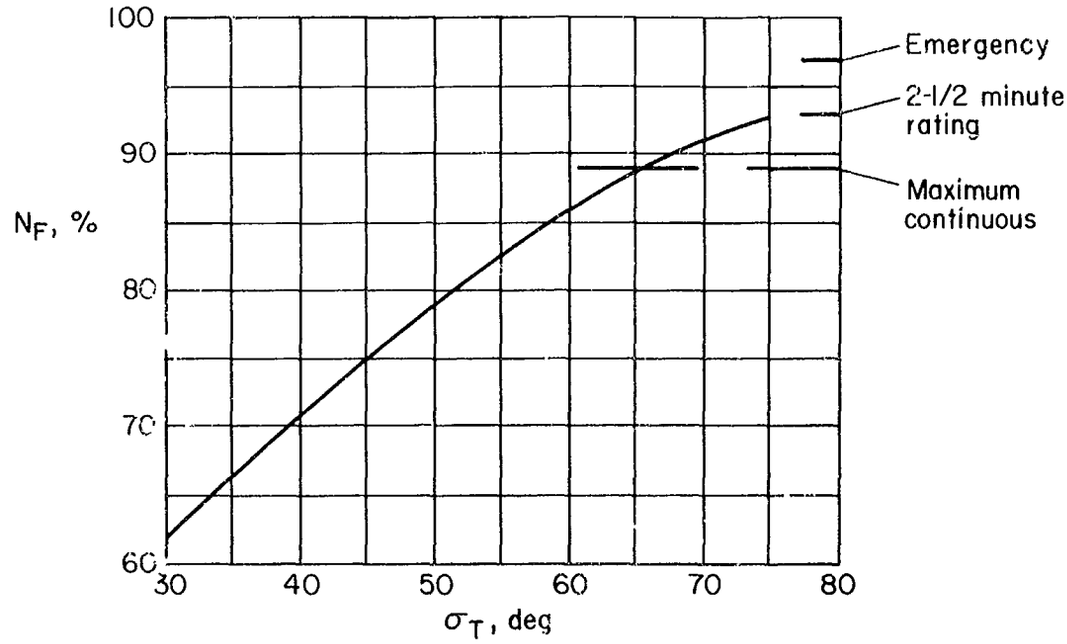

(a) Main engine throttle, length of lever = 220 mm

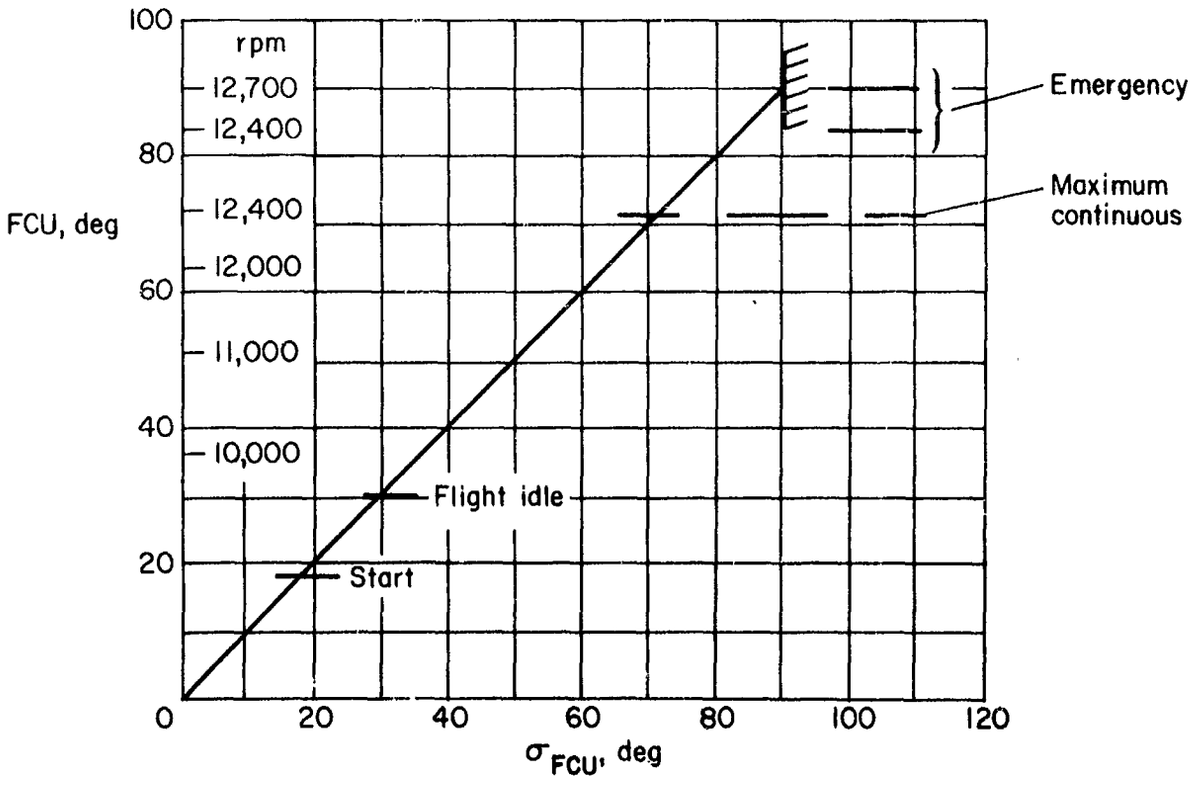

(b) Lift engine throttle, length of lever = 240 mm

Figure 5.- Throttle relations.

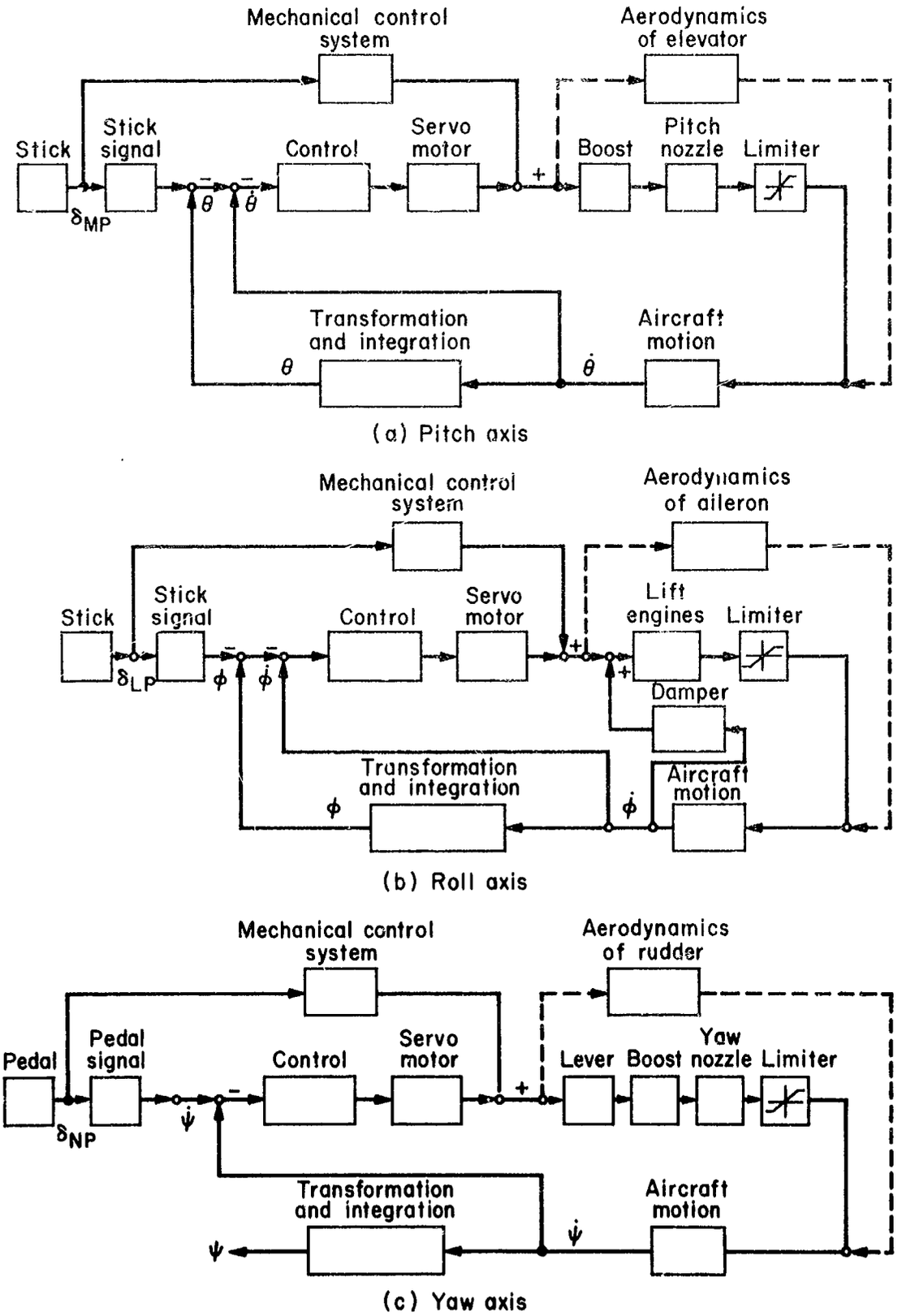

Figure 6.- Block diagram of stabilization and control system; VTOL mode.

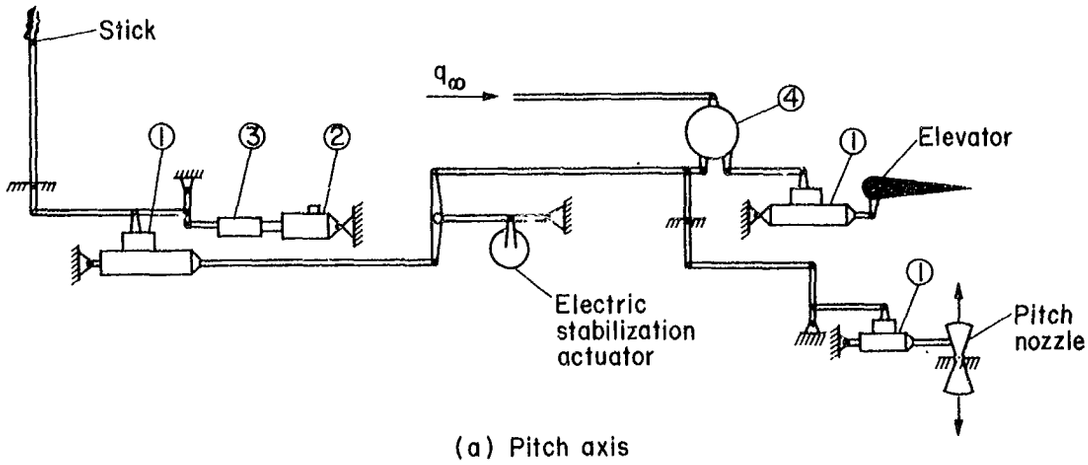

(a) Pitch axis

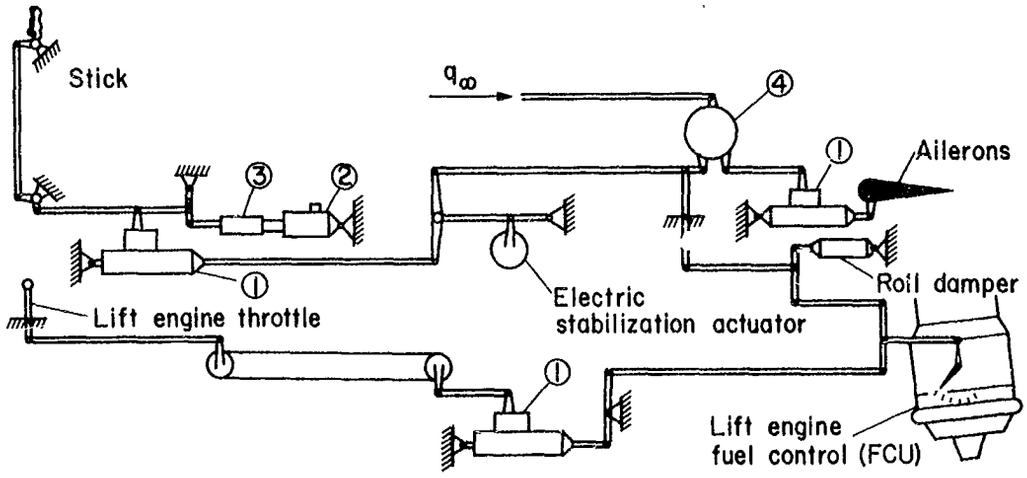

(b) Roll axis

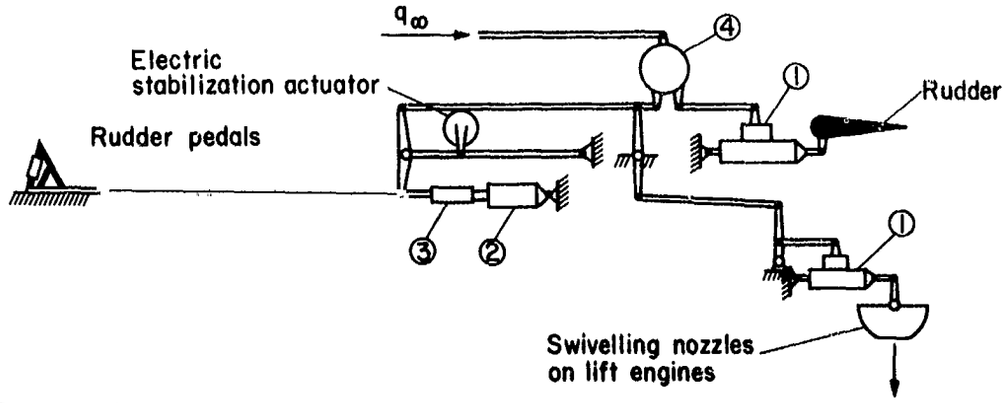

① Hydraulic actuator
② Trim motor in cruise configuration
③ Centering spring
④ Gearchanger, a function of dynamic pressure

(c) Yaw axis

Figure 7.- Schematic of control system.

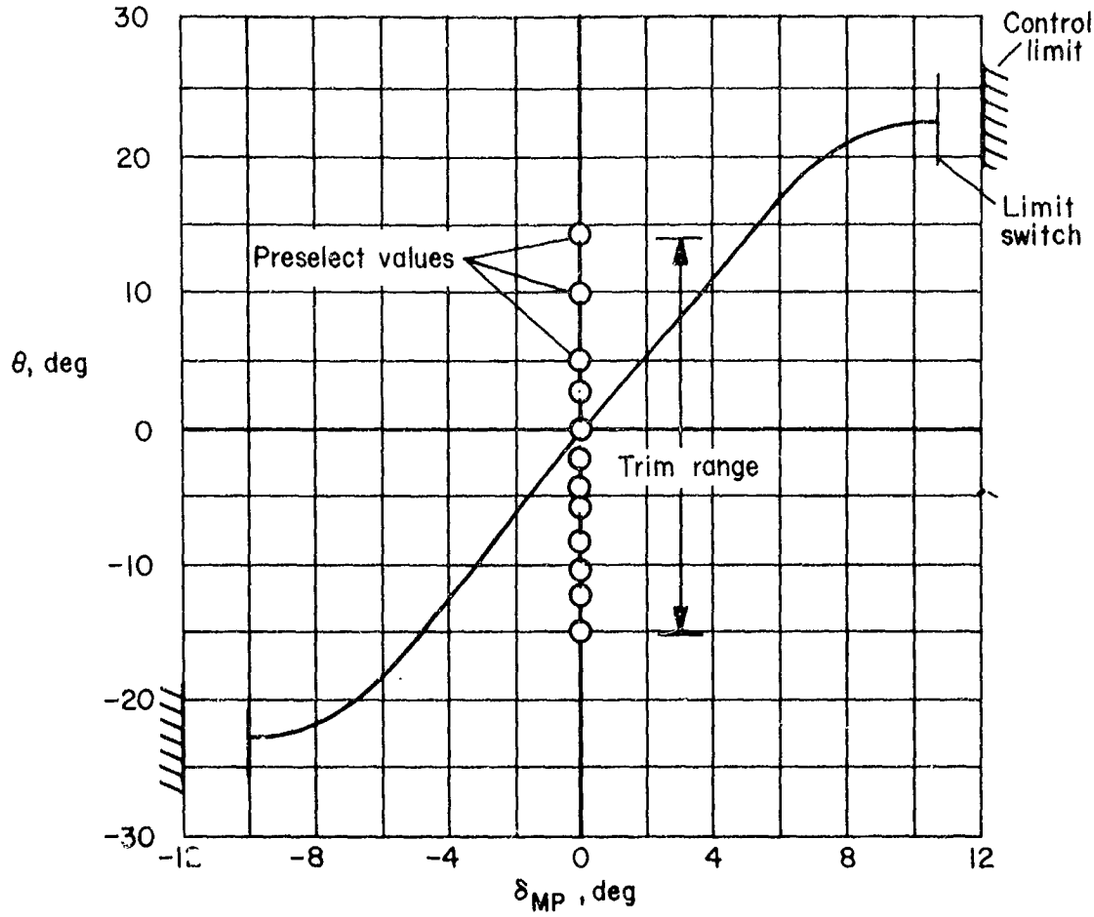

(a) Pitch

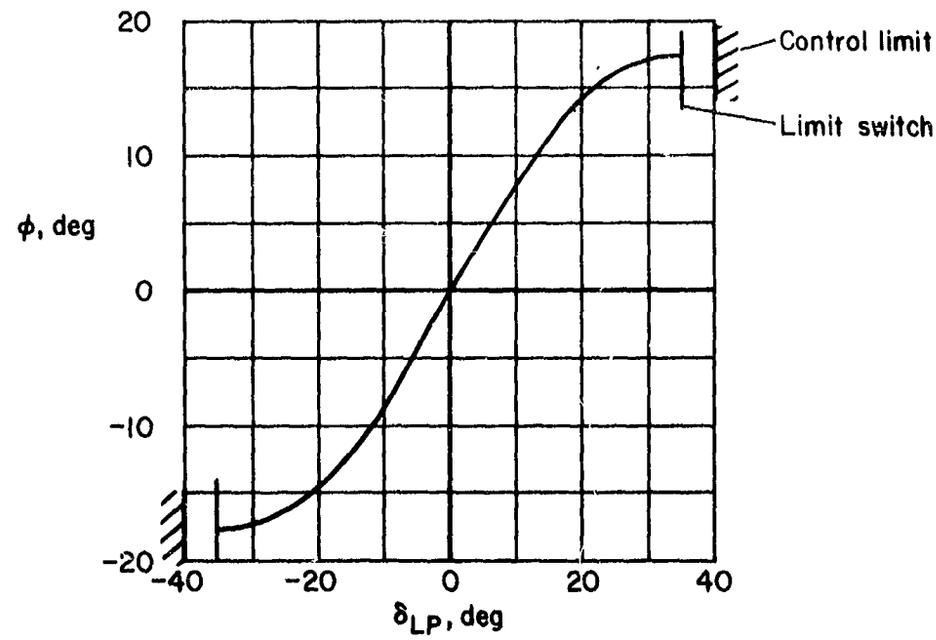

(b) Roll

Figure 8.- Steady-state conditions commanded by pilot control position; VTOL mode.

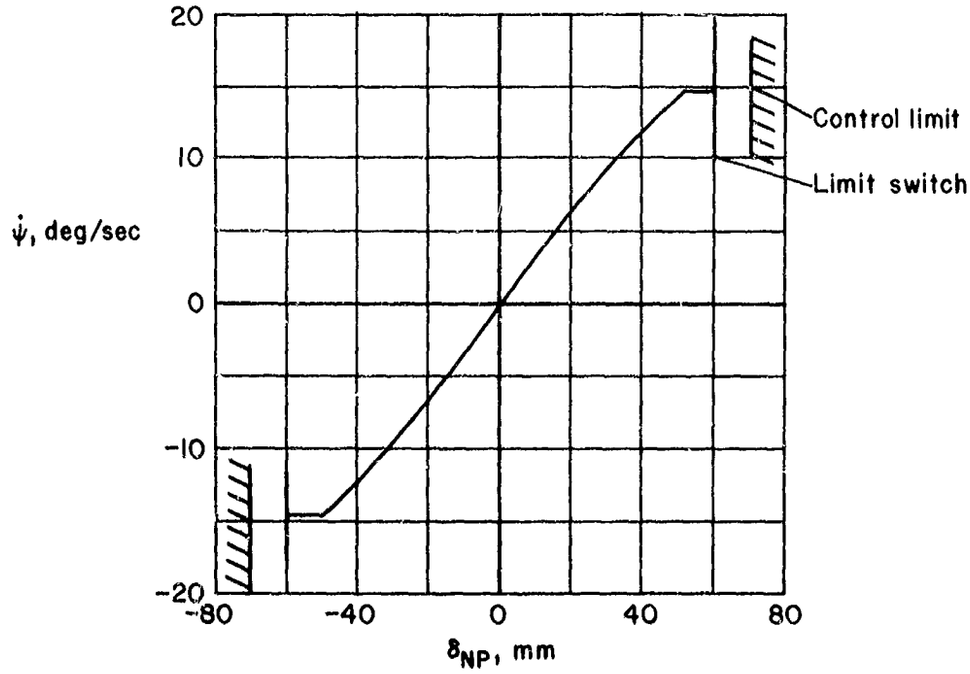

(c) Yaw

Figure 8.- Concluded.

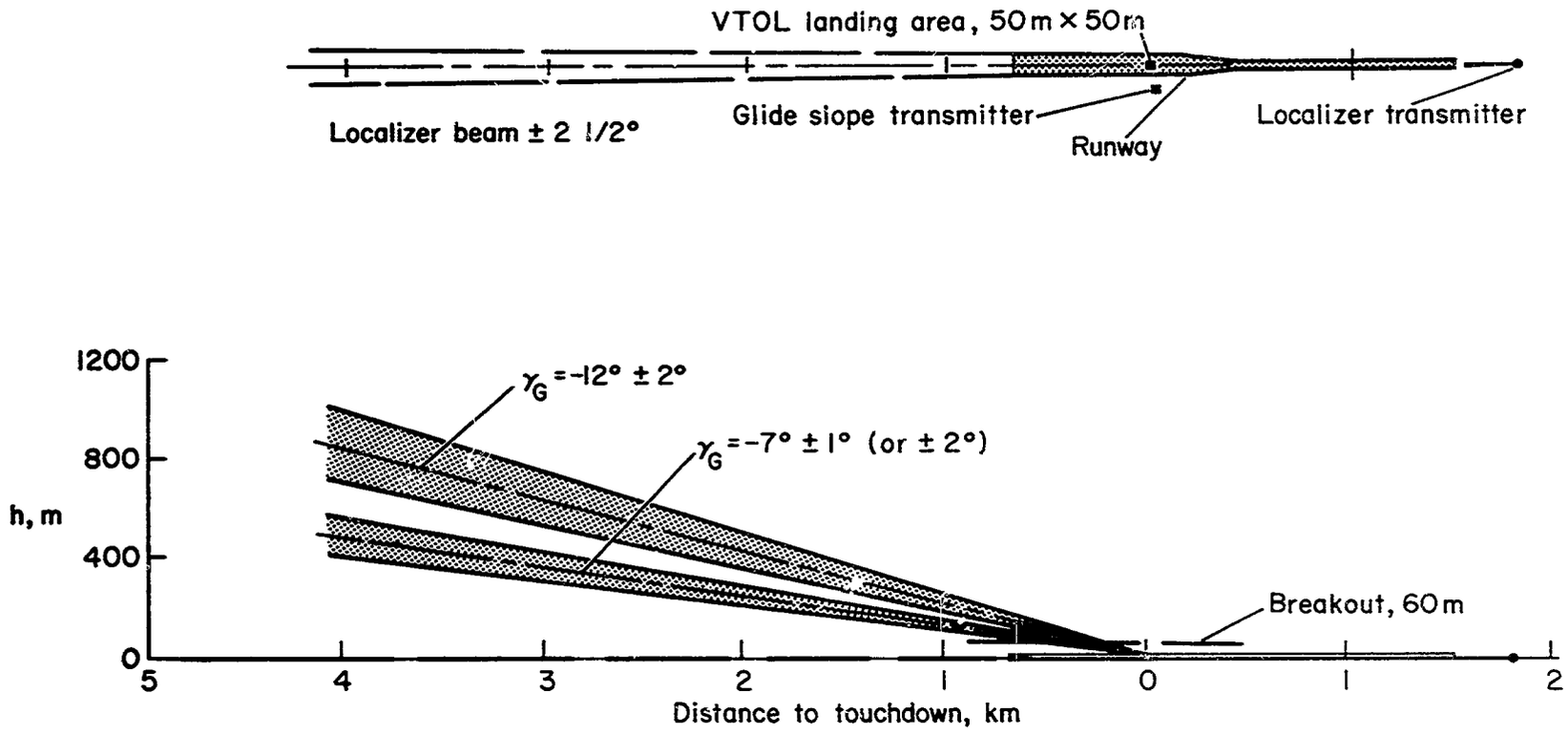

Figure 9.- Runway and guidance characteristics.

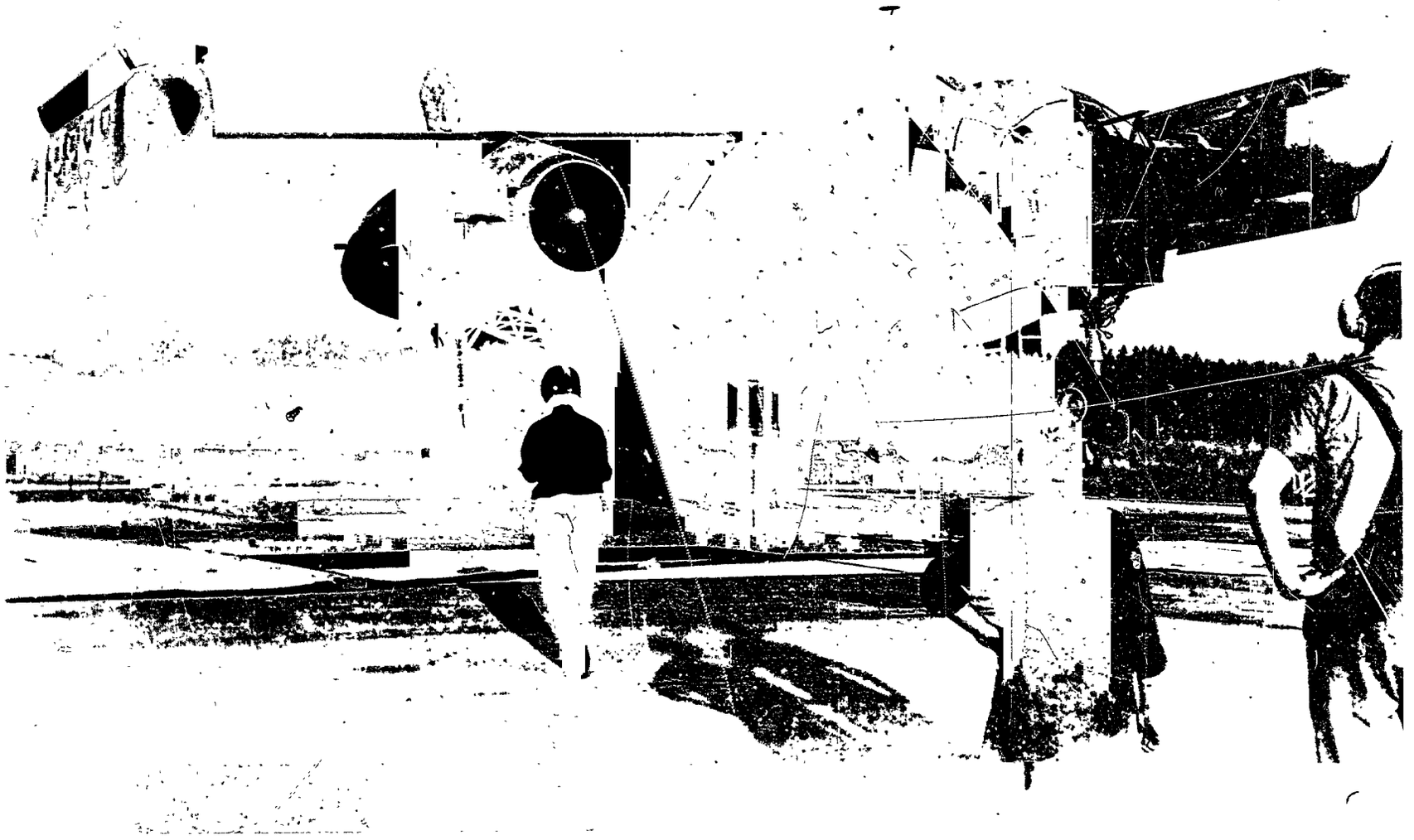

Figure 10.- Hover rig on pedestal.

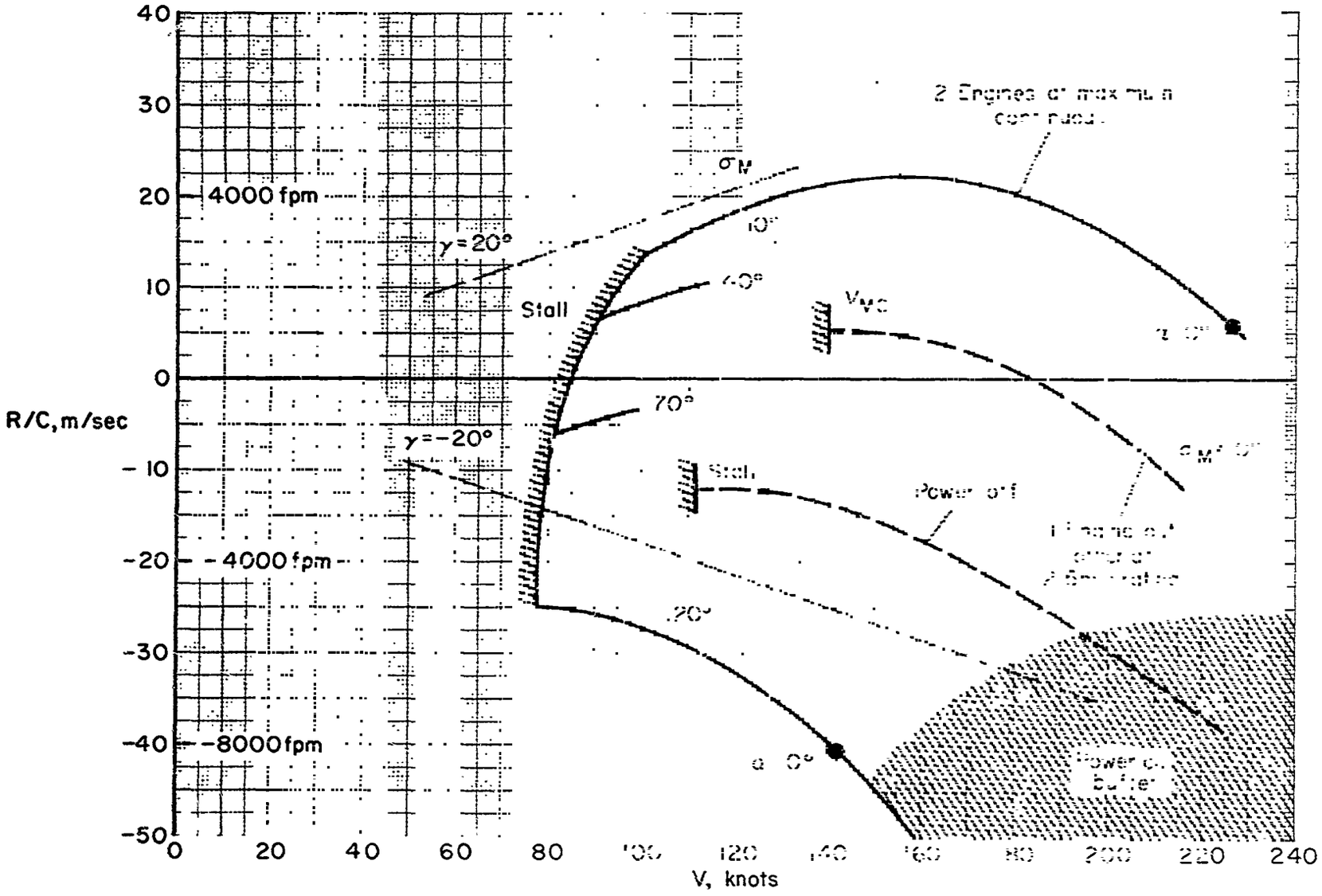

(a) Conventional mode, 2 engines operating, except as noted

Figure 11.- Low-speed characteristics with 45° flaps and gear down; $\frac{dv}{dt} = 0$, m = 19,500 kg, h = 1,000 m, ISA.

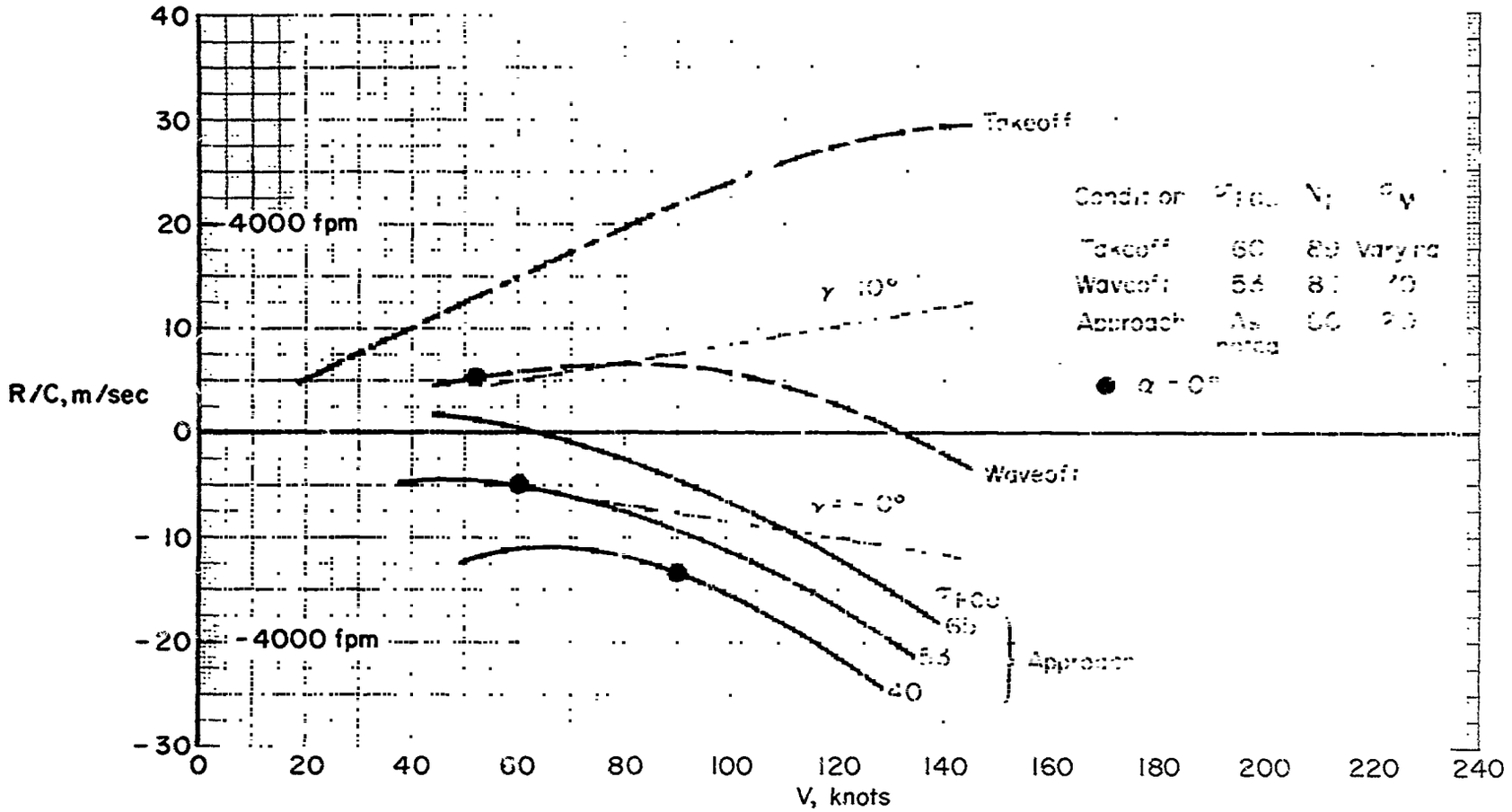

(b) VTOL mode, all engines operating

Figure 11 - concluded

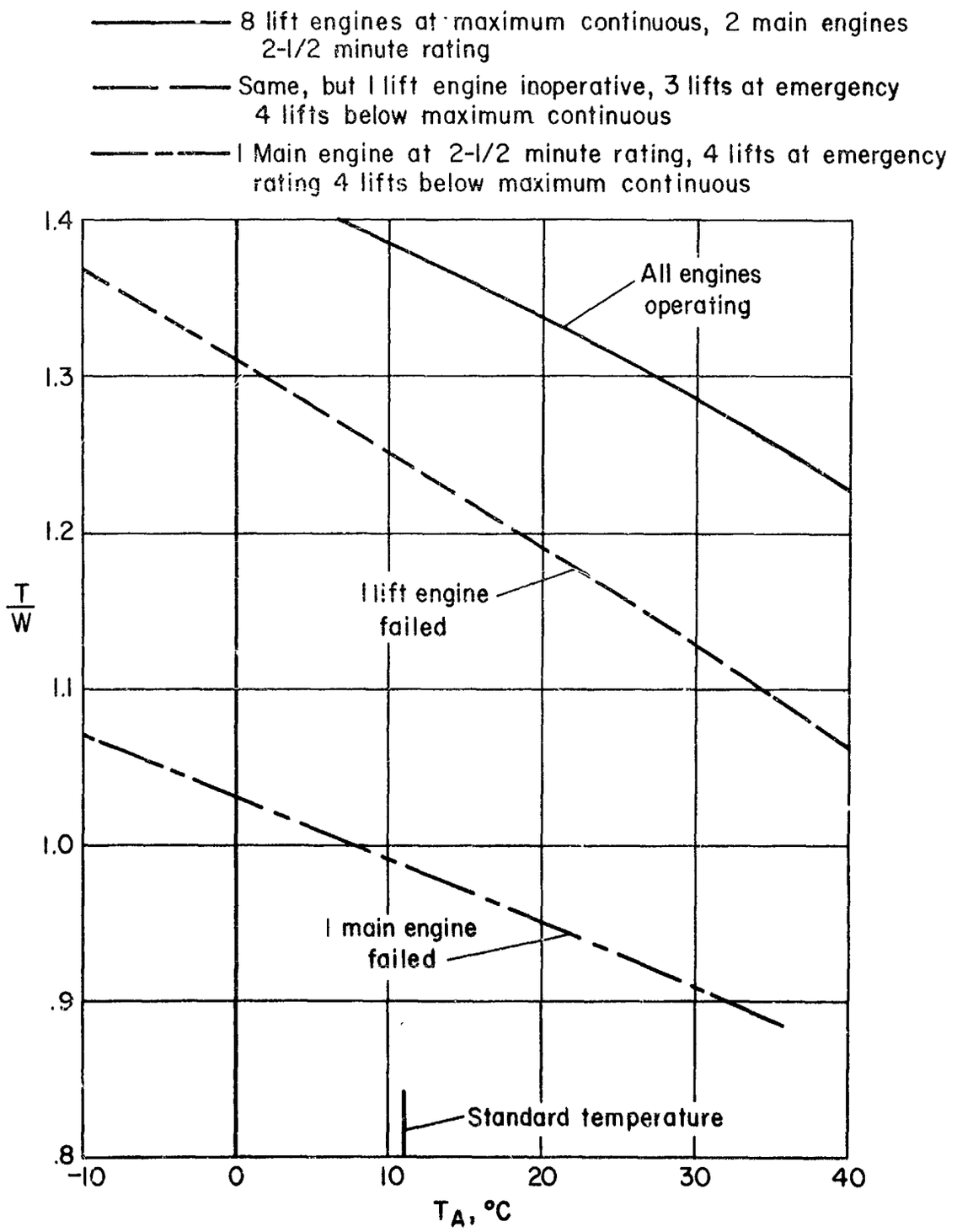

Figure 12.- Thrust-weight ratio in hover out of ground effect and in lateral balance; m = 18,500 kg, h = 600 m, σ_m = 95°, θ = 5°.

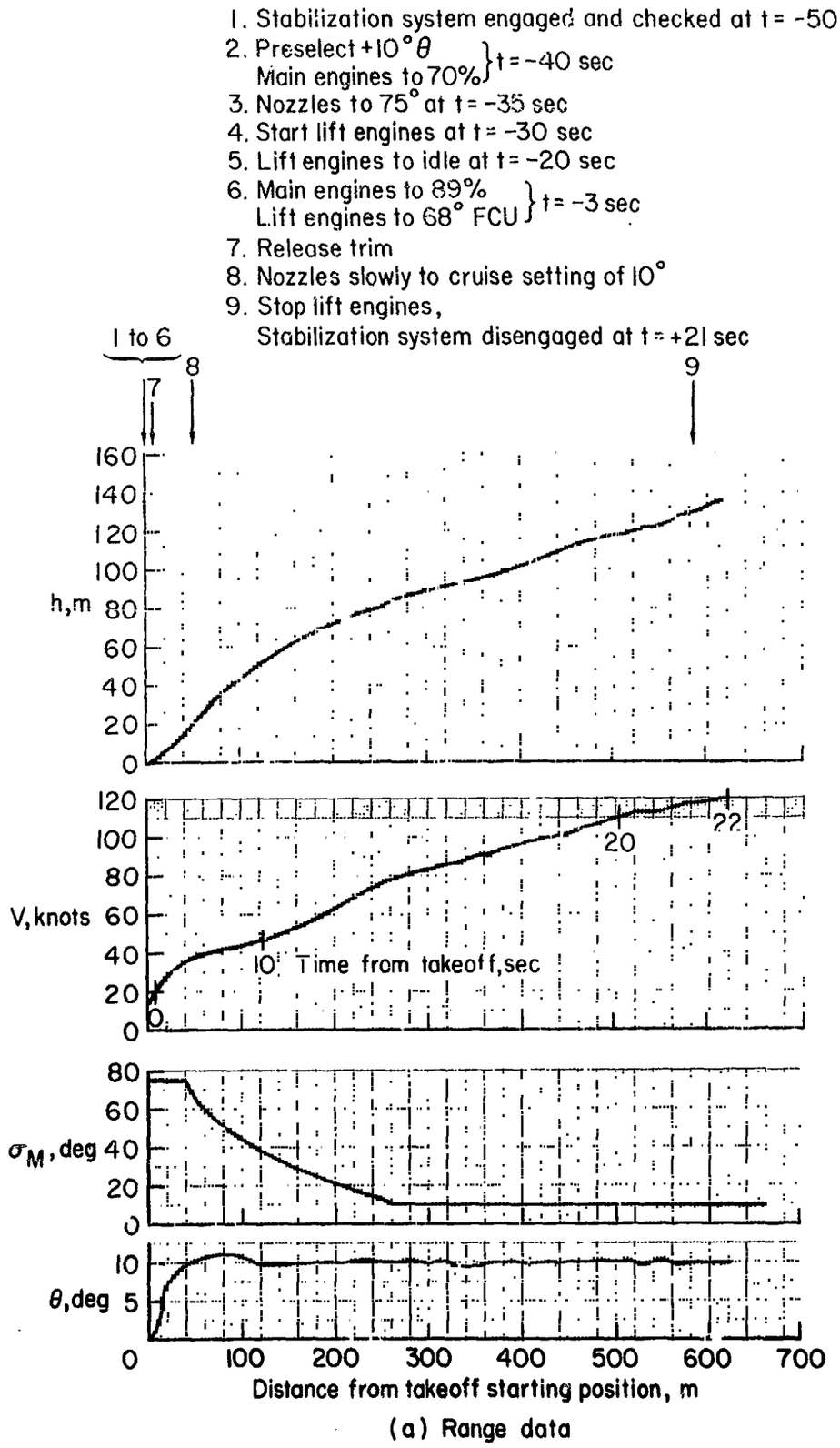

(a) Range data

Figure 13.- Vertical takeoff; m = 21,000 kg, 6-12 knot direct headwind.

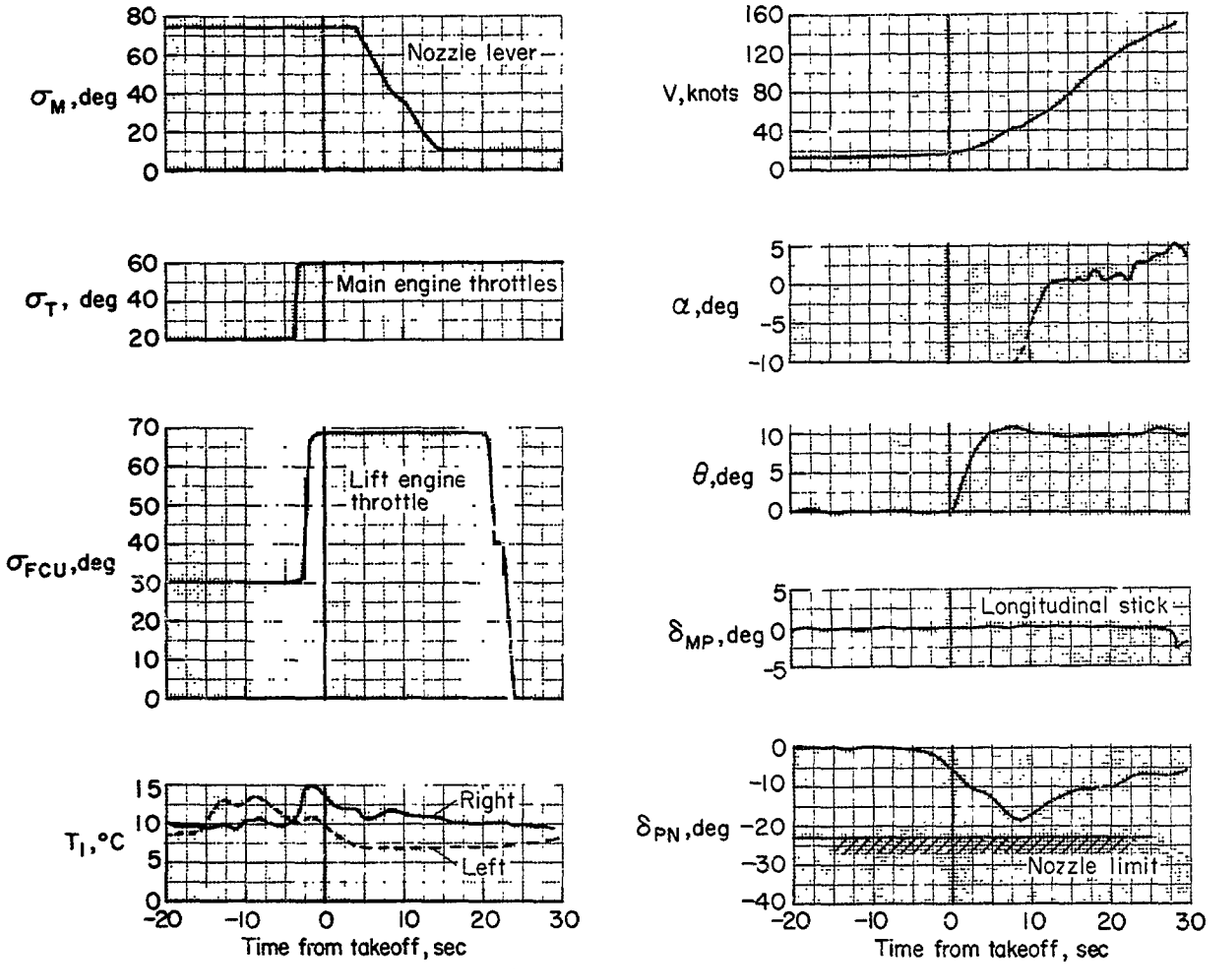

(b) Time history

Figure 13.- Concluded.

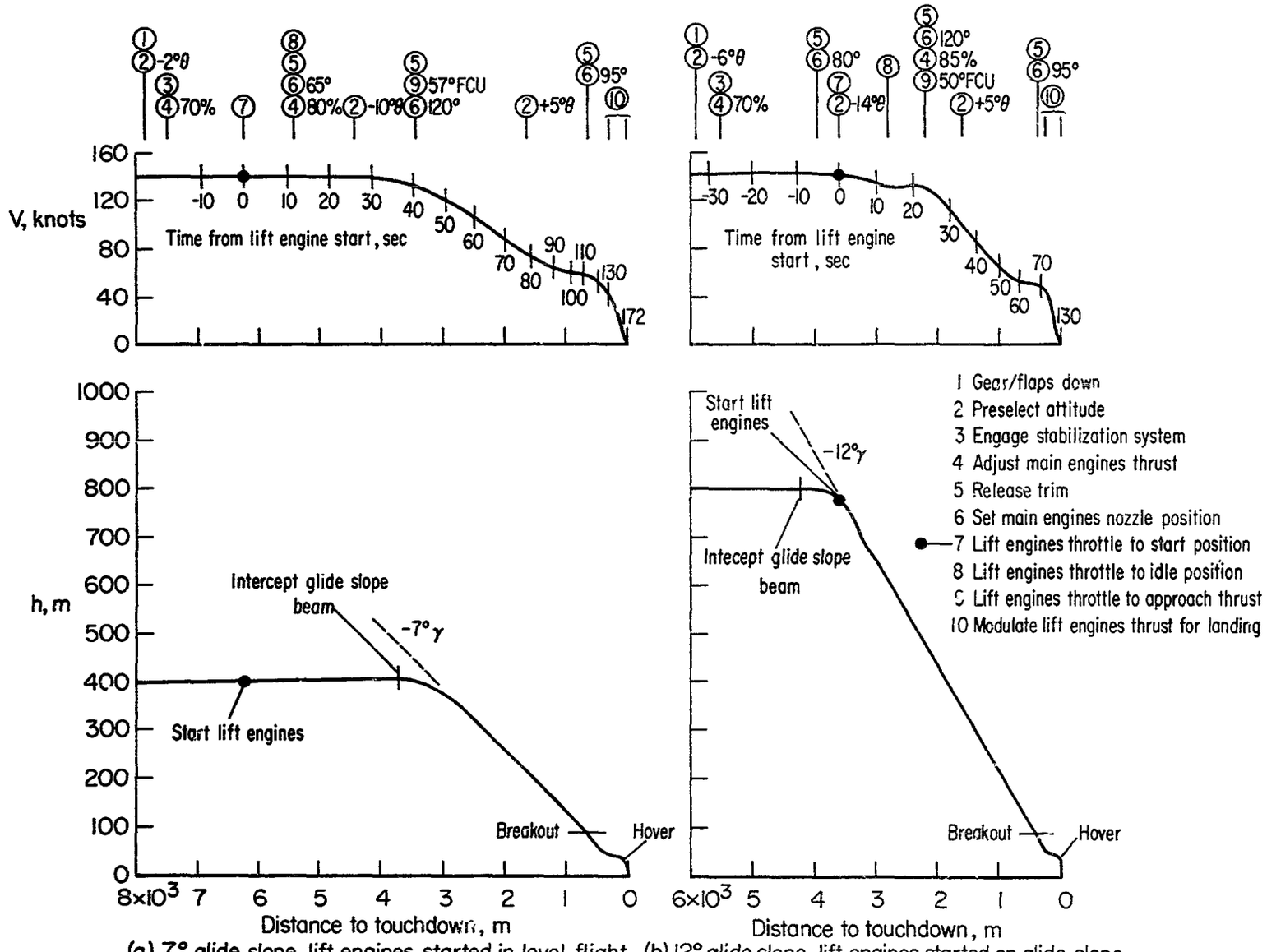

(a) 7° glide slope, lift engines started in level flight (b) 12° glide slope, lift engines started on glide slope

Figure 14.- Schematic of simulated IFR approaches.

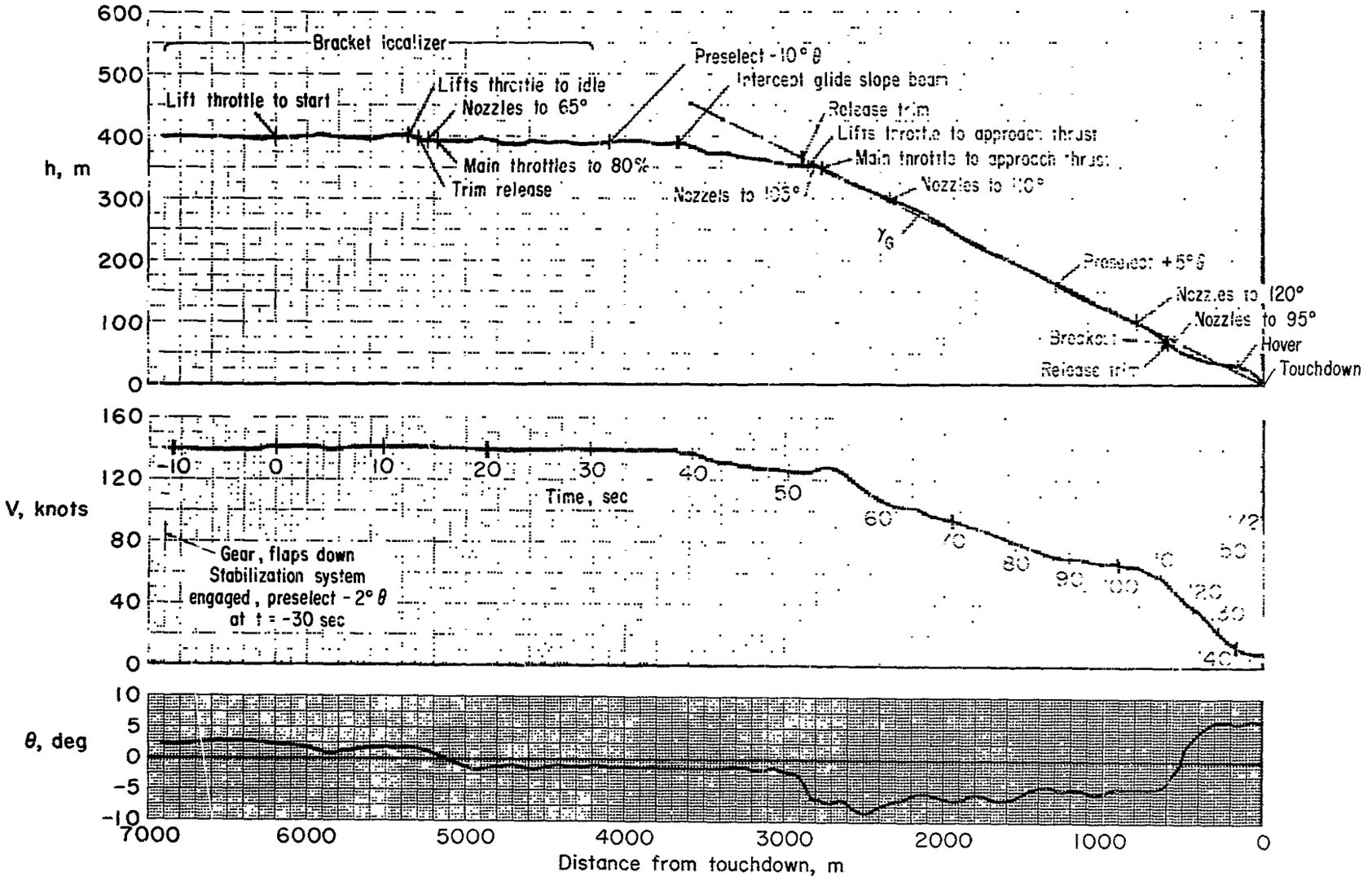

(a) Range data

Figure 15.- 7° simulated IFR approach starting lift engines in level flight; m = 18,750 kg, wind 12-16 knots 60° to 90° from right, $\gamma_G = -7° \pm 1°$.

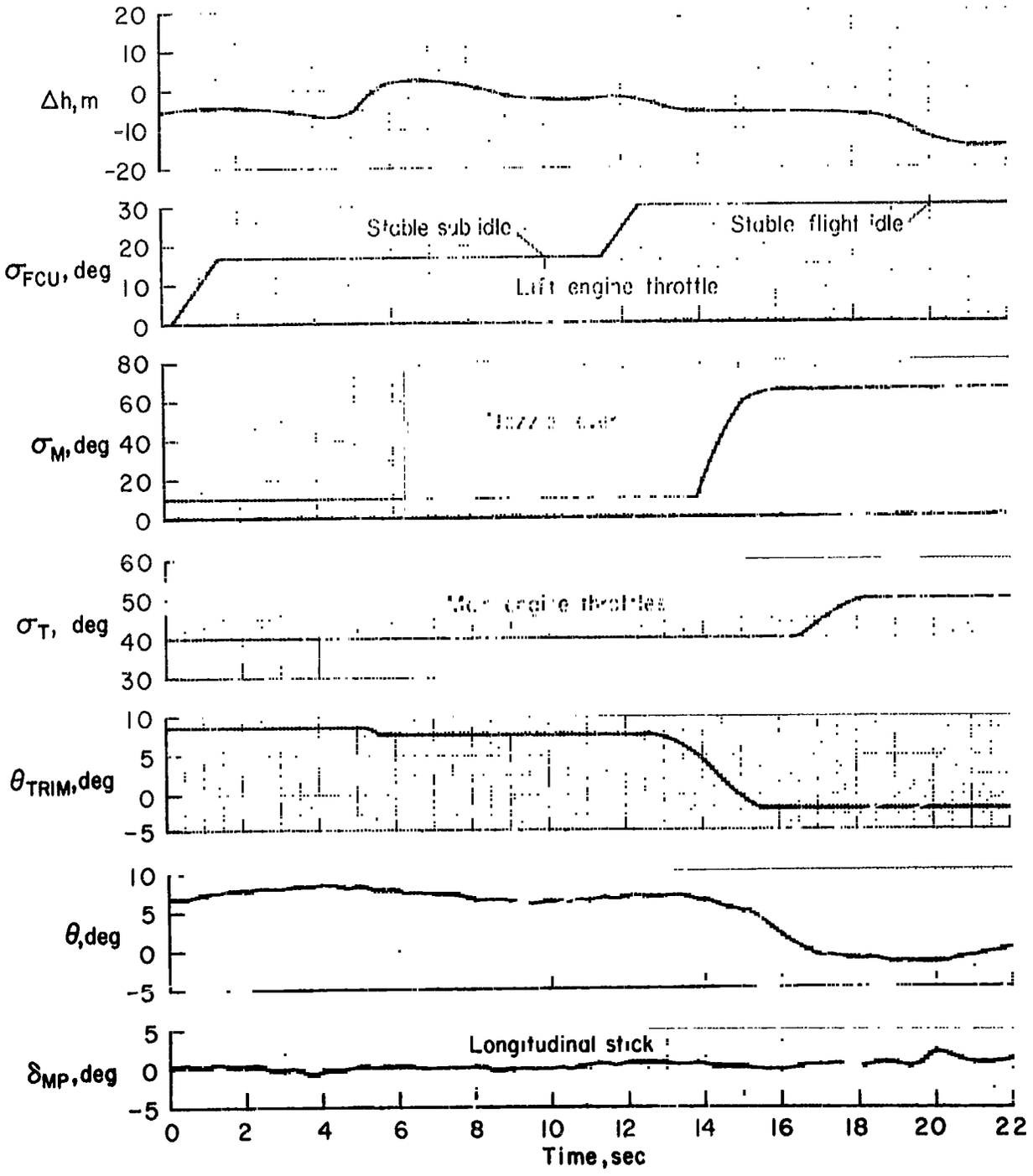

(b) Time history of lift engine start

Figure 15.- Continued.

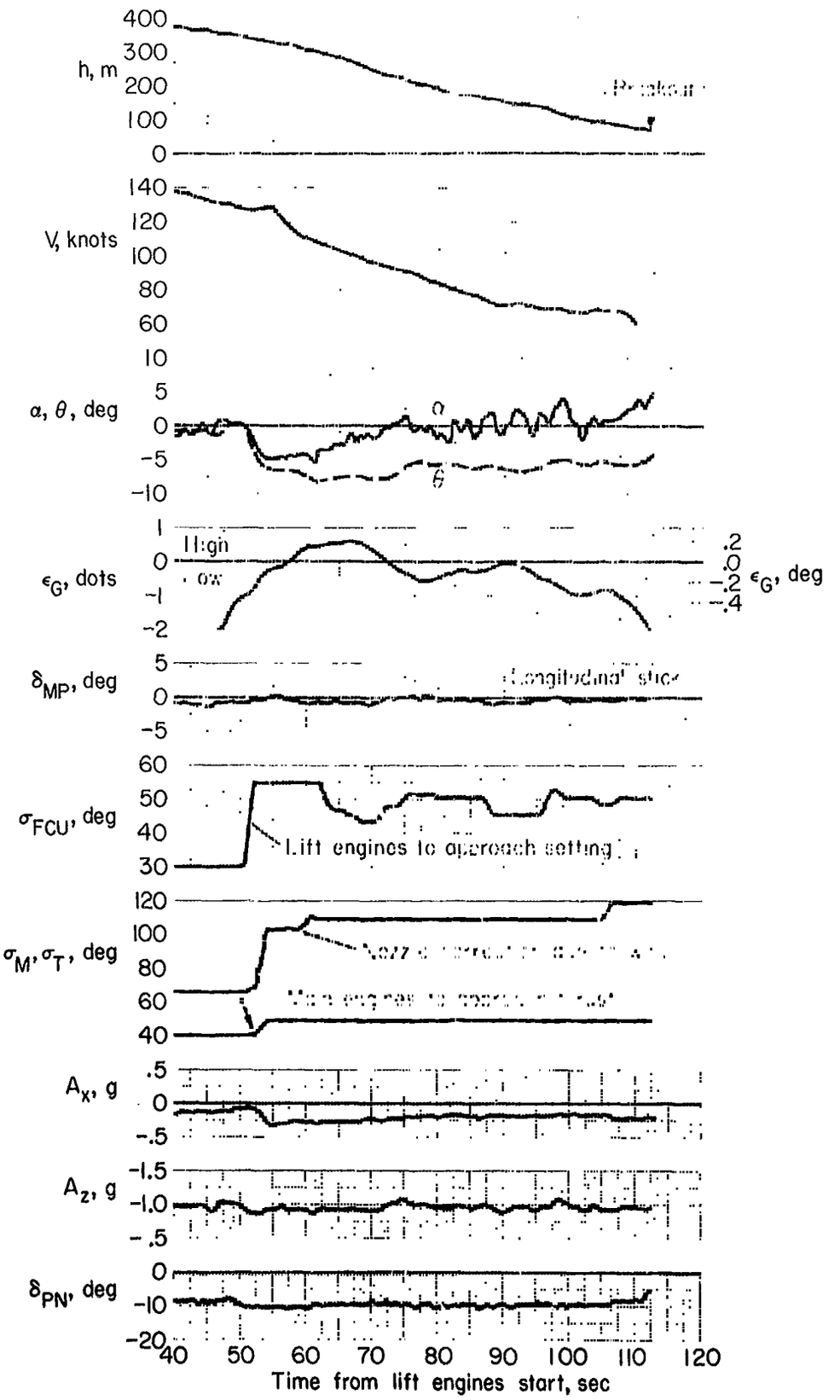

(c) Longitudinal parameters in approach

Figure 15.- Continued.

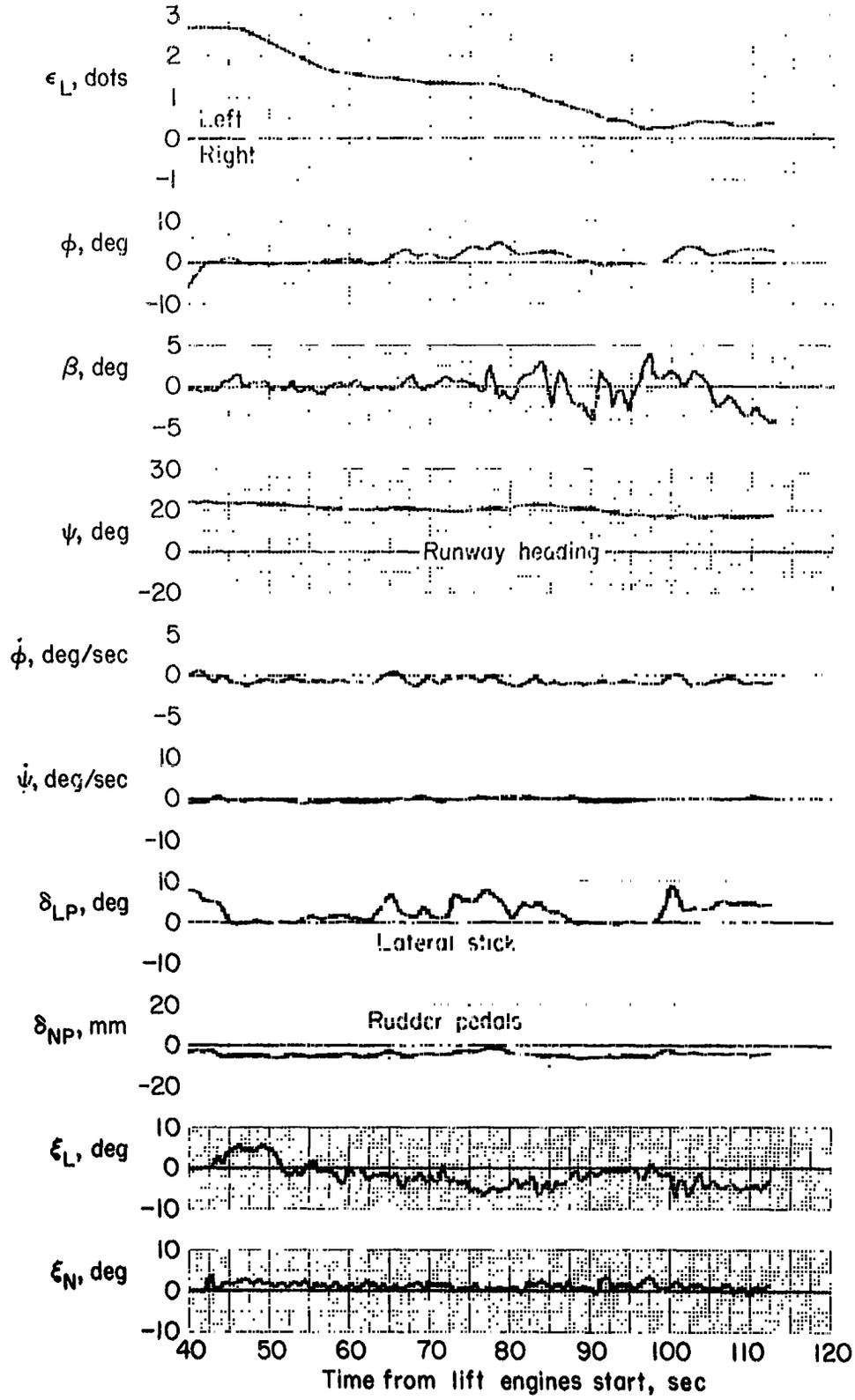

(d) Lateral-directional parameters in approach

Figure 15.- Continued.

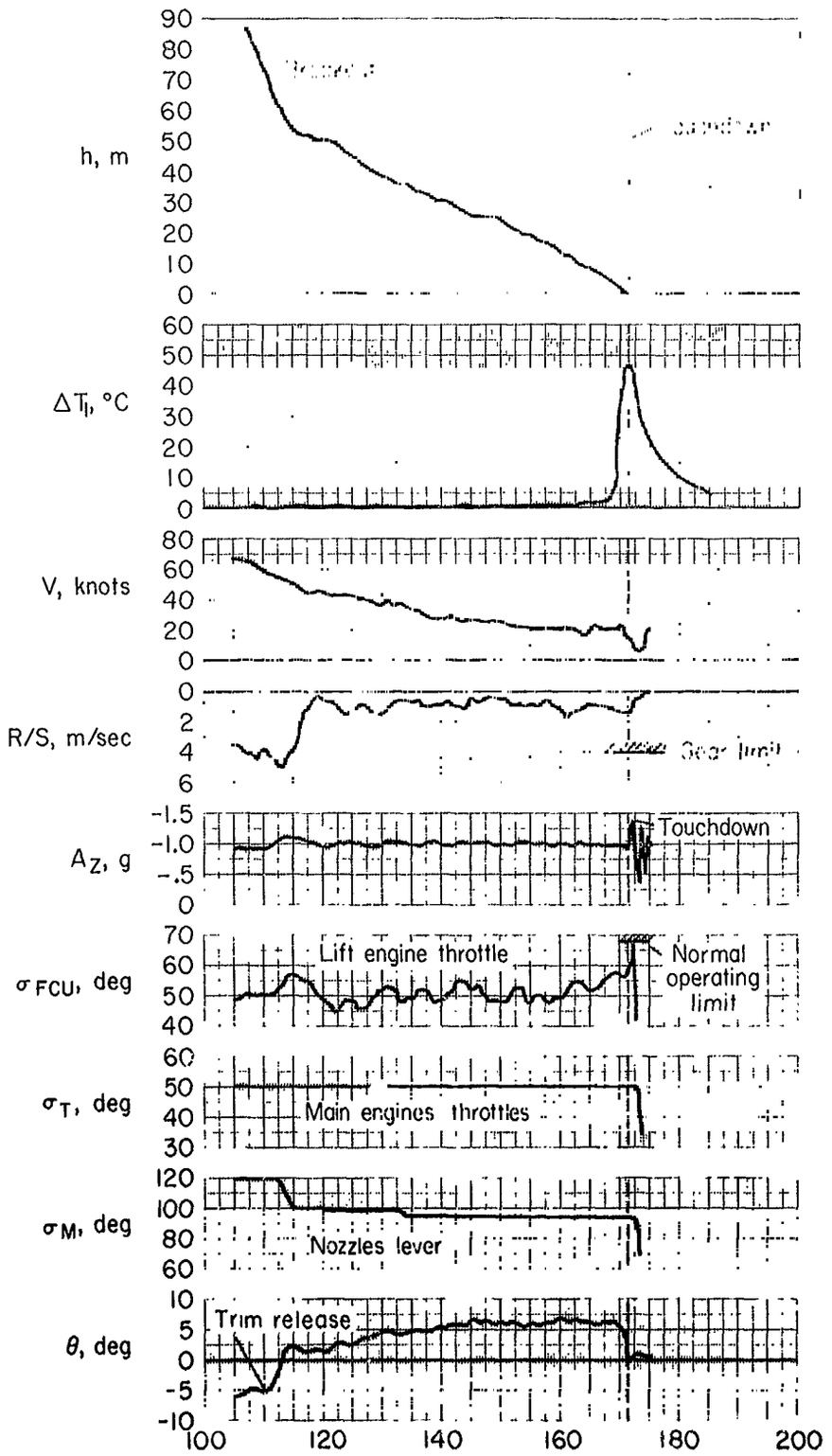

(e) Flare and vertical landing

Figure 15.- Concluded.

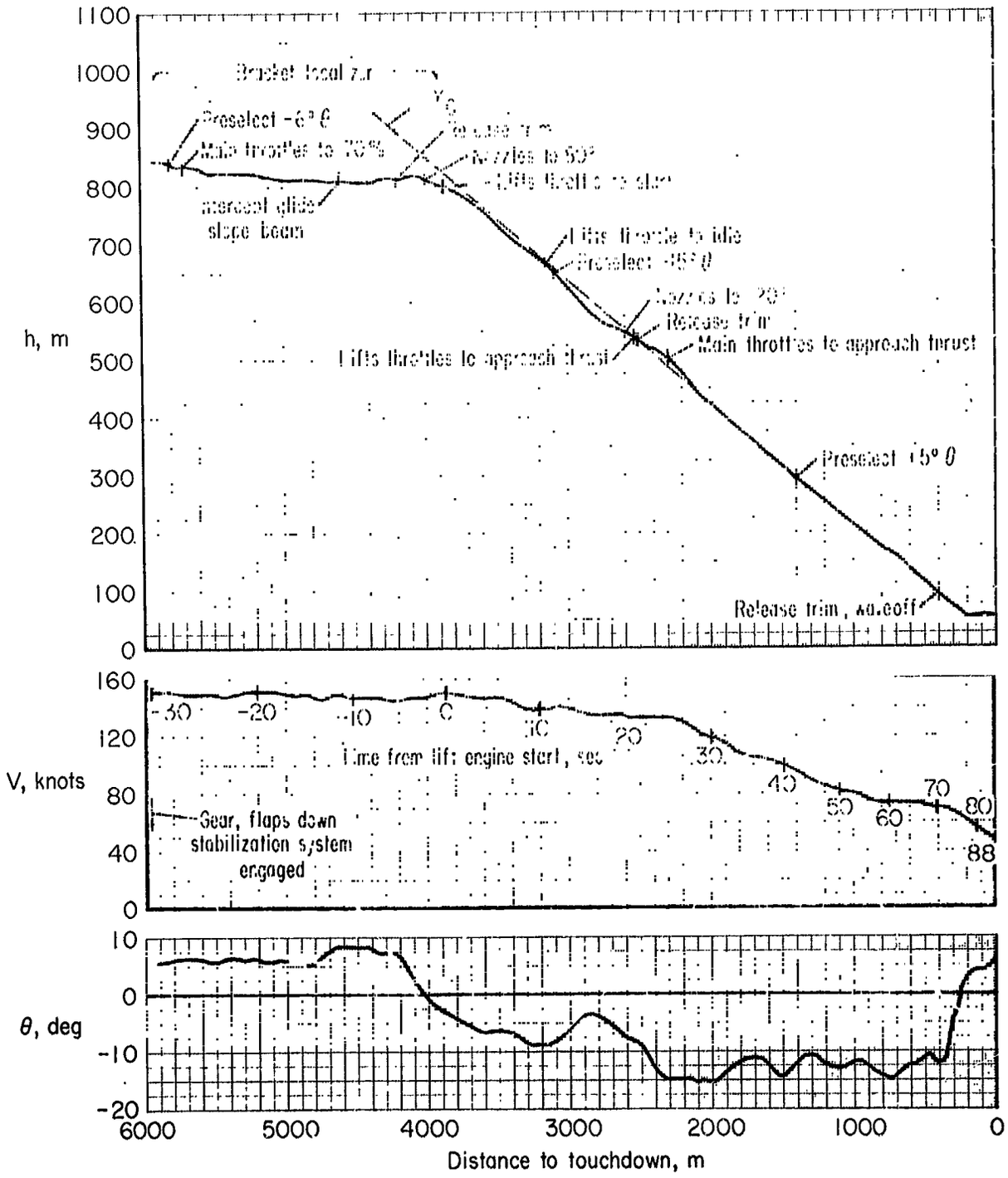

(a) Range data

Figure 16.- 12° simulated IFR approach starting lift engines on glideslope; m = 19,500 kg, wind 15 knots from right, $\gamma_G = -12° \pm 2°$.

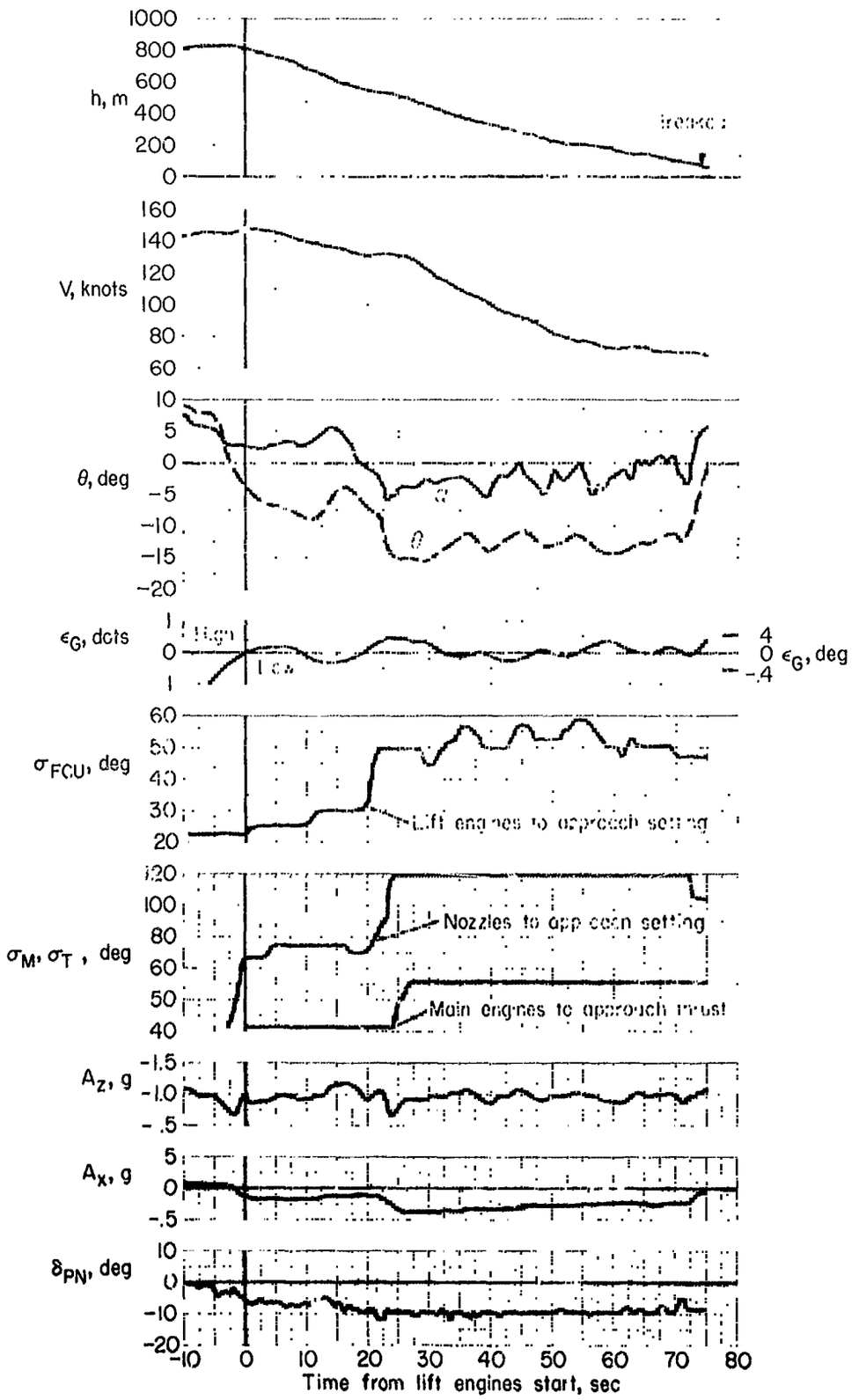

(b) Longitudinal parameters in approach

Figure 16.- Continued.

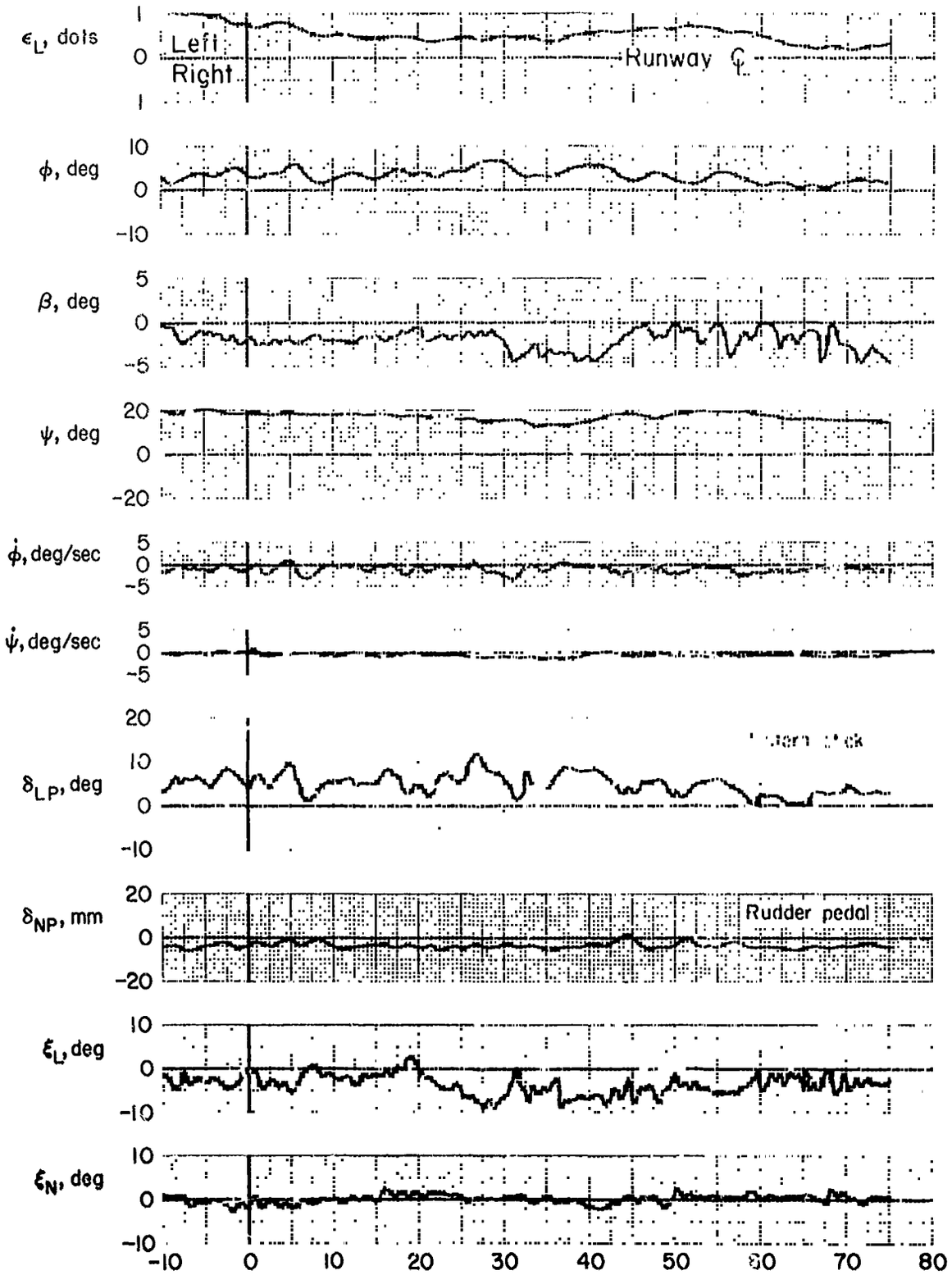

(c) Lateral-directional parameters in approach

Figure 16.- Concluded.

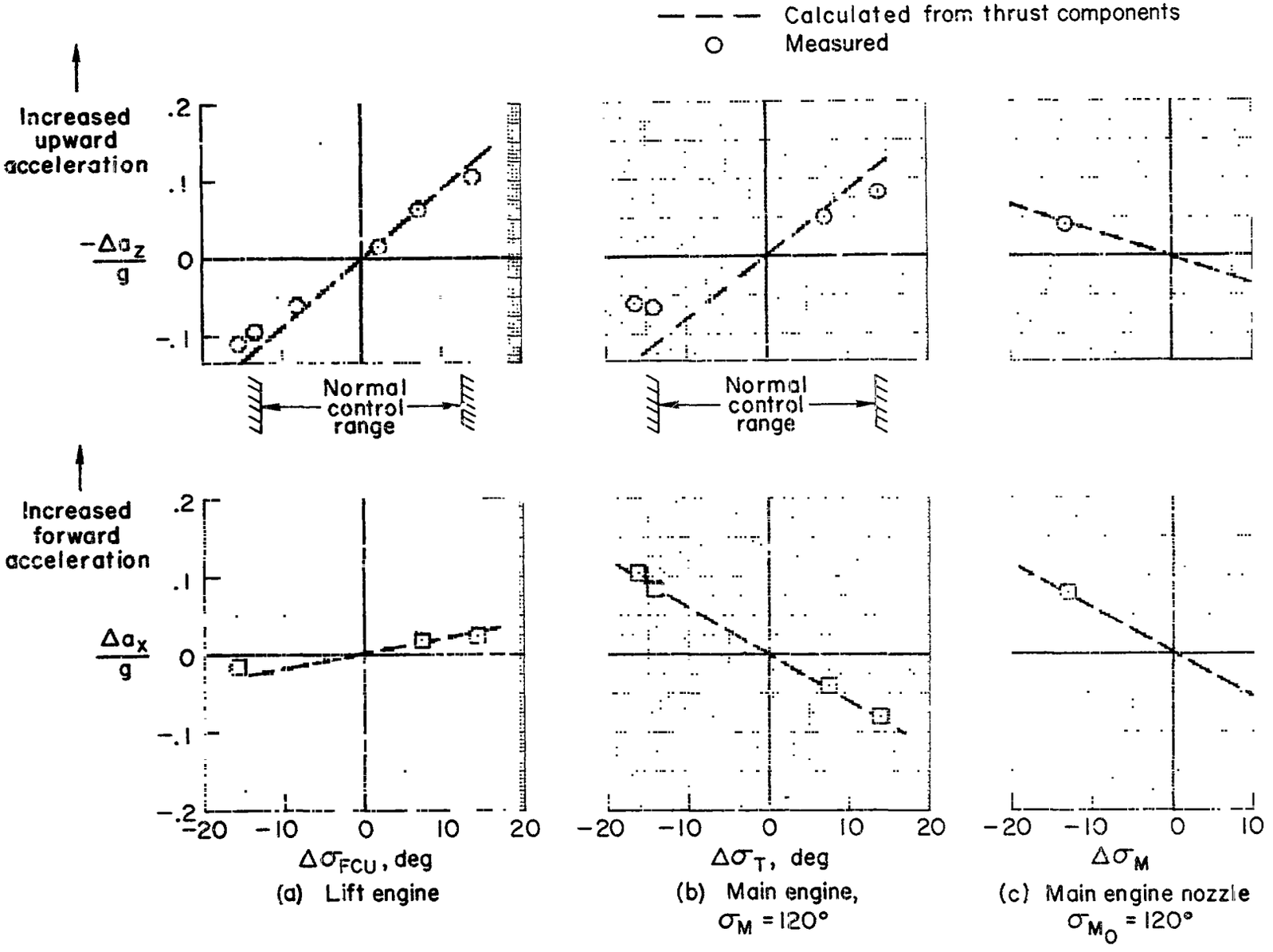

Figure 17.- Incremental accelerations produced by each longitudinal control (with remaining controls fixed). γ_0 about -7°, α_{x_0} about -0.05, V = 50 to 80 knots, m = 19,500 kg.

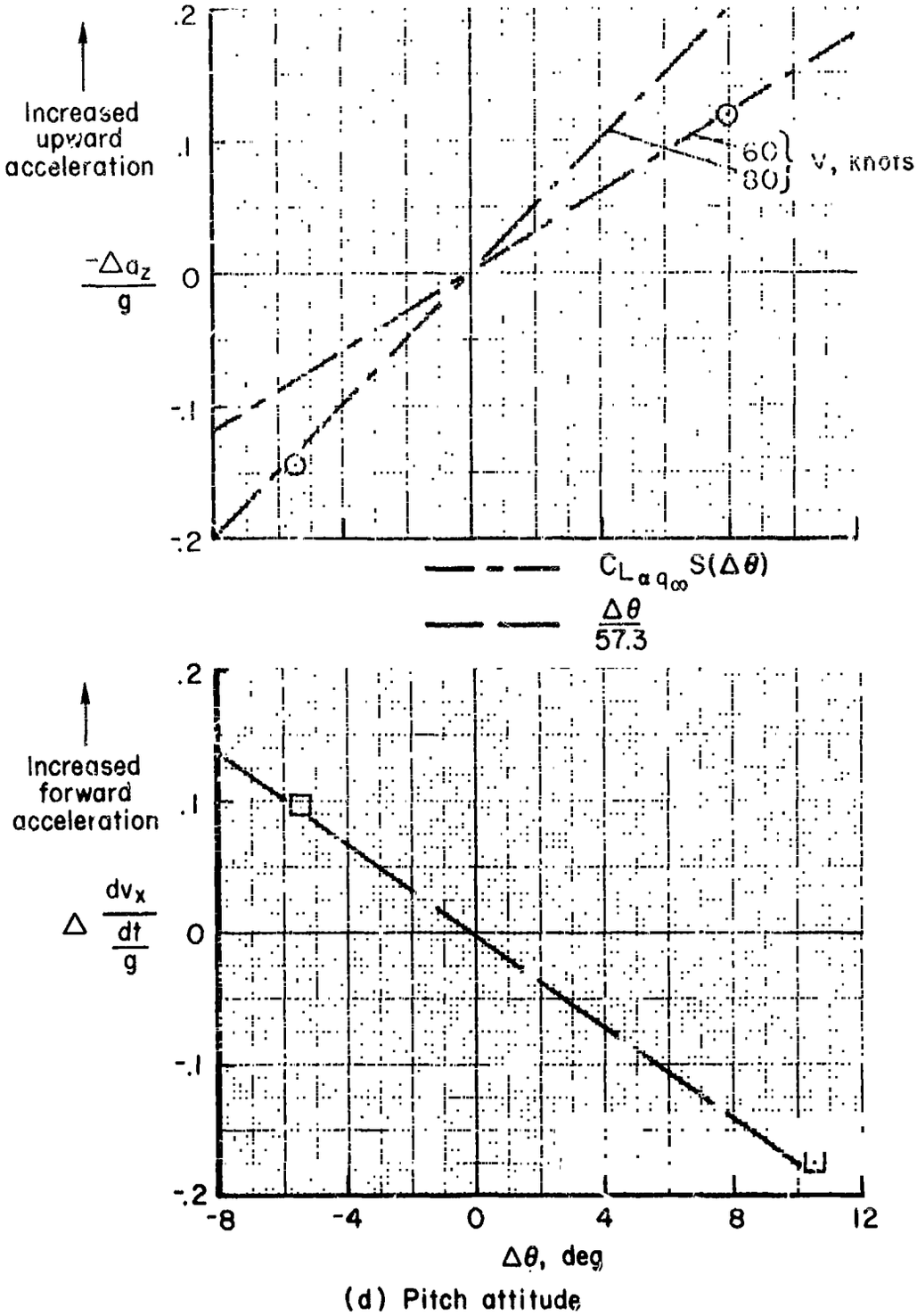

(d) Pitch attitude

Figure 17.- Concluded.

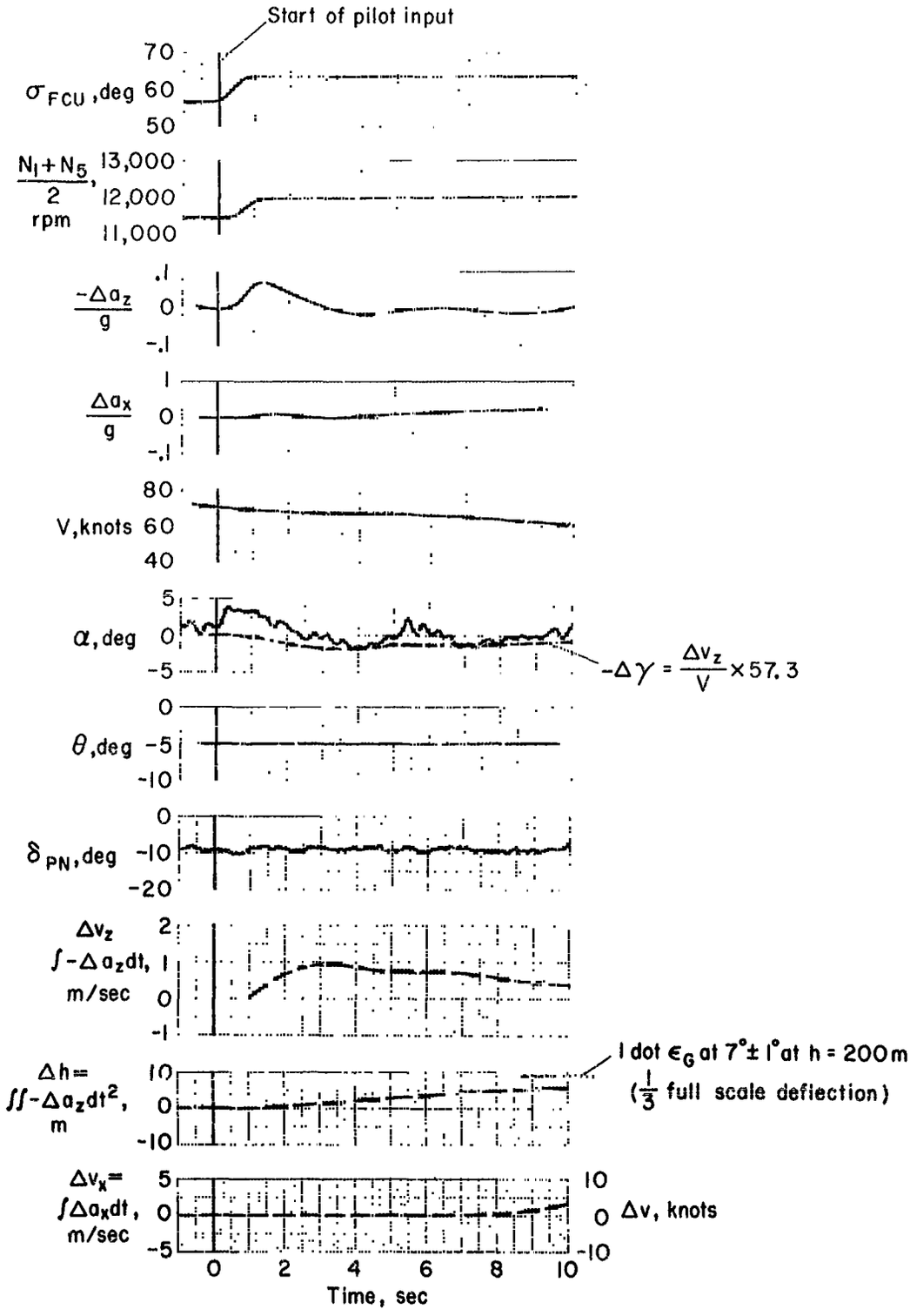

(a) Lift engine step with fixed attitude

Figure 18.- Longitudinal response to different controls; $\gamma_0 = -7°$, M = 19,500 kg.

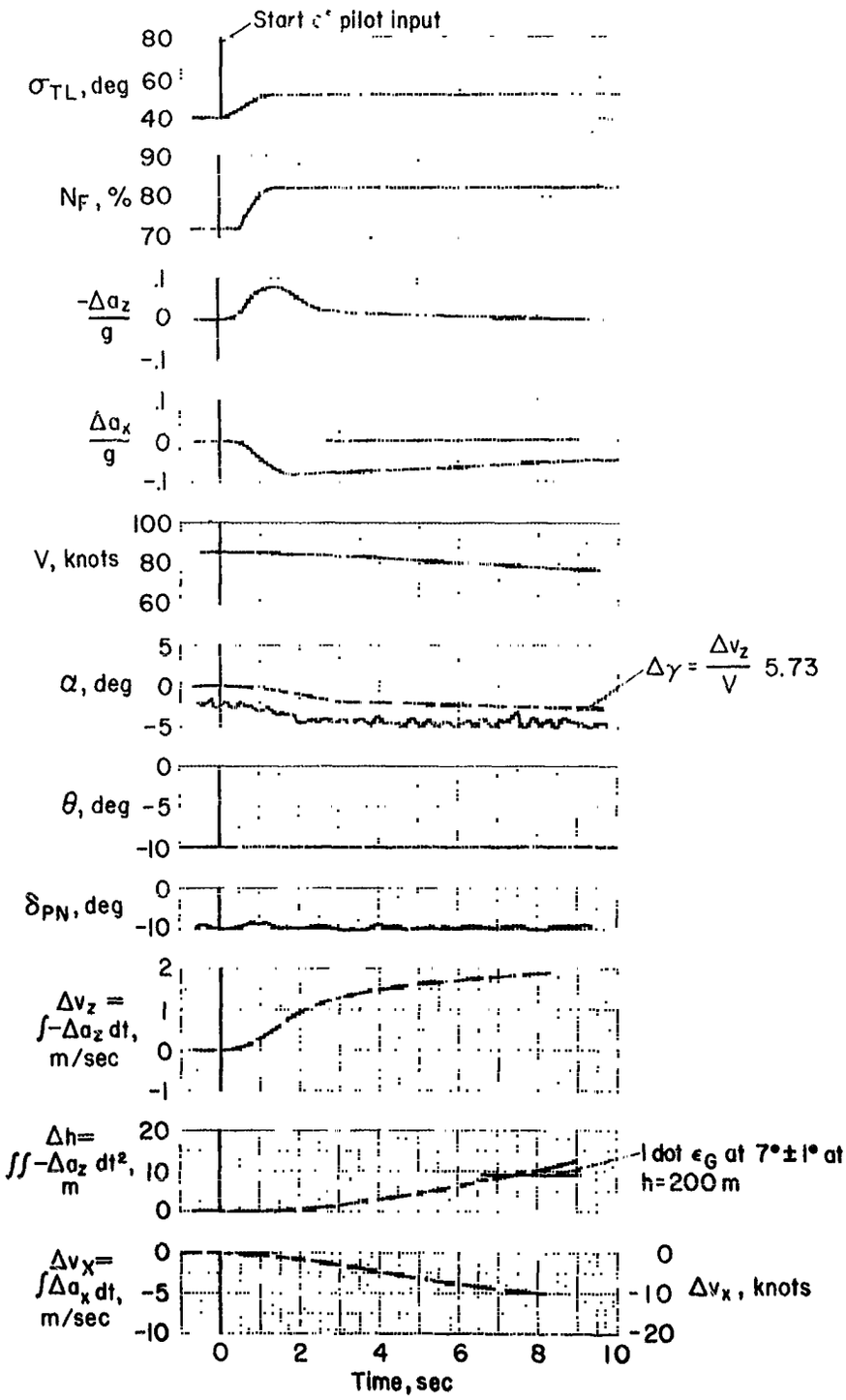

(b) Main engine step with fixed attitude

Figure 18.- Continued.

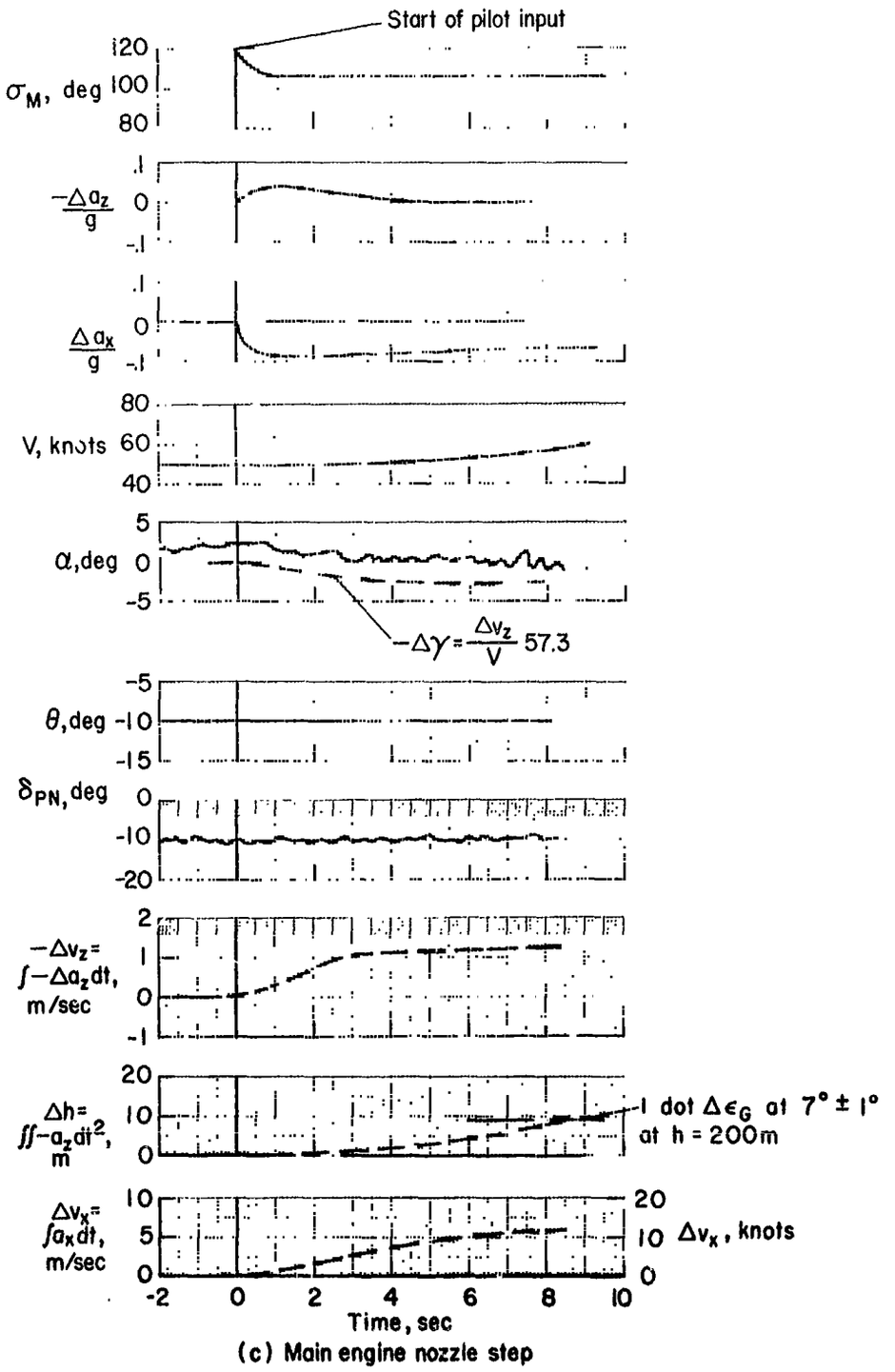

(c) Main engine nozzle step

Figure 18.- Continued.

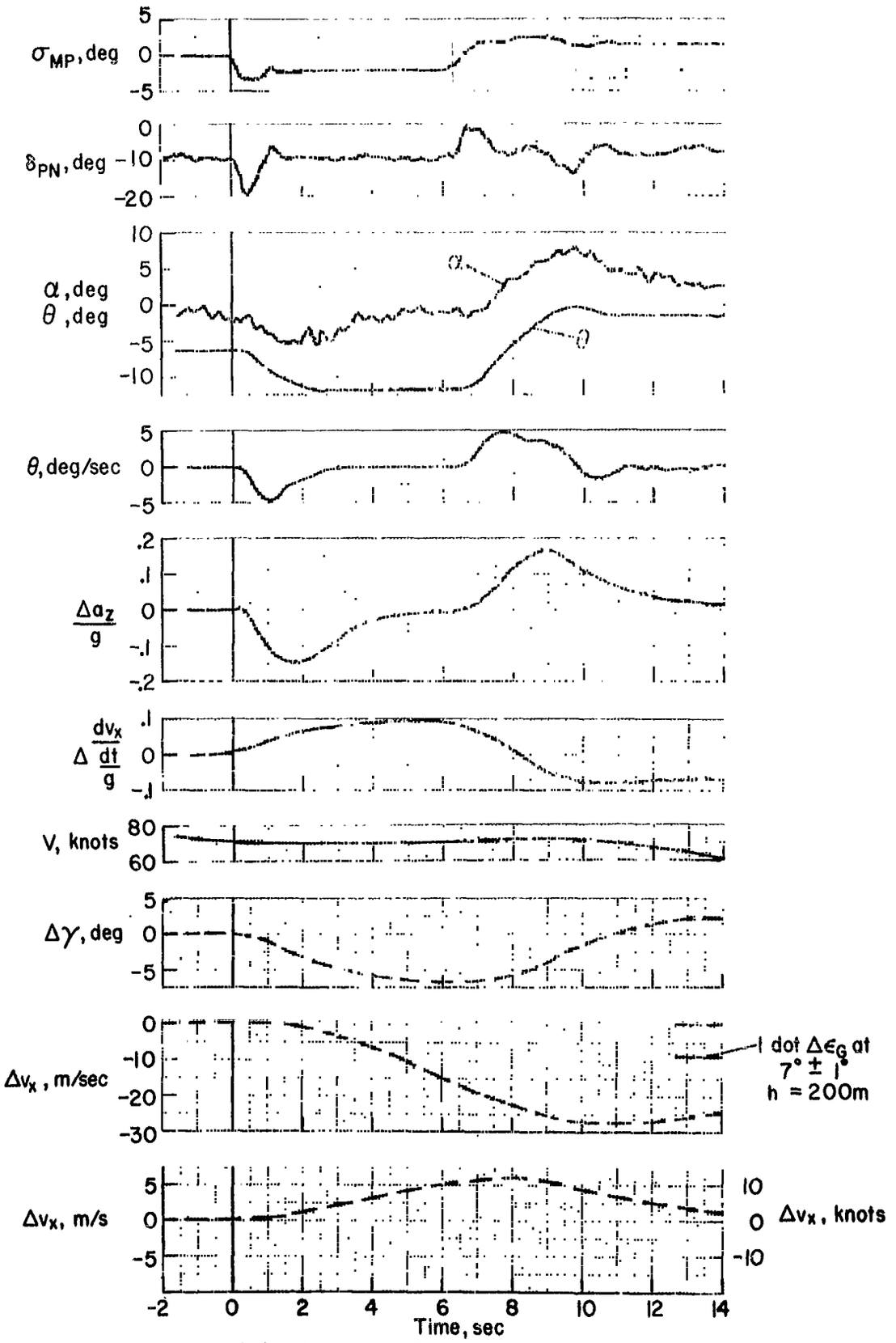

(d) Attitude hold, fixed throttles and nozzle

Figure 18.- Concluded.

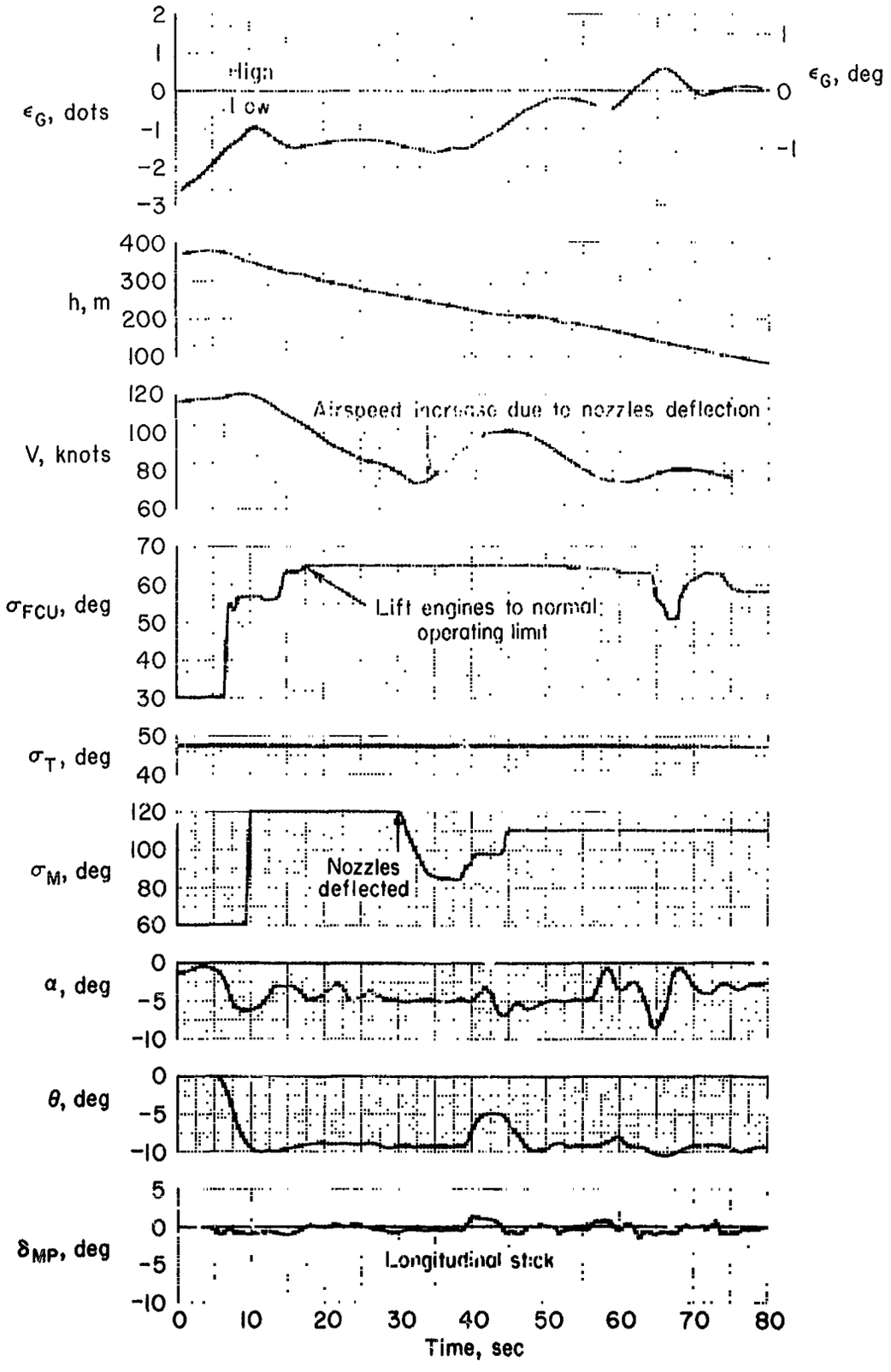

Figure 19.- Correction for 1-1/2 dot low error attempted by lift engines; $\gamma_G = -7° \pm 2°$.

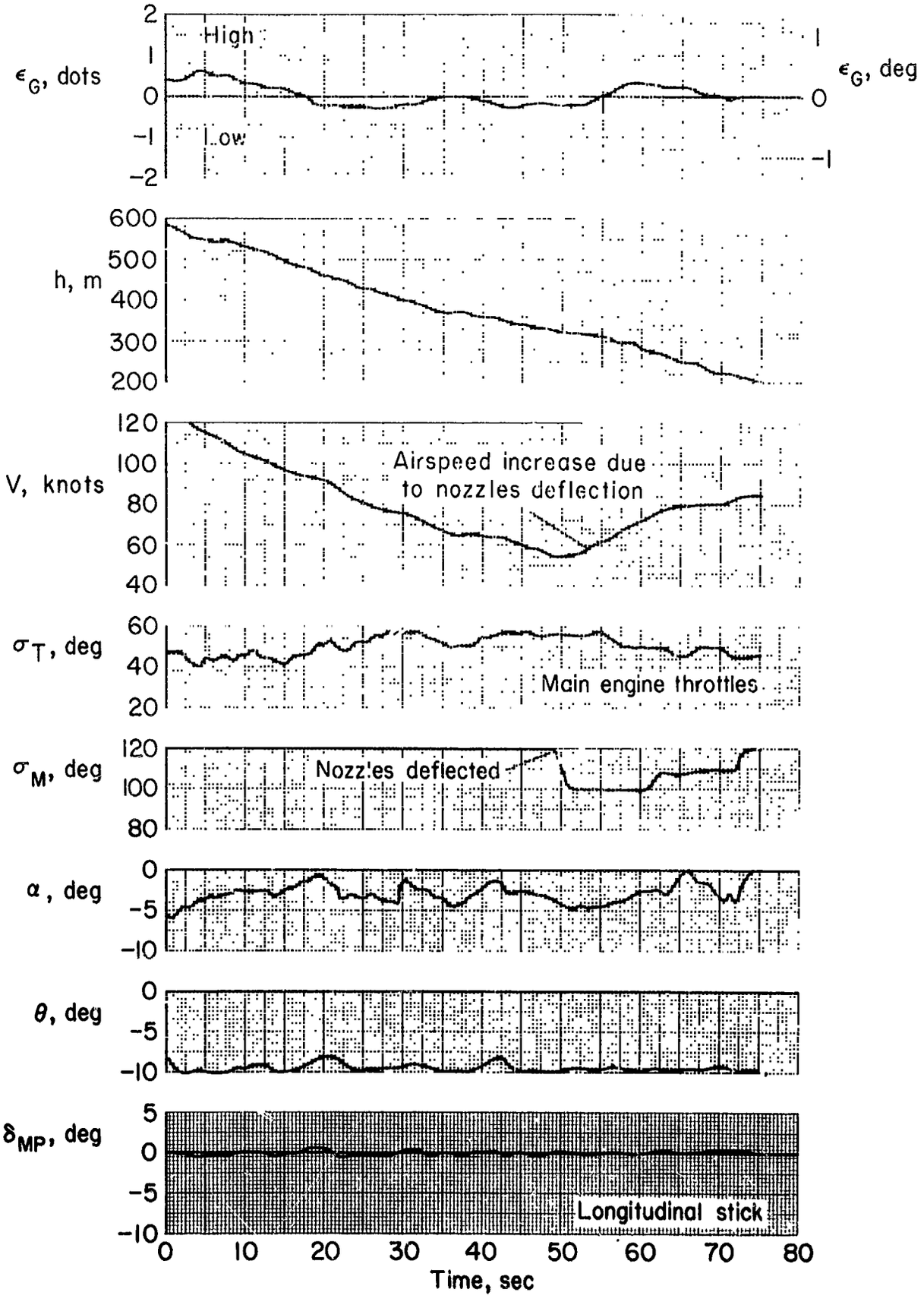

Figure 20.- Effect of main engine thrust modulation on glideslope tracking; $\gamma_G = -7° \pm 2°$.

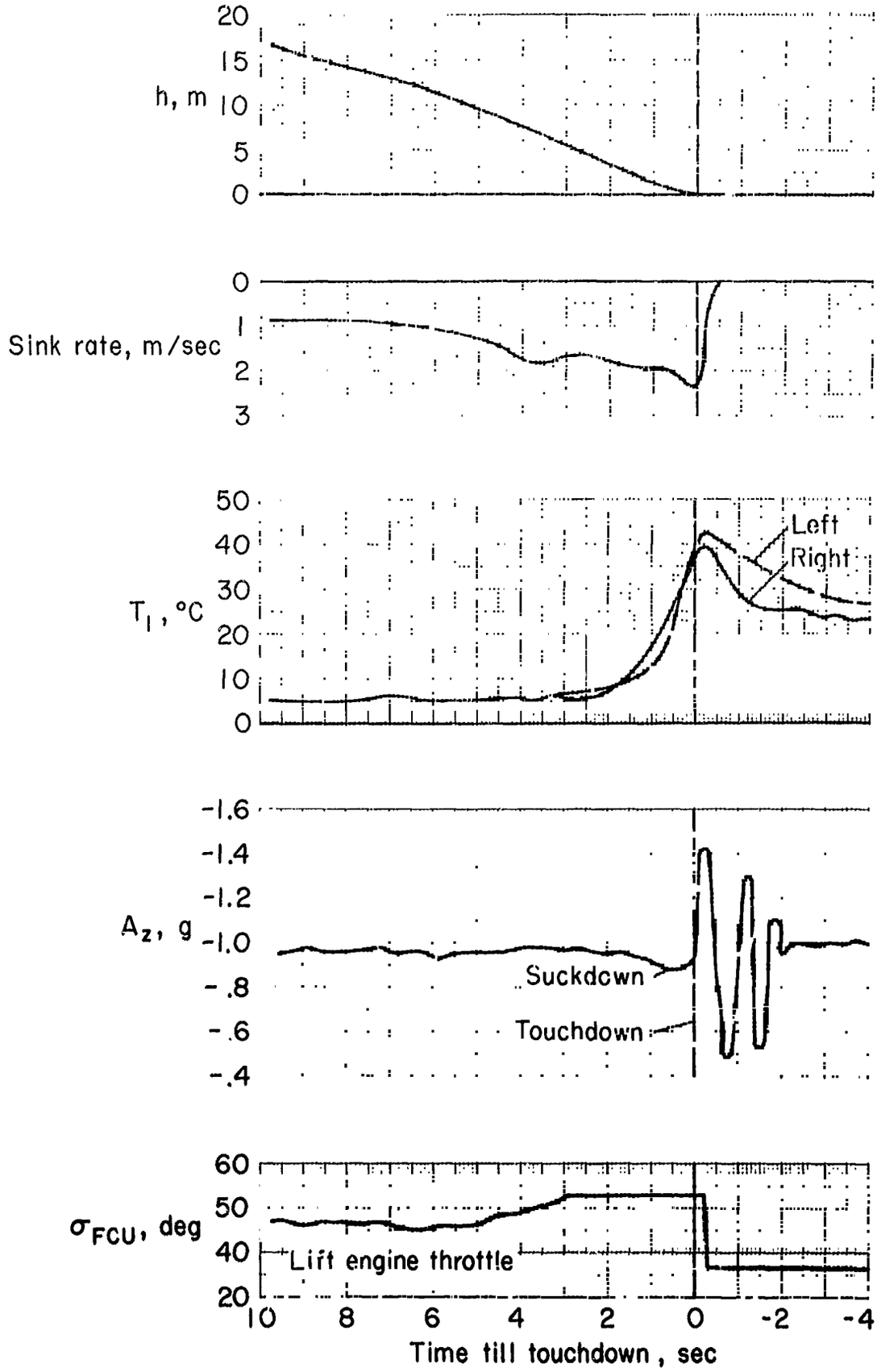

Figure 21.- Lift loss in vertical landing.

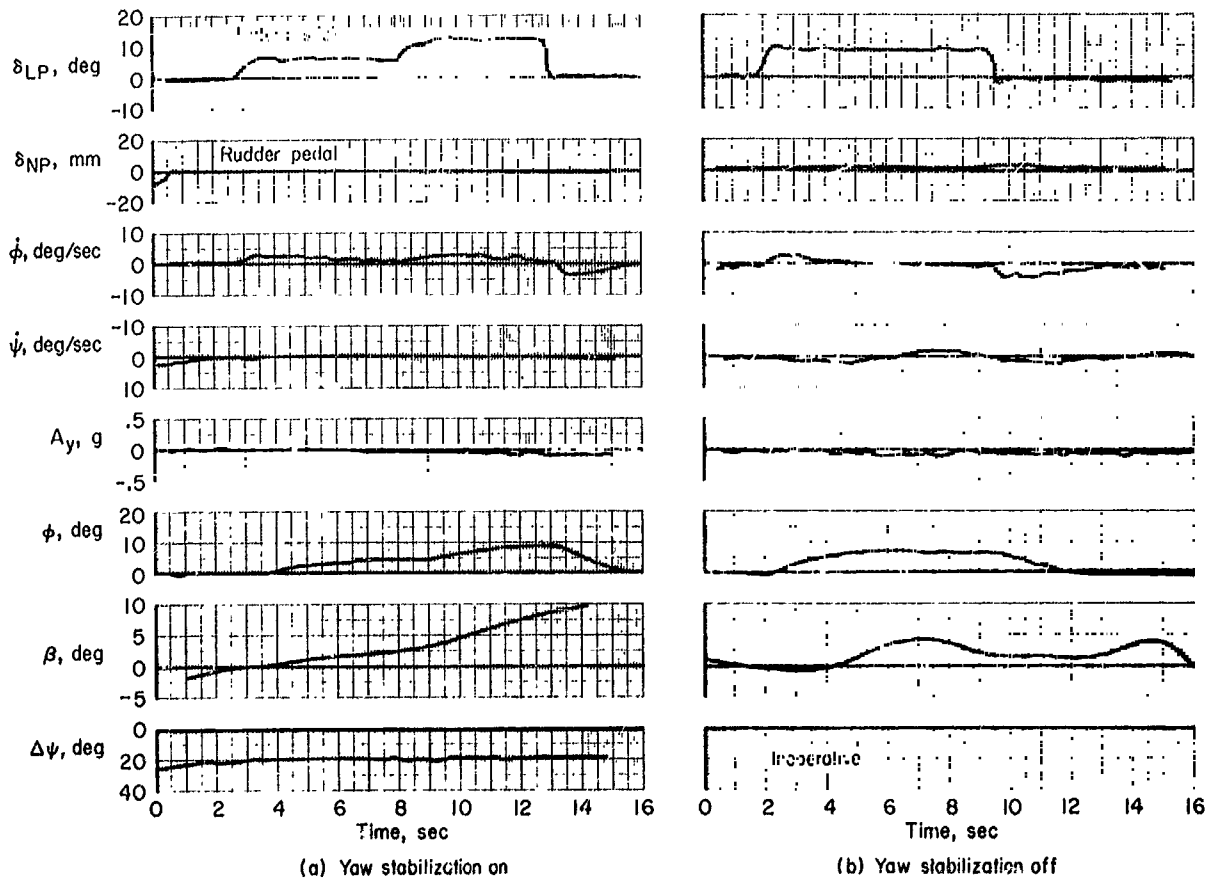

Figure 22.- Lateral attitude steps without directional control inputs; V = 70 to 90 knots, m = 19,500 kg.

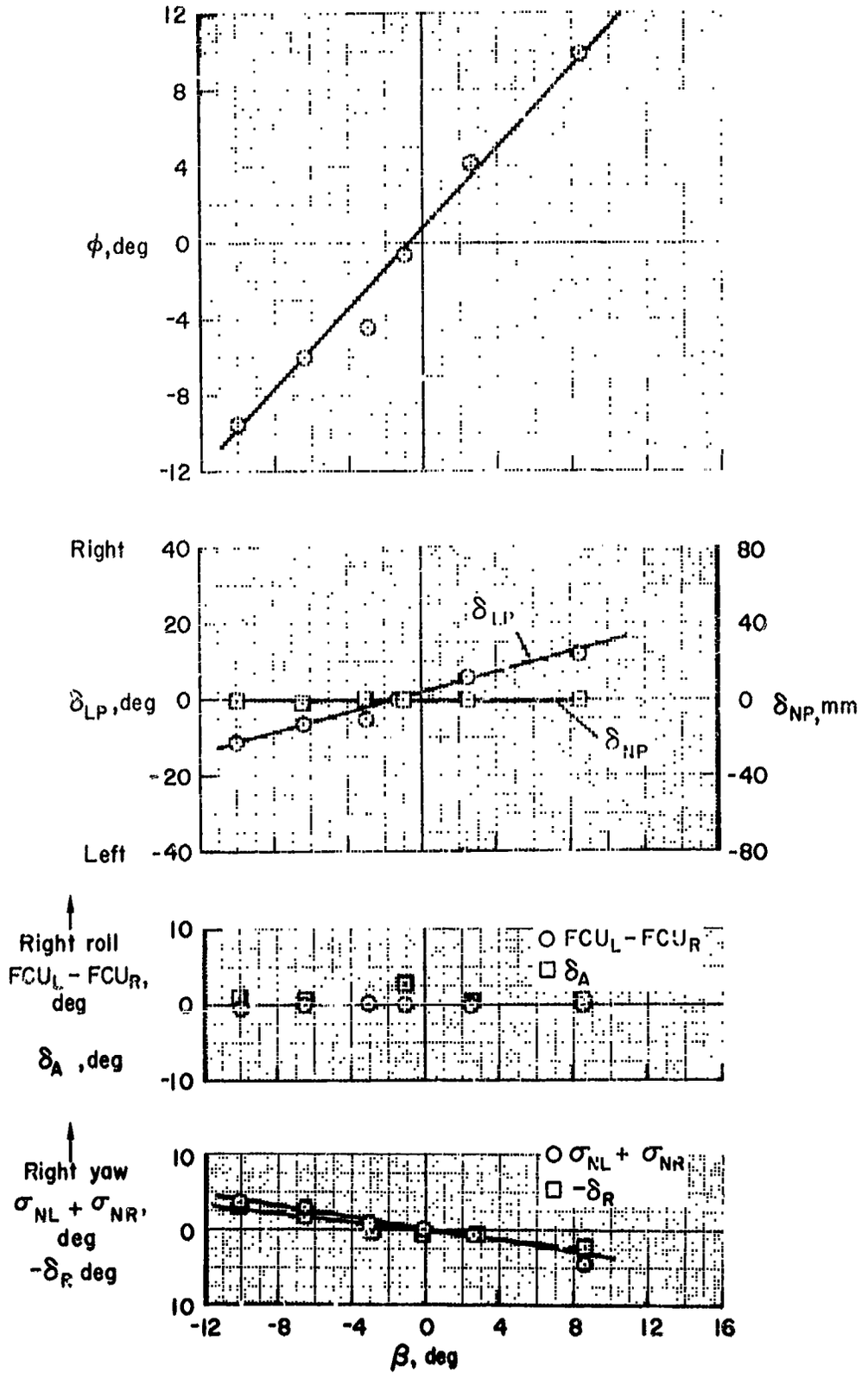

Figure 23.- Static lateral-directional characteristics with stabilization engaged; V = 70-90 knots, γ_0 = -7°, σ_{FCU} = 57°, N_F = 80 percent, σ_m = 120°, m = 19,500 kg.

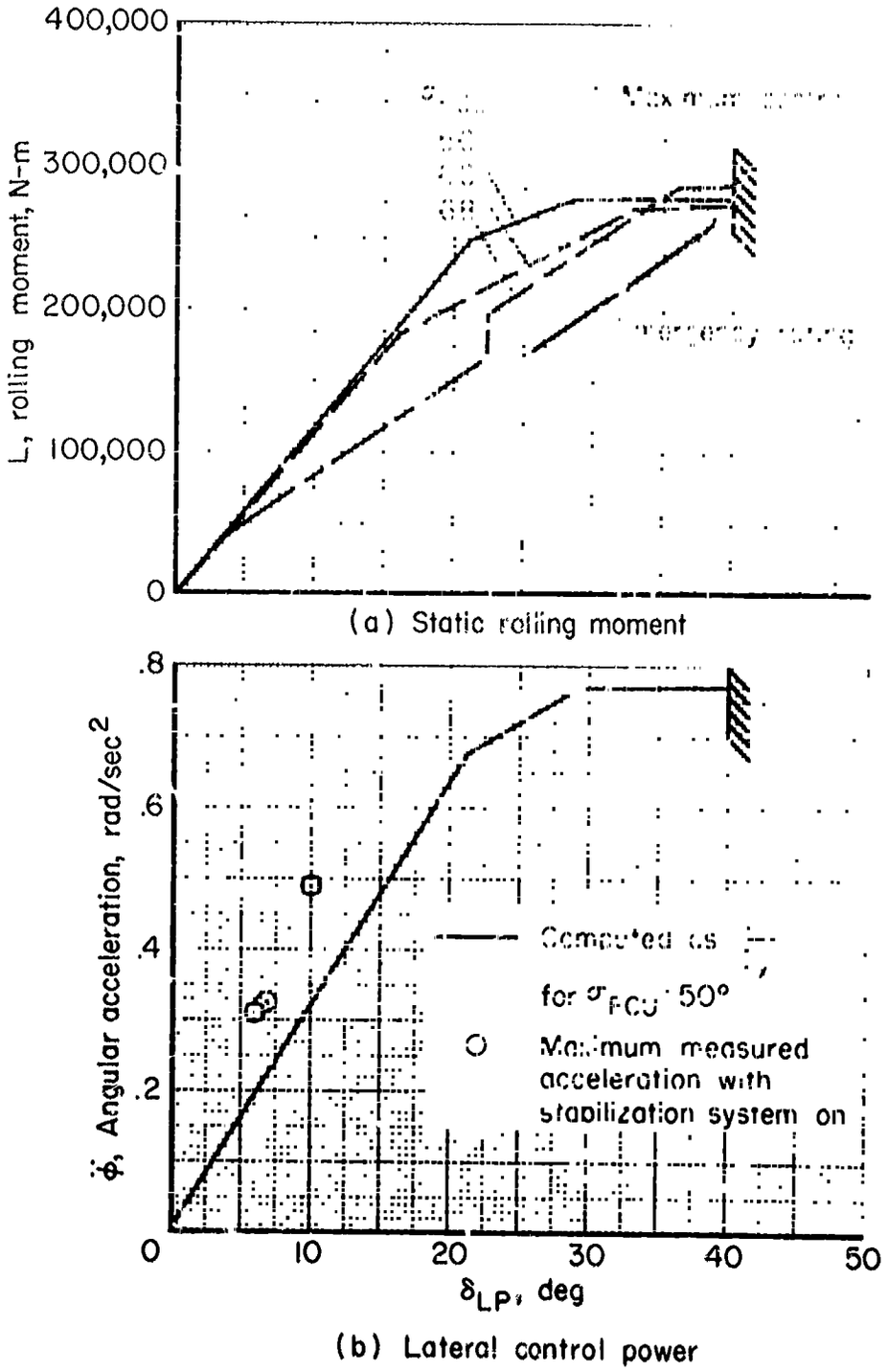

Figure 24.- Lateral control capability in hover; m = 19,000 kg, I_x = 385,000 kg-m^2.

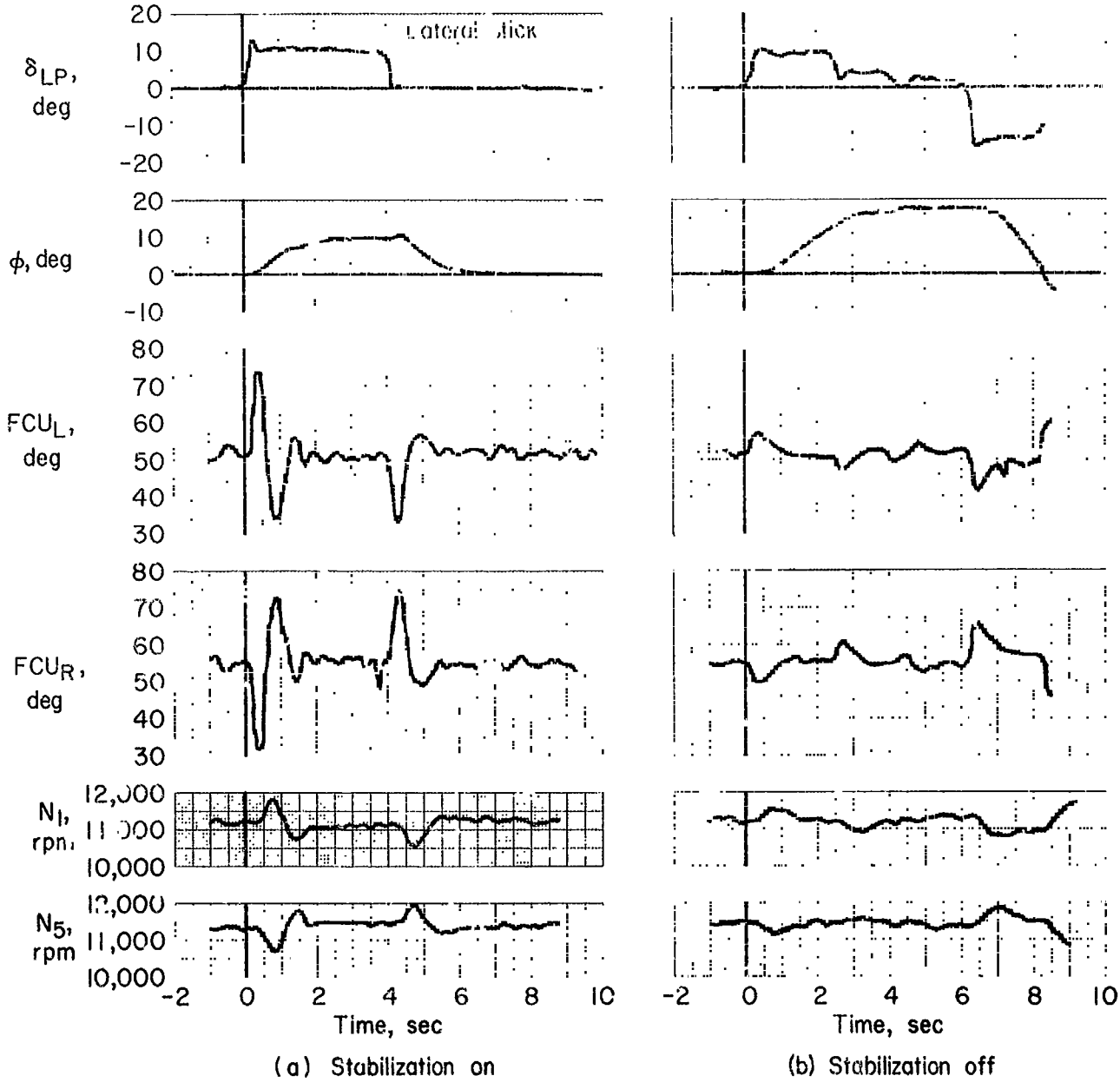

Figure 25.- Response to lateral control input; hover rig on pedestal.

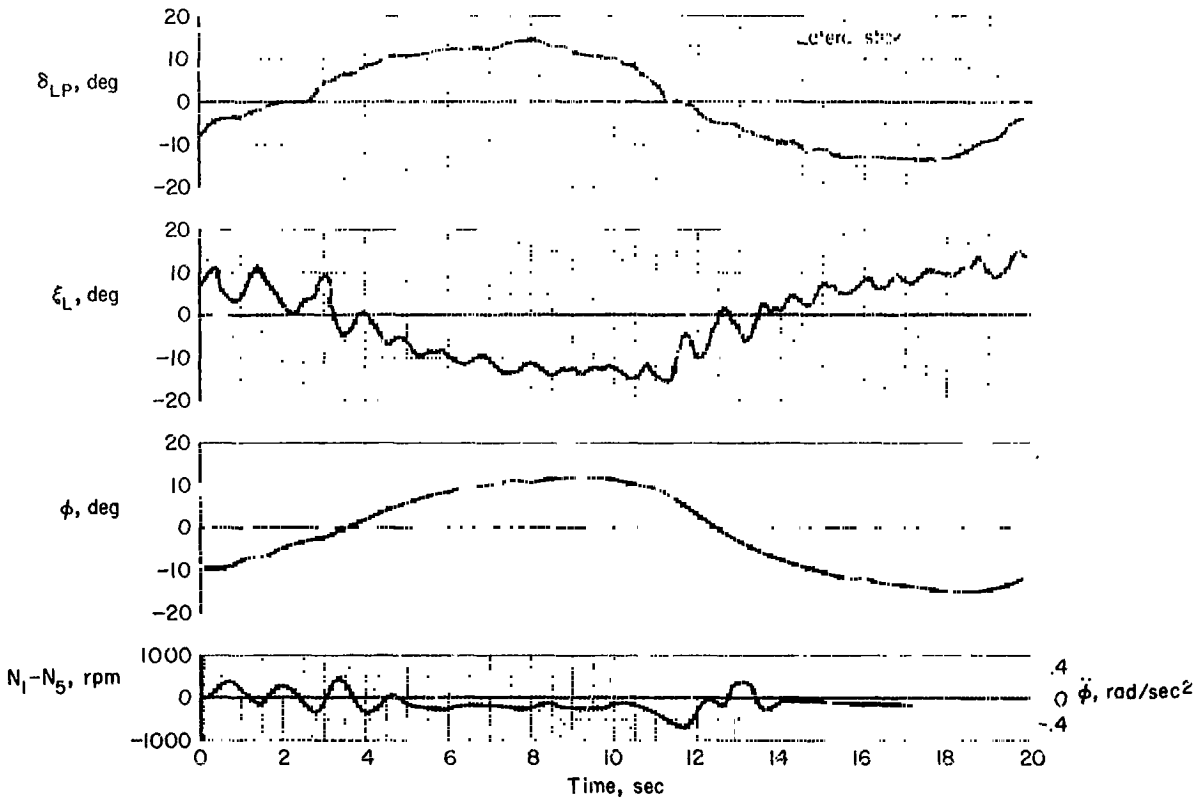

Figure 26.- Lateral maneuvering in hover.

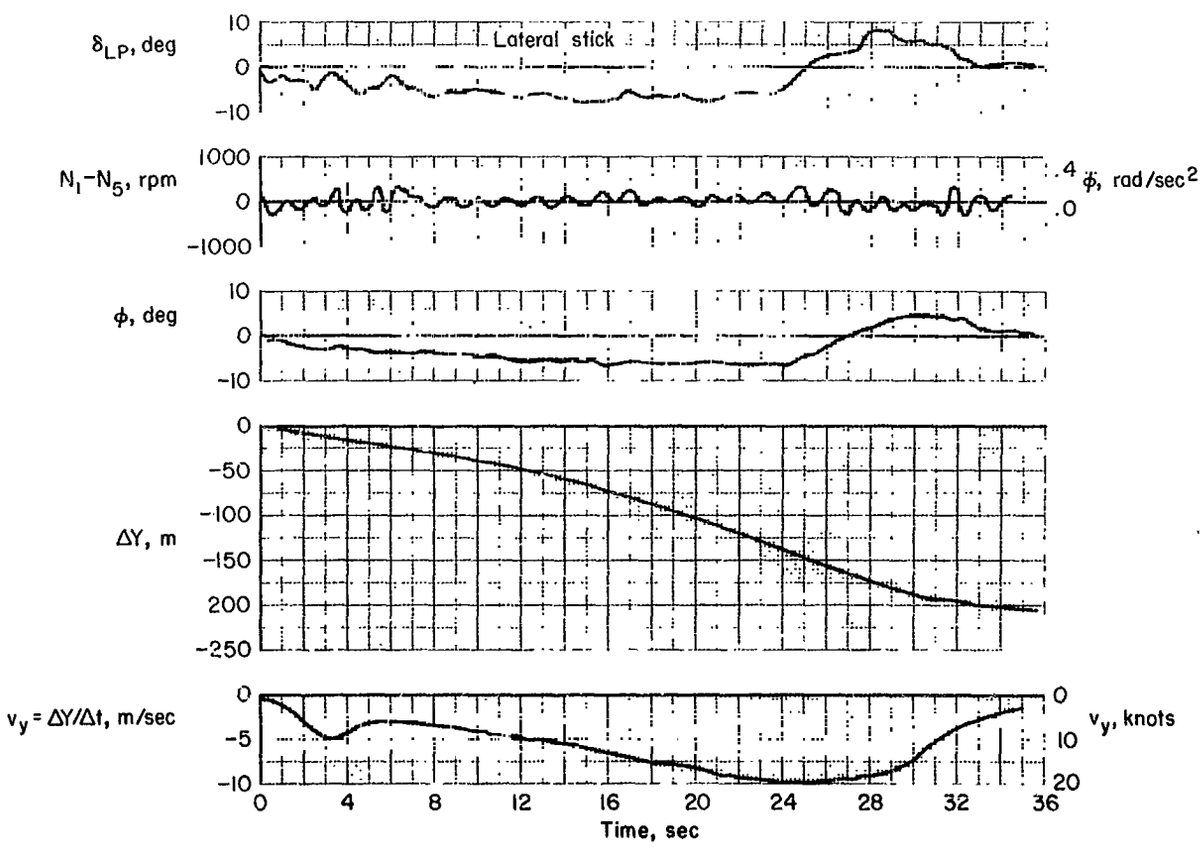

Figure 27.- Slow buildup to maximum desired lateral translational velocity in hover.

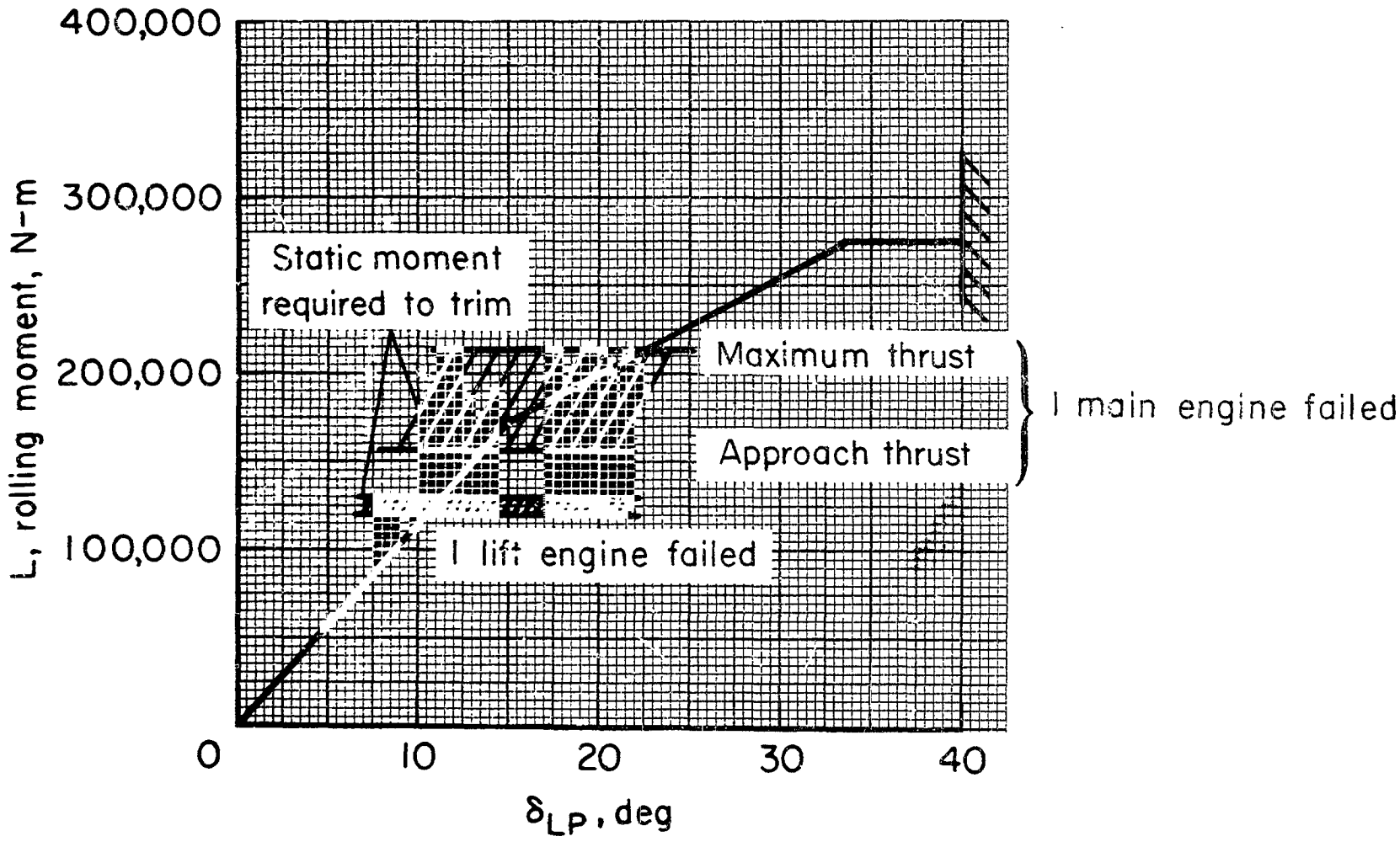

Figure 28.- Lateral control to balance an engine failure; $\sigma_{FCU} = 60°$.

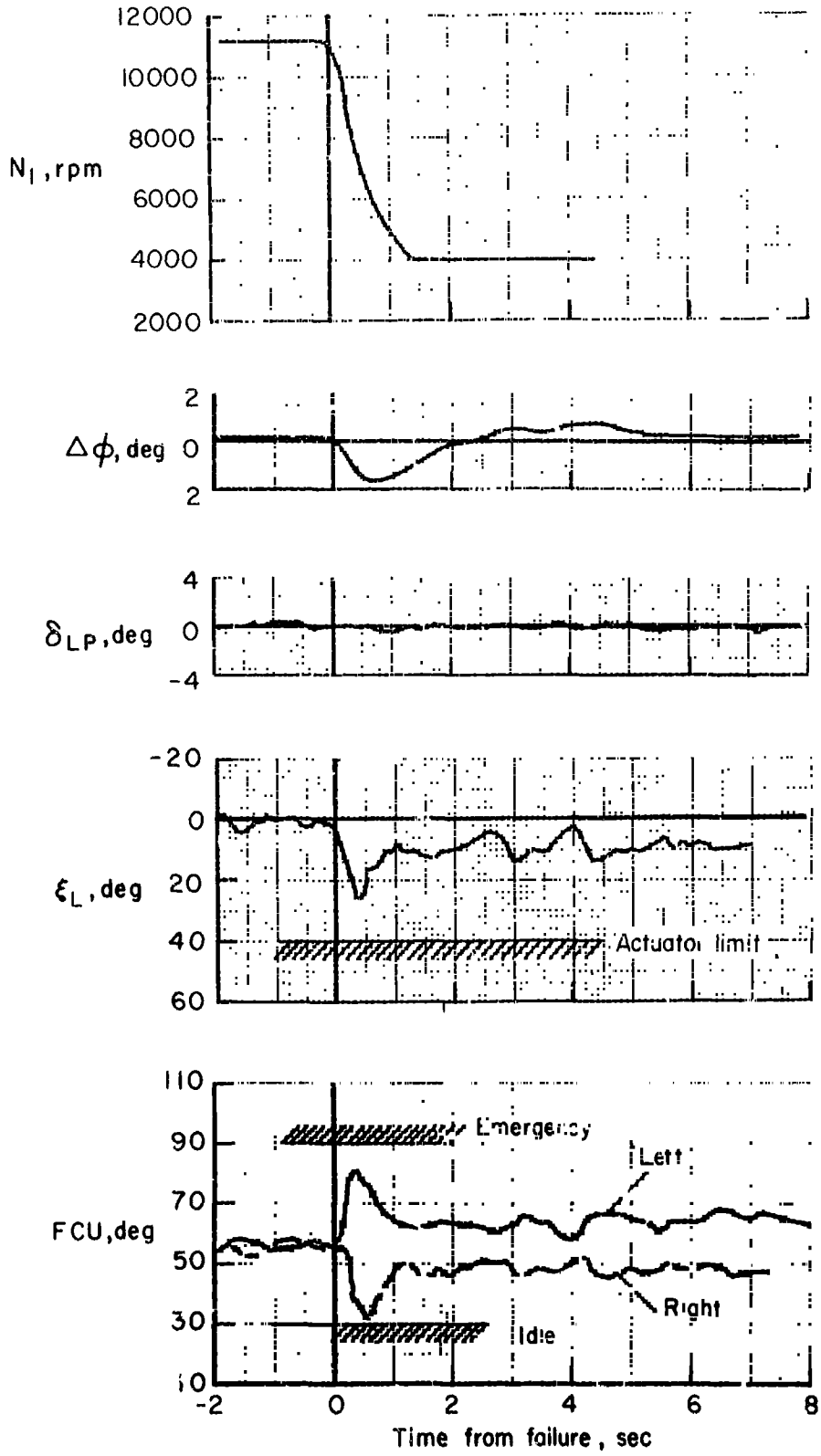

Figure 29.- Lateral response to lift engine failure without pilot correction; hover rig on pedestal.

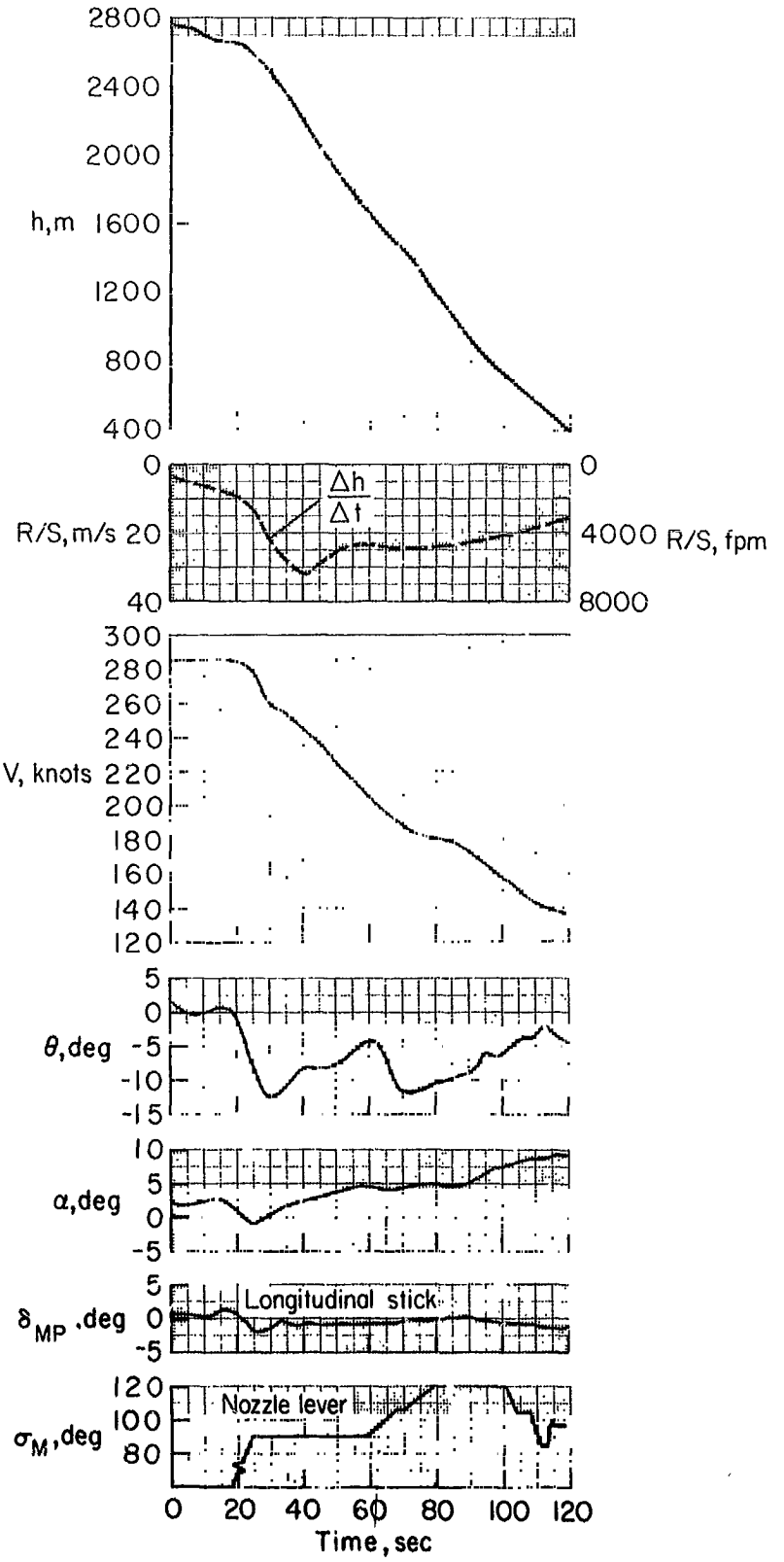

Figure 30.- Letdown from cruise to pre-approach using main engine nozzle deflection; N_F = 72 percent.

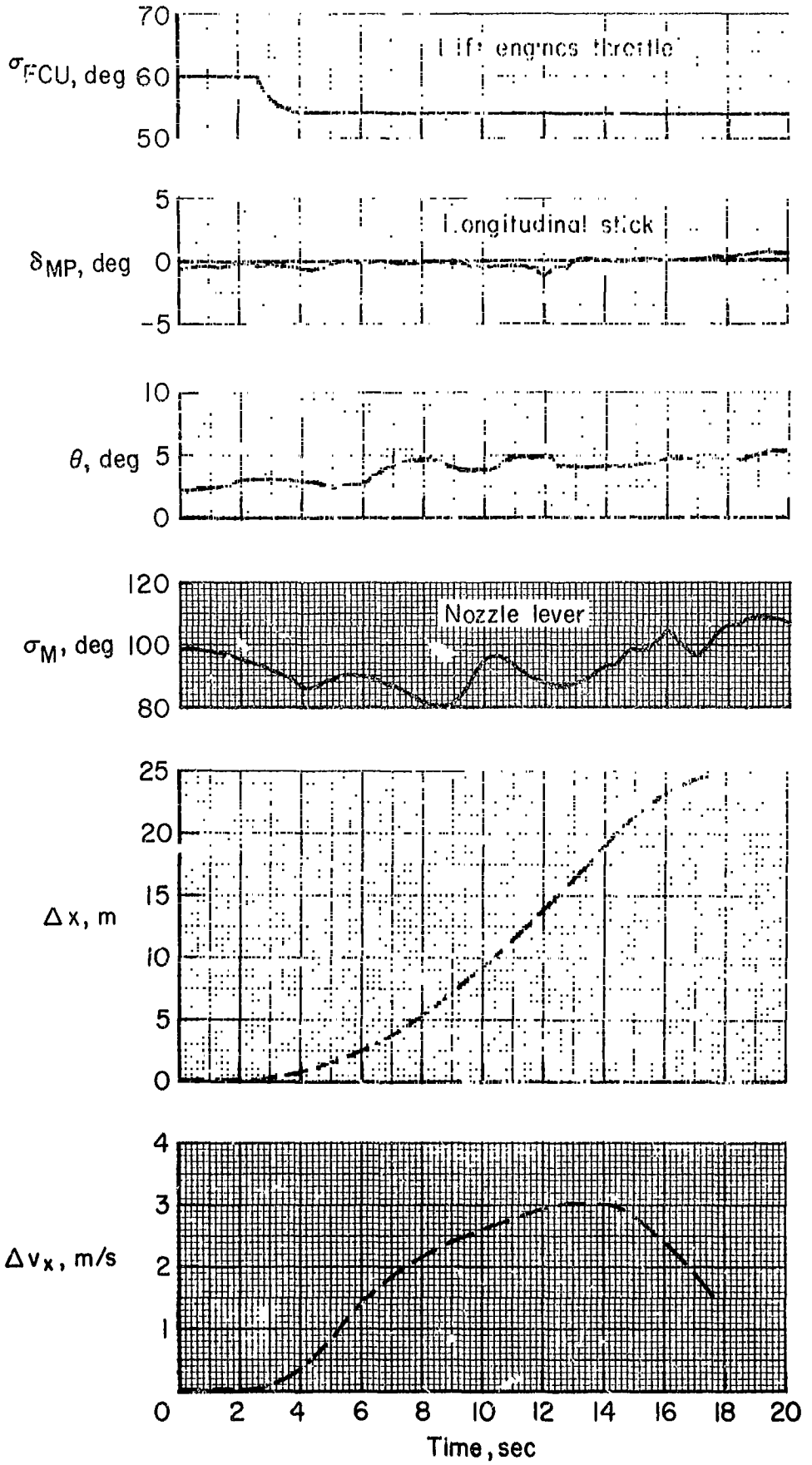

(a) By main engine nozzle deflection

Figure 31.- Longitudinal translation in hover.

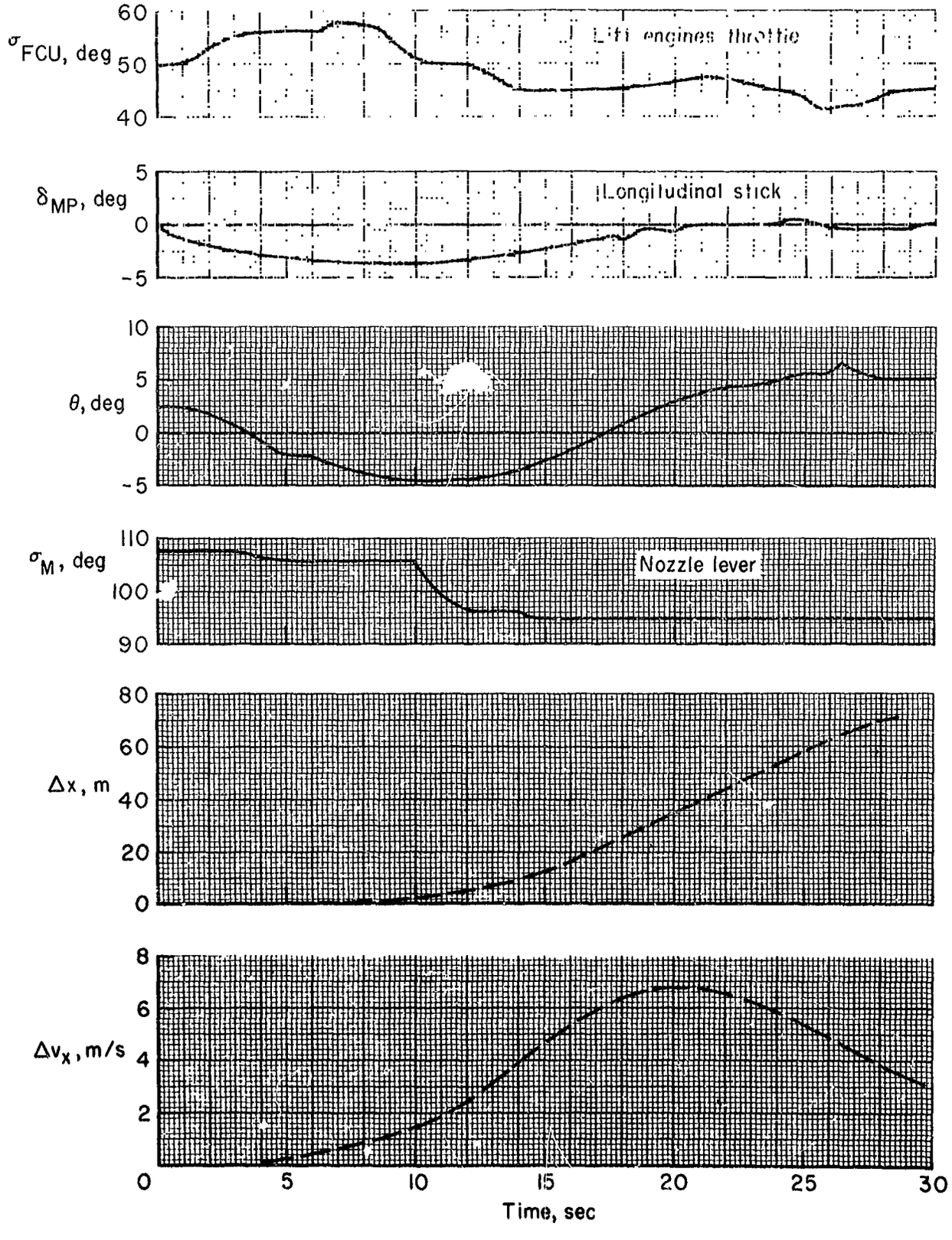

(b) By attitude and nozzle

Figure 31.- Concluded.

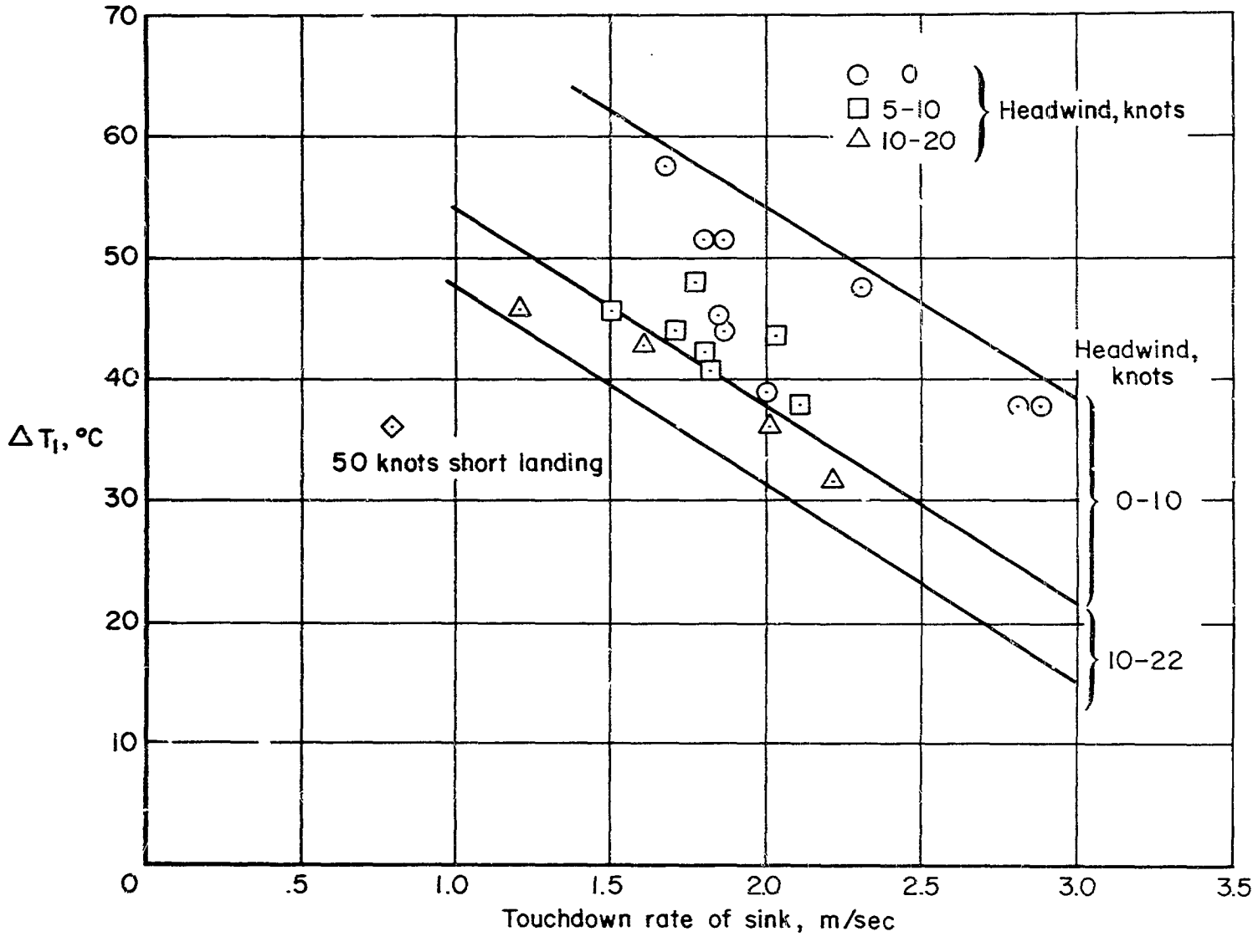

Figure 32.- Effect of sink rate and wind on reingestion.

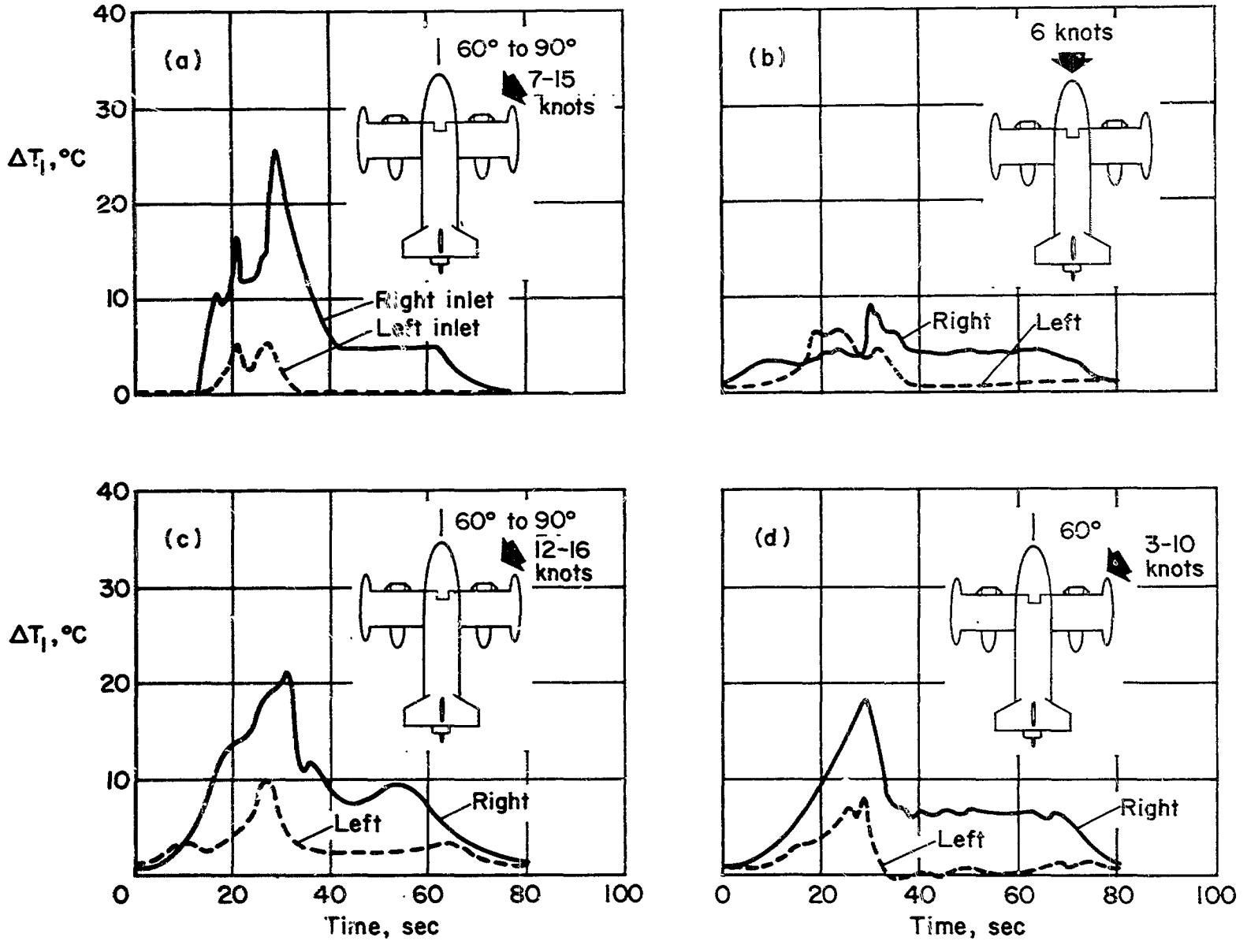

Figure 33.- Vertical takeoff reingestion with different wind conditions.

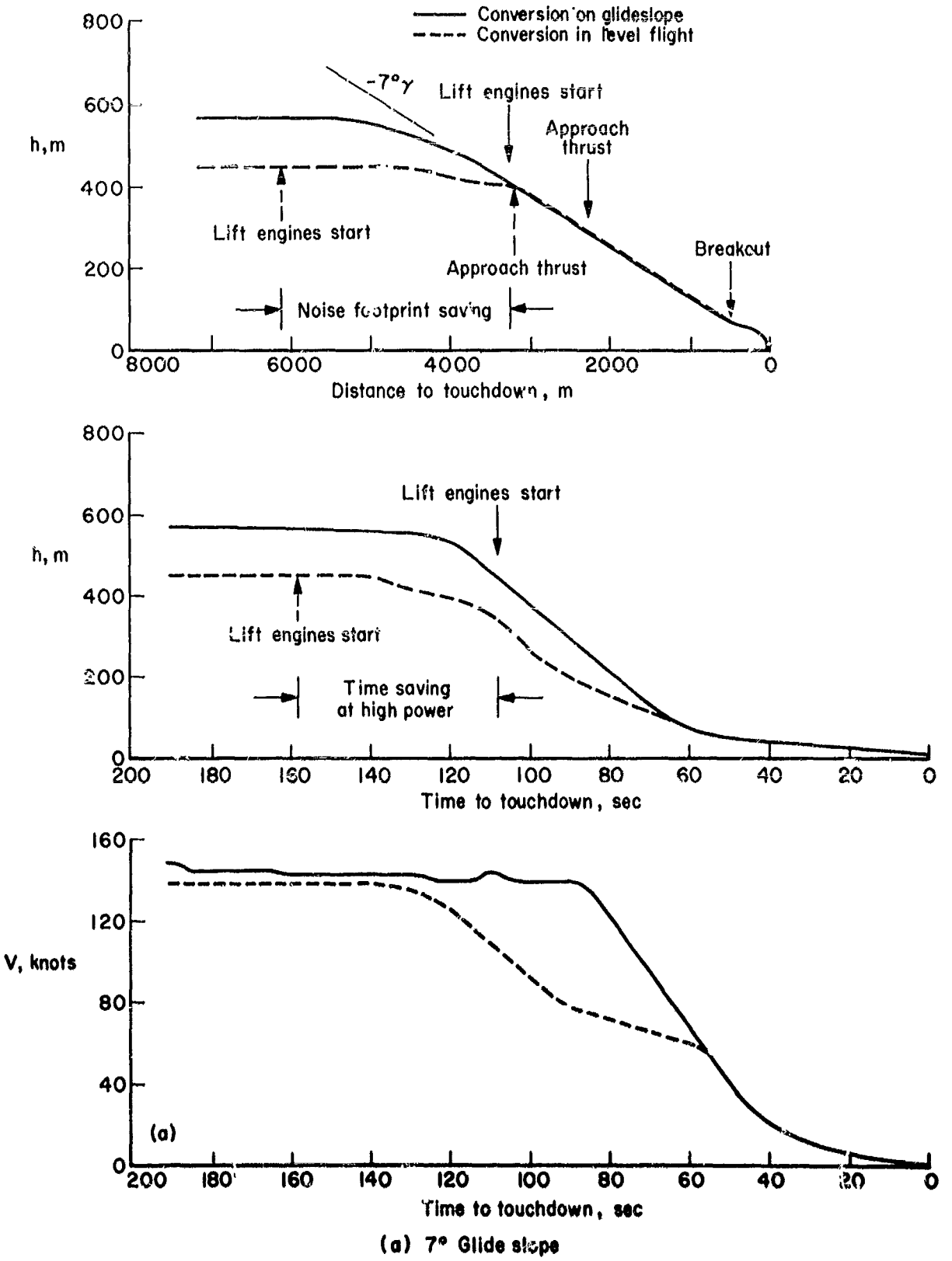

(a) 7° Glide slope

Figure 34.- Comparison of time and distance for different approaches.

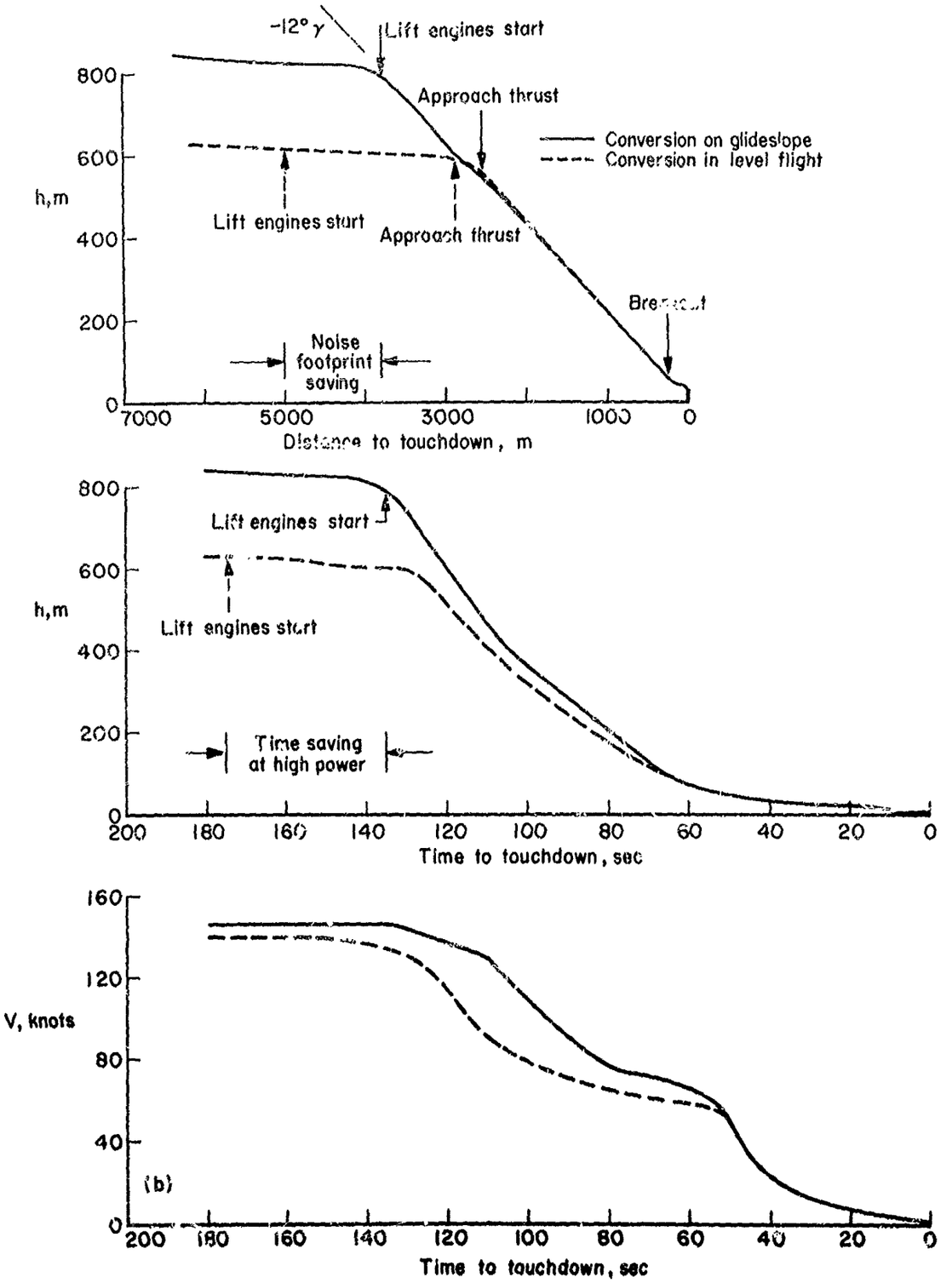

(b) 12° Glide slope

Figure 34.- Concluded.

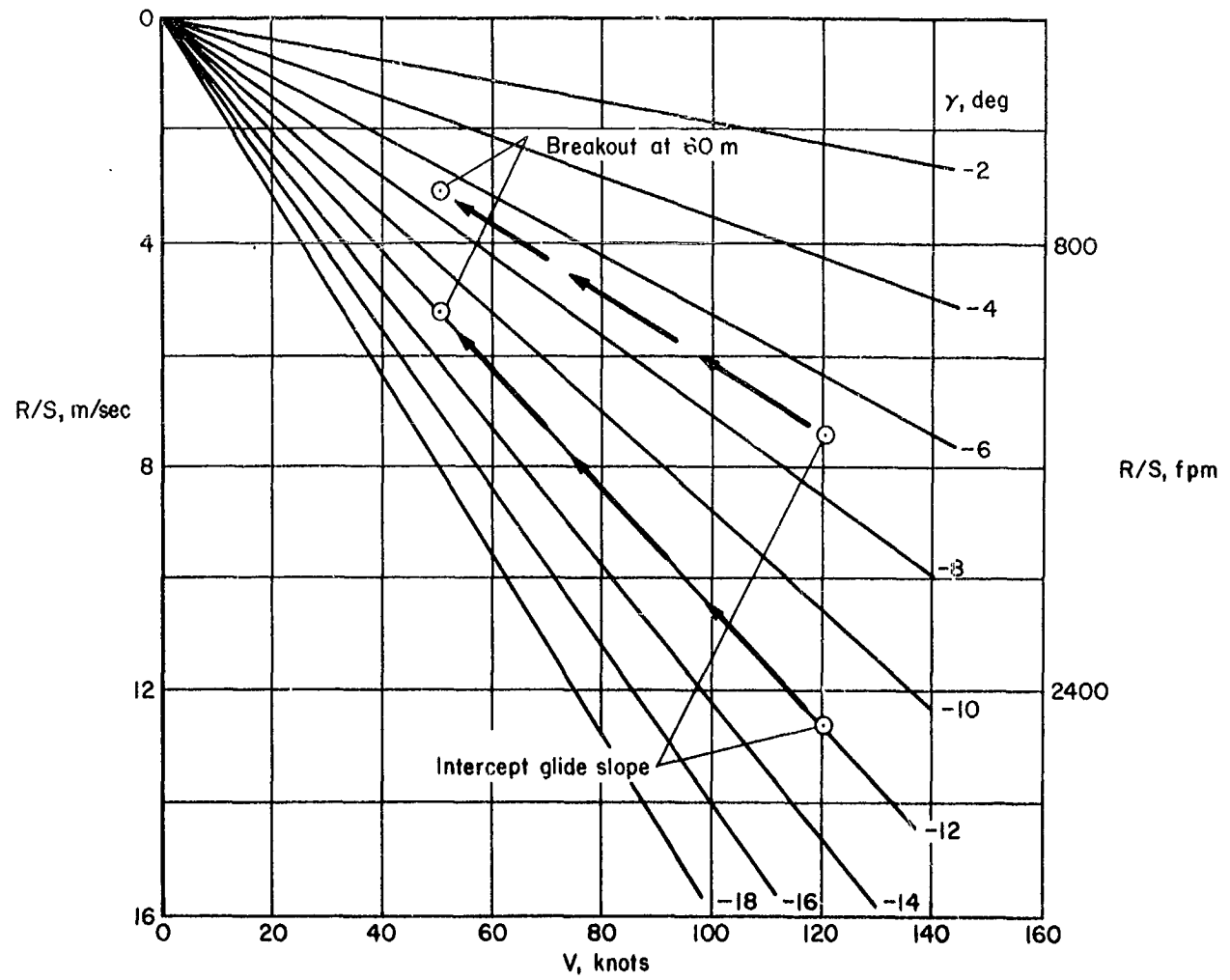

Figure 35.- Variation of rate of sink with airspeed and flight-path angle, zero wind.

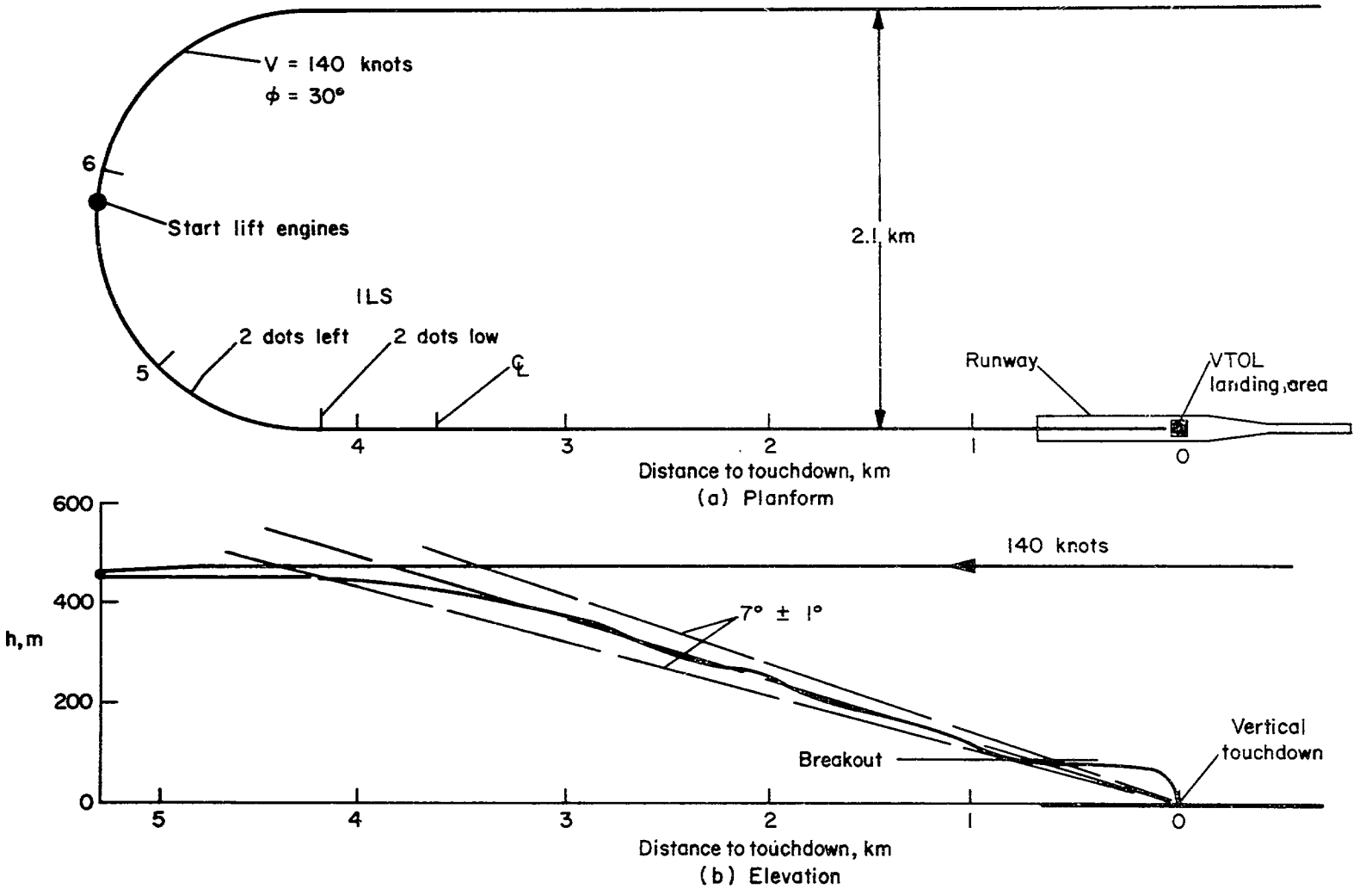

Figure 36.- Close in pattern, starting lift engines during turn.

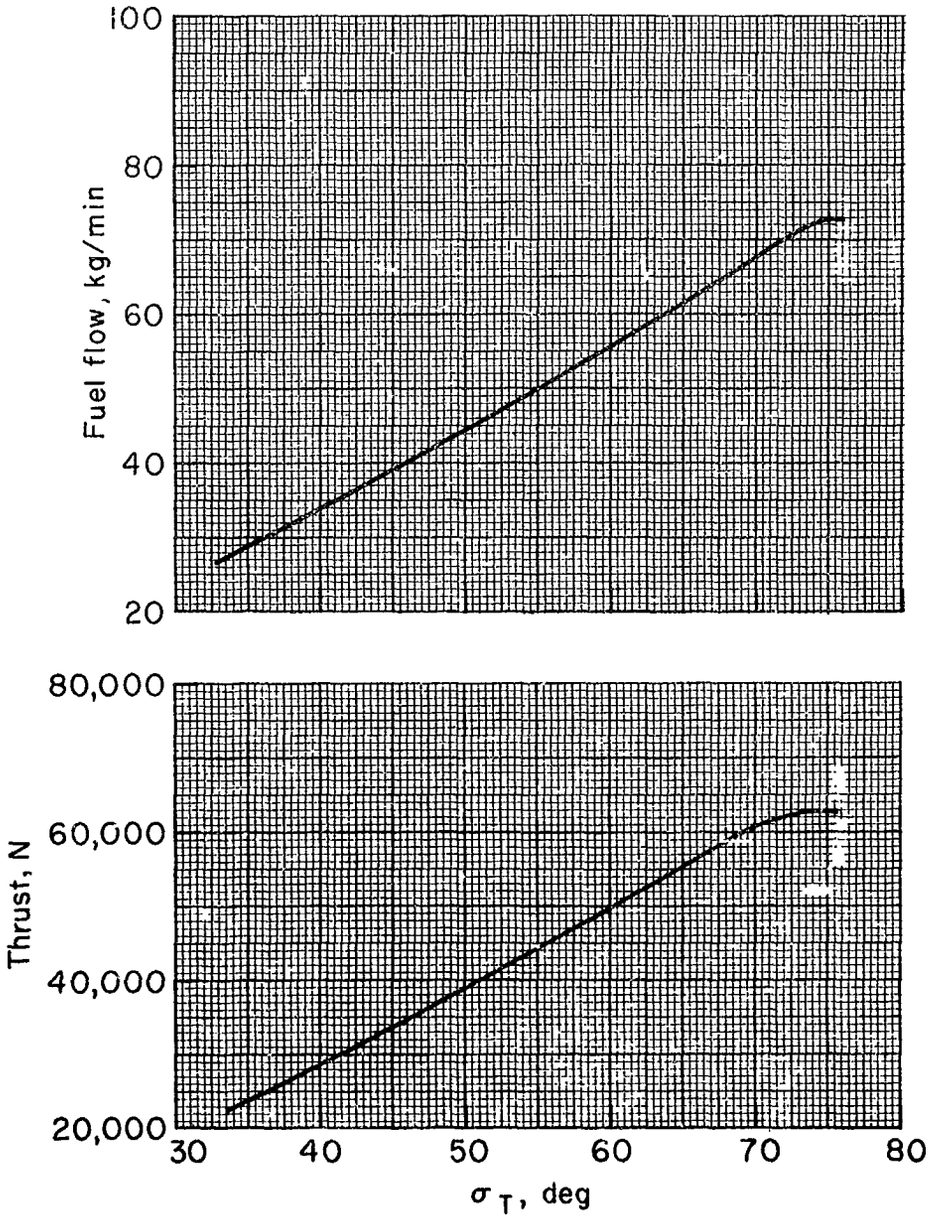

(a) One main engine

Figure 37.- Thrust and fuel flow characteristics at V = 0, h = 600 M, T_A = 11° C.

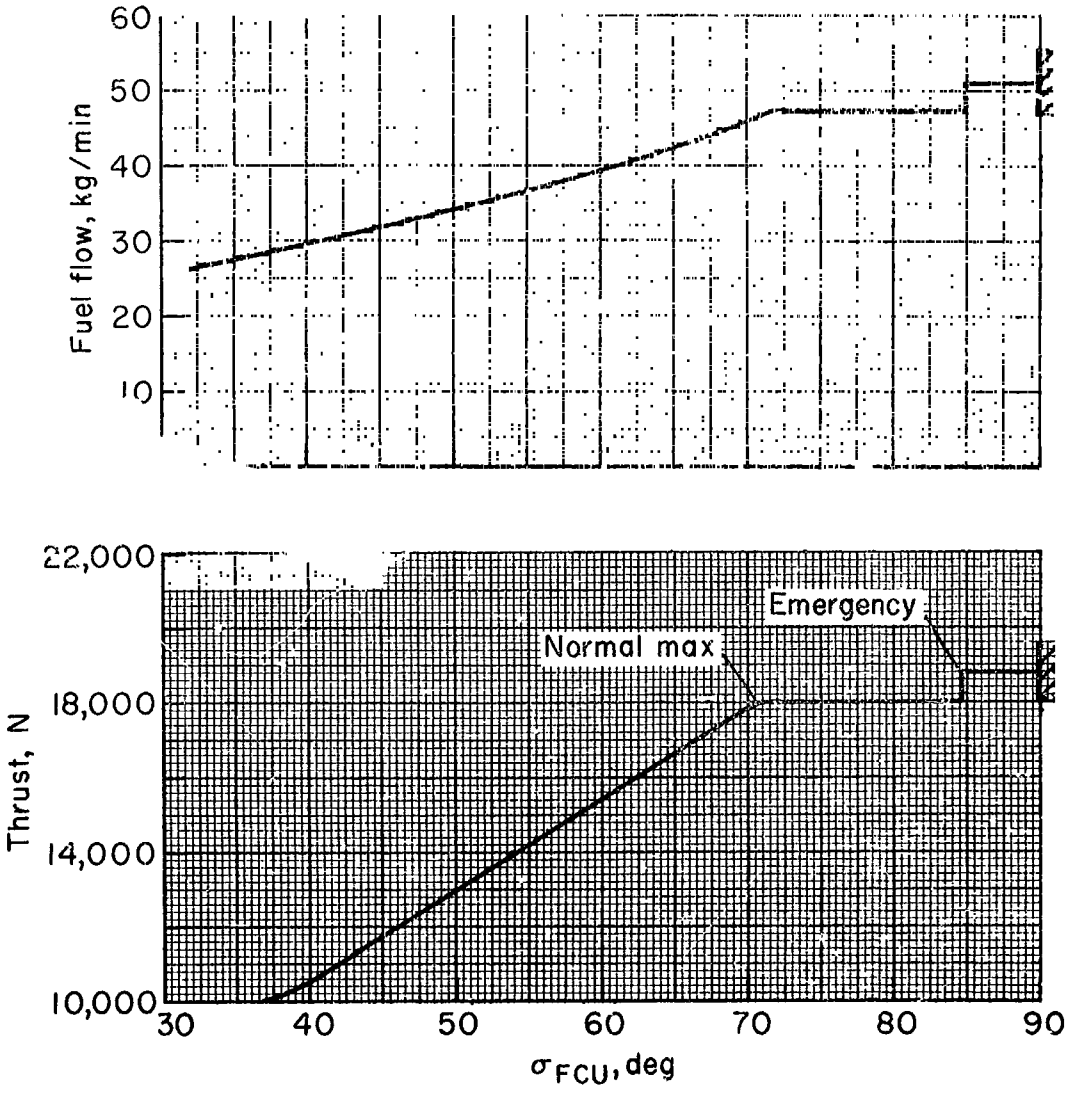

(b) One lift engine

Figure 37.- Concluded.

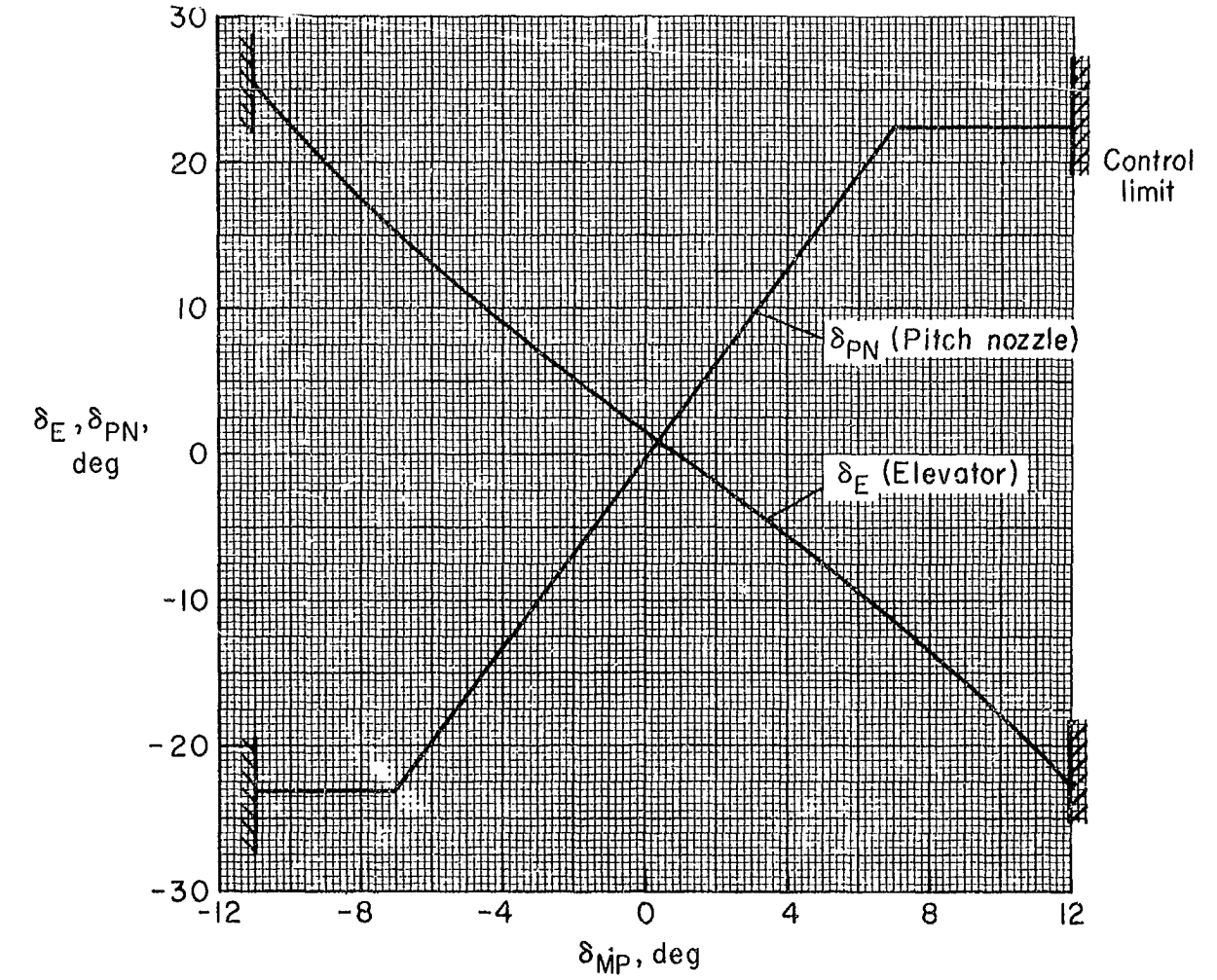

(a) In hover maximum angular acceleration is ±0.22 radian/second squared at $N_F = 80\%$, m = 20,000 kg

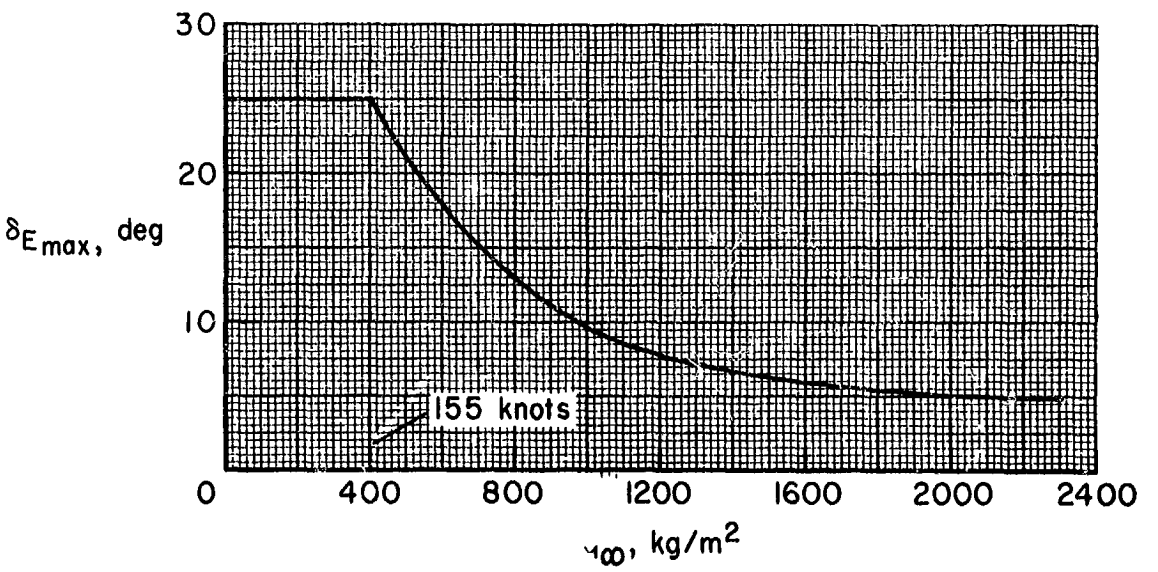

(b) Gearchanger relations

Figure 38.- Longitudinal control relations.

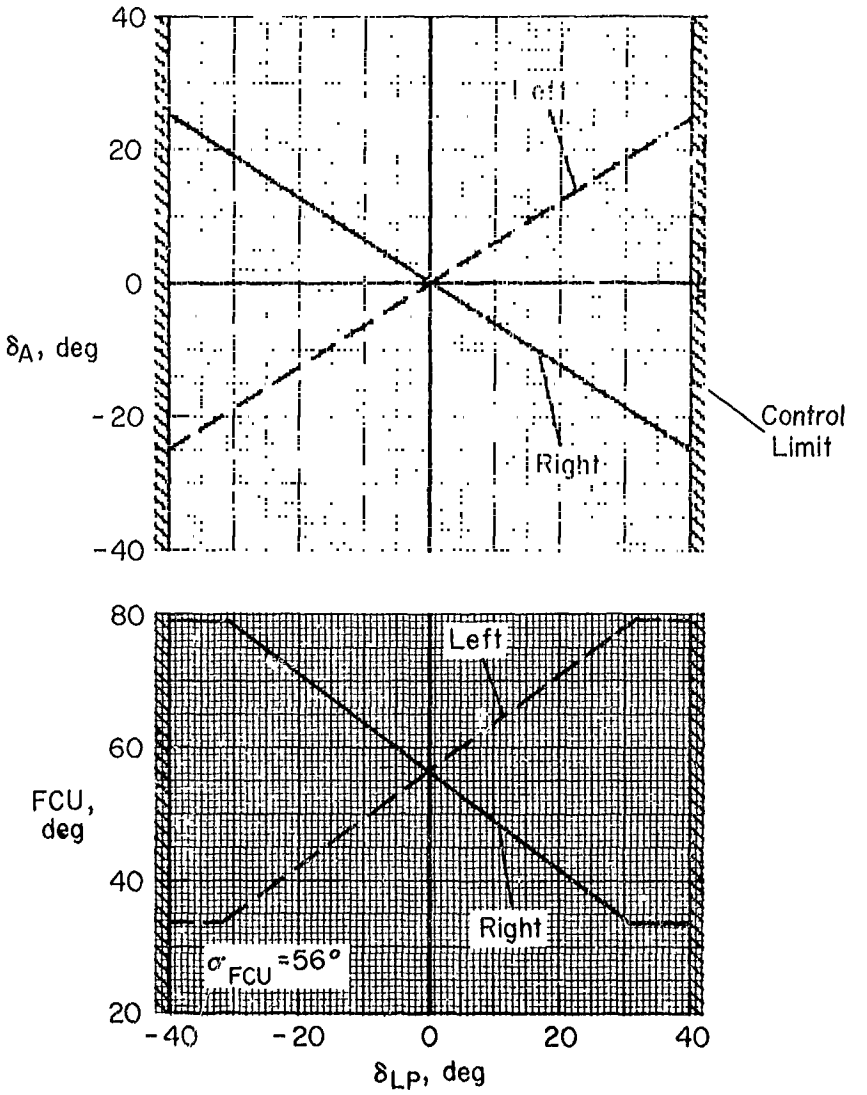

(a) In hover maximum angular acceleration is ±0.78 rad/second squared at m=20,000 kg

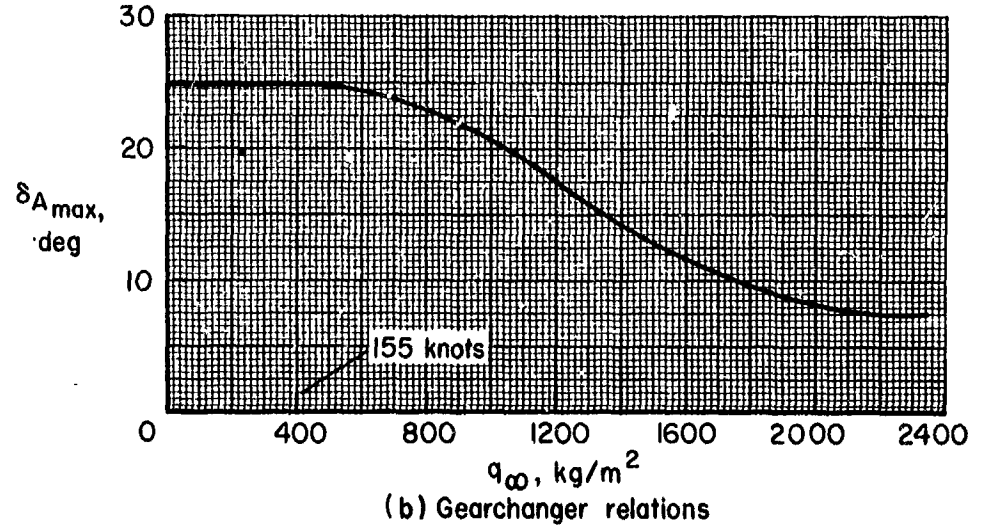

(b) Gearchanger relations

Figure 39.- Lateral control relations.

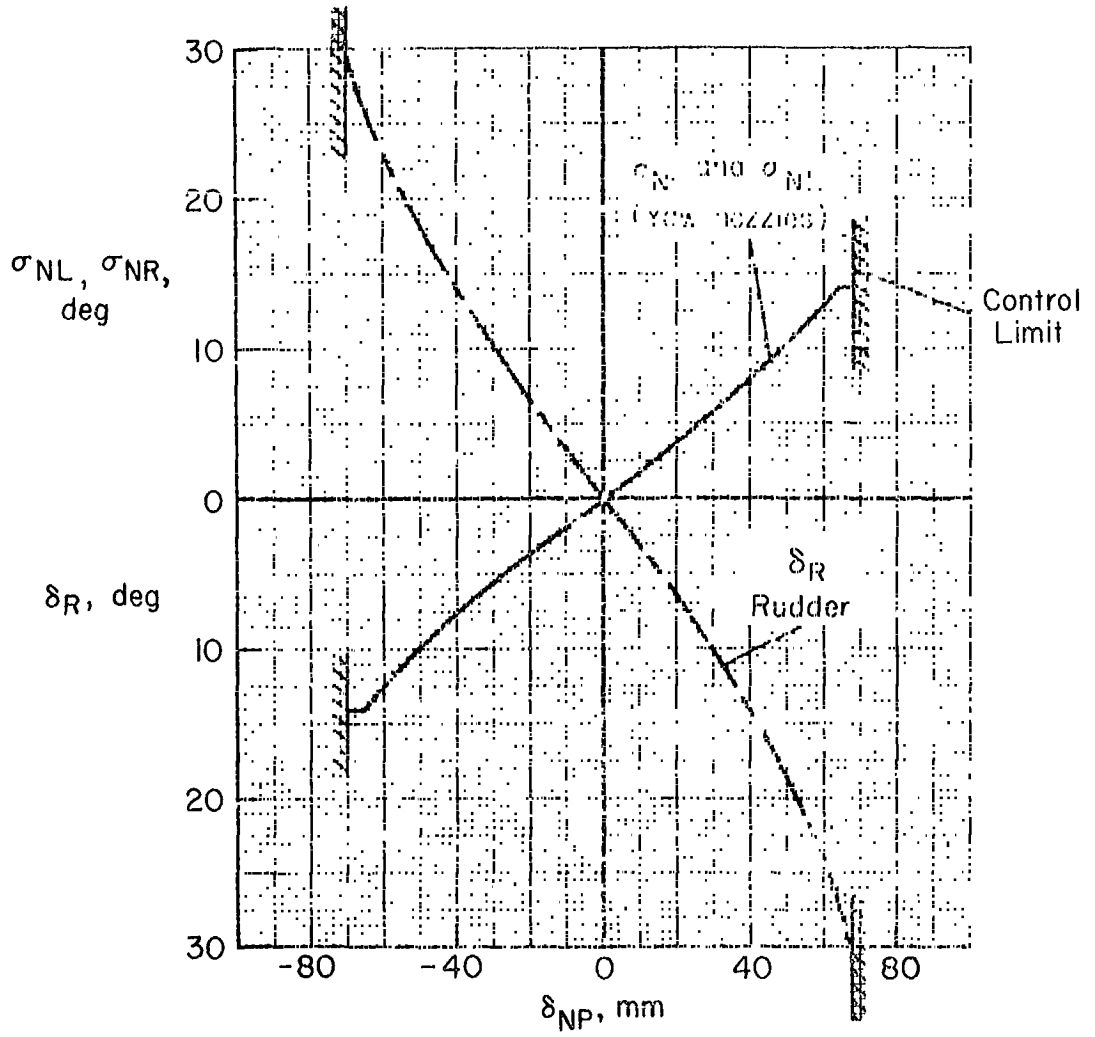

(a) In hover maximum angular acceleration is ±0.38 radians per second squared at m = 20,000 kg

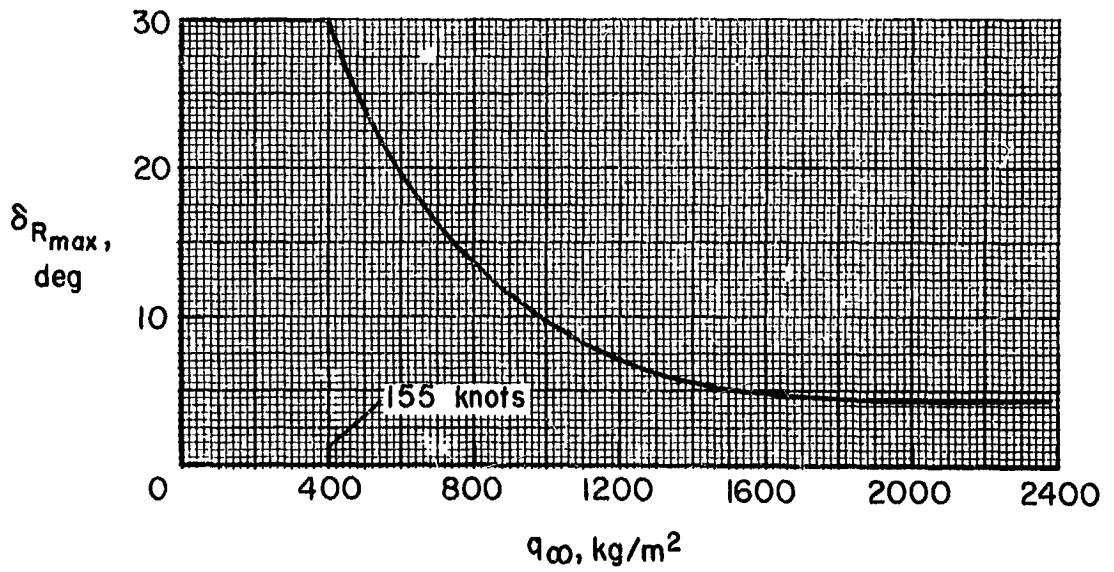

(b) Gearchanger relations

Figure 40.- Directional control relations.